GDAŃSK UNIVERSITY OF TECHNOLOGY

Management of broth after biomass hydrolysis to improve biohydrogen production

DOCTORAL DISSERTATION

Zhila Honarmandrad

Gdańsk, 2025

Załącznik nr 1/3
do Zarządzenia Rektora PG nr 5/2015 z 10 lutego 2015 r.

GDAŃSK UNIVERSITY OF TECHNOLOGY
Faculty of Chemistry

FACULTY OF CHEMISTRY

The author of the PhD dissertation: Zhila Honarmandrad
Scientific discipline: Chemical Sciences

DOCTORAL DISSERTATION

Title of PhD dissertation: Management of broth after biomass hydrolysis to improve biohydrogen production

Title of PhD dissertation (in Polish): Zarządzanie bulionem po hydrolizie biomasy w celu poprawy produkcji biowodoru

Supervisor *signature*
PhD, Dr. habil. Jacek Gębicki, prof. GUT

Gdańsk, 2025

GDAŃSK UNIVERSITY OF TECHNOLOGY
Faculty of Chemistry

FACULTY OF CHEMISTRY

STATEMENT

The author of the PhD dissertation: Zhila Honarmandrad
I,the undersigned, agree that my PhD dissertation entitled:

Management of broth after biomass hydrolysis to improve biohydrogen production

may be used for scientific or didactic purposes.[1]

Gdańsk, 04-07-2025.

Zhila Honarmandrad
.....
signature of the PhD student

Aware of criminal liability for violations of the Act of 4th February 1994 on Copyright and Related Rights (Journal of Laws 2006, No. 90, item 631) and disciplinary actions set out in the Law on Higher Education (Journal of Laws 2012, item 572 with later amendments),2 as well as civil liability, I declare, that the submitted PhD dissertation is my own work.

Ideclare, that the submitted PhD dissertation is my own work performed under and in cooperation with the supervision of PhD, PhD, Dr. habil. Jacek Gębicki, prof. GUT

This submitted PhD dissertation has never before been the basis of an official procedure associated with the awarding of a PhD degree.

All the information contained in the above thesis which is derived from written and electronic sources is documented in a list of relevant literature in accordance with art. 34 of the Copyright and Related Rights Act. I confirm that this PhD dissertation is identical to the attached electronic version.

Gdańsk, 04-07-2025.

Zhila Honarmandrad
.....
signature of the PhD student

I, the undersigned, agree to include an electronic version of the above PhD dissertation in the open, institutional, digital repository of Gdańsk University of Technology, Pomeranian Digital Library, and for it to be submitted to the processes of verification and protection against misappropriation of authorship.

Gdańsk, 04-07-2025.

Zhila Honarmandrad
.....
signature of the PhD student

[1] Decree of Rector of Gdansk University of Technology No. 34/2009 of 9th November 2009, TUG archive instruction addendum No. 8.

[2] Act of 27th July 2005, Law on Higher Education: Chapter 7, Criminal responsibility of PhD students, Article 226.

GDAŃSK UNIVERSITY OF TECHNOLOGY
Faculty of Chemistry

FACULTY OF CHEMISTRY

DESCRIPTION OF DOCTORAL DISSERTATION

The Author of the PhD dissertation: Zhila Honarmandrad

Title of PhD dissertation: Management of broth after biomass hydrolysis to improve biohydrogen production

Title of PhD dissertation in Polish: Zarządzanie bulionem po hydrolizie biomasy w celu poprawy produkcji biowodoru

Language of PhD dissertation: English

Supervision: PhD, Dr. habil. Jacek Gębicki, prof. GUT

Date of doctoral defense:

Keywords of PhD dissertation in Polish: Hydrolizaty lignocelulozowe; Usuwanie inhibitorów; Zielone techniki ekstrakcji/sorpcji; Detoksykacja biomasy w procesie wstępnej obróbki; Zwiększenie wydajności produkcji bio-wodoru

Keywords of PhD dissertation in English: Lignocellulosic hydrolysates; Inhibitor removal; Green extraction/sorption techniques; Biomass pretreatment detoxification; Biohydrogen yield enhancement

Summary of PhD dissertation in Polish: Rosnący globalny popyt na zrównoważoną energię zwiększył zainteresowanie produkcją biowodoru z biomasy lignocelulozowej. Jednak hydroliza takiej biomasy generuje różne związki hamujące, takie jak furfural (FF), hydroksymetylofurfural (HMF), hydrochinon (HQ) i wanilina (VAN), które znacznie utrudniają aktywność mikrobiologiczną i zmniejszają wydajność produkcji biowodoru. Celem badań było opracowanie i ocena zaawansowanych, przyjaznych dla środowiska metod sorpcji/ekstrakcji, aby skutecznie usuwać te inhibitory z brzeczki fermentacyjnej. Zbadano trzy innowacyjne podejścia: hydrofobowe magnetyczne rozpuszczalniki głęboko eutektyczne (HMDES), supramolekularne rozpuszczalniki głęboko eutektyczne (SUPRADES) i oparte na strukturze metaloorganicznej pseudo-DES (MOF@pseudo-DES). Parametry sorpcji/ekstrakcji zoptymalizowano za pomocą projektów statystycznych (Plackett-Burman i Box-Behnken, a ich wydajność sprawdzono na rzeczywistych próbkach hydrolizatu. Spośród badanych metod SUPRADES wykazała najwyższą selektywność dla HQ i VAN, podczas gdy HMDES oferowała szybką, magnetycznie odzyskiwalną sorpcję odpowiednią do zastosowań przemysłowych. MOF@pseudo-DES zapewniał szeroką kompatybilność z różnymi matrycami próbek. Wszystkie metody wykazały się znaczną możliwością ponownego użycia i przyczyniły się do poprawy produkcji biowodoru poprzez znaczne zmniejszenie stężeń inhibitorów. W niniejszym badaniu przedstawiono nowe, skalowalne i ekologiczne systemy sorpcyjne/ekstrakcyjne, które oferują obiecujące rozwiązania w zakresie zwiększania wydajności i zrównoważonego rozwoju produkcji biowodoru.

GDAŃSK UNIVERSITY OF TECHNOLOGY
Faculty of Chemistry

FACULTY OF CHEMISTRY

Summary of PhD dissertation in English: The increasing global demand for sustainable energy has intensified interest in biohydrogen production from lignocellulosic biomass. However, the hydrolysis of such biomass generates various inhibitory compounds such as furfural (FF), hydroxymethylfurfural (HMF), hydroquinone (HQ), and vanillin (VAN) that significantly hinder microbial activity and reduce hydrogen yield. This doctoral research aims to develop and evaluate advanced, environmentally friendly sorption-based extraction methods to effectively remove these inhibitors from fermentation broth. Three innovative approaches were investigated: hydrophobic magnetic deep eutectic solvents (HMDES), supramolecular deep eutectic solvents (SUPRADES), and metal-organic framework-based pseudo-DES (MOF@pseudo-DES). Extraction parameters were optimized through statistical designs (Plackett-Burman and Box-Behnken, and their performance was validated on real hydrolysate samples. Among the studied methods, SUPRADES demonstrated the highest selectivity for HQ and VAN, while HMDES offered rapid, magnetically recoverable extraction suitable for industrial settings. MOF@pseudo-DES provided broad compatibility with diverse sample matrices. All methods exhibited notable reusability and contributed to improved biohydrogen production by significantly reducing inhibitor concentrations. This study introduces novel, scalable, and green extraction systems that offer promising solutions for enhancing the efficiency and sustainability of lignocellulosic biohydrogen production.

Table of contents

Abstract

The increasing global demand for sustainable energy has intensified interest in biohydrogen production from lignocellulosic biomass. However, the hydrolysis of such biomass generates various inhibitory compounds such as furfural (FF), hydroxymethylfurfural (HMF), hydroquinone (HQ), and vanillin (VAN) that significantly hinder microbial activity and reduce hydrogen yield. This doctoral research aims to develop and evaluate advanced, environmentally friendly sorption-based extraction methods to effectively remove these inhibitors from fermentation broth. Three innovative approaches were investigated: hydrophobic magnetic deep eutectic solvents (HMDES), supramolecular deep eutectic solvents (SUPRADES), and metal-organic framework-based pseudo-DES (MOF@pseudo-DES). Extraction parameters were optimized through statistical designs (Plackett-Burman and Box-Behnken, and their performance was validated on real hydrolysate samples. Among the studied methods, SUPRADES demonstrated the highest selectivity for HQ and VAN, while HMDES offered rapid, magnetically recoverable extraction suitable for industrial settings. MOF@pseudo-DES provided broad compatibility with diverse sample matrices. All methods exhibited notable reusability and contributed to improved biohydrogen production by significantly reducing inhibitor concentrations. This study introduces novel, scalable, and green extraction systems that offer promising solutions for enhancing the efficiency and sustainability of lignocellulosic biohydrogen production.

Acknowledgements

The present studies were financially supported by the National Science Centre, Poland, under the OPUS research grant no. UMO-2021/41/B/ST8/02395, which enabled me to conduct the research presented in this dissertation.

1. INTRODUCTION

The utilization of non-renewable energy resources, such as coal, oil, and natural gas, has played a crucial role in the progress of industrial civilizations throughout the last two centuries. Nevertheless, the reliance on these limited resources has resulted in significant repercussions. The ongoing extraction and consumption of non-renewable energy sources inevitably lead to their depletion, posing a danger to the long-term sustainability of future energy supplies. In addition, the environmental consequences are significant: the burning of fossil fuels emits substantial quantities of greenhouse gases, especially carbon dioxide, into the atmosphere. The buildup of greenhouse gases is the main cause of climate change, resulting in global warming, rising sea levels, and more frequent and intense weather phenomena.

In addition, the extraction methods used for these resources frequently lead to substantial ecological damage, such as the destruction of habitats, erosion of soil, and pollution of water. With the increasing awareness of these concerns, there has been a significant surge in the adoption of sustainable energy solutions. Green technologies, which prioritize energy efficiency and strive for minimal environmental effect, are leading the way in this transformation. In addition to these technologies, the idea of a circular economy is becoming increasingly popular. The circular economy, in contrast to the linear economy, adopts a model that focuses on prolonging the use of resources, maximizing their value throughout use, and recovering and regenerating goods and materials at the end of their service life. This technique not only preserves resources but also minimizes waste and environmental footprint. Renewable energy sources play a crucial role in the pursuit of sustainable energy. The sources mentioned, including sun, wind, hydro, geothermal, and biomass, possess the characteristic of being able to organically replenish themselves within short time frames. Renewable energy sources, in contrast to fossil fuels, have less greenhouse gas emissions during energy generation, making them a more environmentally friendly option. Solar and wind power utilize natural mechanisms to produce electricity without emitting pollution. Hydropower, harnessed from the kinetic energy of water, has been employed for millennia and continues to be a vital element of several national energy networks. Biomass is notable among renewable energy sources for its adaptability and capacity for extensive use. Biomass energy is obtained from organic matter, including plant and animal waste, agricultural crops, and forestry products. These materials can be combusted to generate heat or transformed into biofuels, such as ethanol and biodiesel, which are suitable for use in transportation and industry. An important benefit of biomass is its ability to convert waste products, such as agricultural leftovers, food waste, and municipal solid waste, into valuable sources of energy. This not only offers a sustainable energy source but also aids to trash management and minimization. Biomass energy is classified as carbon-neutral due to the fact that the carbon dioxide emitted during burning is balanced out by the carbon dioxide assimilated by plants throughout their development. Nevertheless, it is crucial to effectively oversee biomass resources in a manner that guarantees the consumption rate does not

surpass the rate of regeneration. Sustainable biomass production includes measures such as conscientious forest management, systematic crop rotation, and the utilization of agricultural wastes instead of specific energy crops. To summarize, the shift from non-renewable to renewable energy sources is not only crucial for the environment but also essential for the economy and society. The future of energy lies in green technology and the circular economy, which prioritize sustainability, efficiency, and resource conservation. Biomass, due to its capacity to transform waste into energy and its carbon-neutral characteristics, plays a crucial role in the context of renewable energy. By adopting these advancements, we can alleviate the negative consequences of climate change, diminish pollution, and guarantee a long-lasting energy future for future generations [1, 2].

2. NON-RENEWABLE FUELS

Non-renewable fuels, which primarily include fossil fuels such as coal, oil, and natural gas, have been the mainstay of global energy production since the beginning of the Industrial Revolution. Non-renewable fuels are so named because they are derived from the ancient remnants of plants and animals. These remains suffered intense heat and pressure over millions of years, making it impossible for them to be replaced within a period meaningful to humans. Although it is evident that they have played a crucial role in history and have contributed to economic progress and contemporary comforts, their ongoing utilization poses considerable difficulties [3].

The production and consumption of non-renewable fuels pose several environmental and health risks. Coal mining results in significant land disturbance, resulting in the destruction of habitats and the erosion of soil. Additionally, miners are exposed to dangerous circumstances that heighten the likelihood of developing respiratory ailments. Likewise, the process of extracting oil frequently entails drilling in bodies of water, a practice that carries the potential for oil spills. These spills may cause significant harm to marine ecosystems, impacting both animals and populations residing along the coast. Hydraulic fracturing, often known as fracking, which is employed for the extraction of natural gas, has been associated with the pollution of groundwater and the escalation of seismic events.

Fossil fuel combustion is the main contributor to the release of greenhouse gases, specifically carbon dioxide (CO_2). These emissions make a substantial contribution to global warming by intensifying the greenhouse effect, in which gases capture heat in the Earth's atmosphere. This increase in temperature results in a series of climatic alterations, such as elevated sea levels, more frequent and intense weather phenomena, and changing weather patterns that impact agriculture and biodiversity. Coal burning emits not just CO_2 but other pollutants such as sulfur dioxide (SO_2), nitrogen oxides (NO_x), and particulate matter. These pollutants contribute to the deterioration of air quality and can lead to respiratory health problems [4].

From an economic perspective, depending on non-renewable fuels brings about instability because of the unpredictable pricing impacted by geopolitical tensions, market dynamics, and interruptions in the supply chain.

Due to the limited nature of non-renewable resources, their depletion is unavoidable. The limited availability of resources increases the expenses associated with their exploitation, as the remaining resources become more difficult to get. This is demonstrated by the use of deep-sea drilling and tar sand mining. Furthermore, the energy return on investment (EROI] for fossil fuels has been diminishing, indicating that a greater amount of energy is now necessary to extract these fuels compared to previous periods. Consequently, their economic viability has decreased over time [5].

To address these difficulties, there has been a worldwide effort to promote sustainable energy options. Renewable energy sources such as solar, wind, and hydroelectric power are becoming more economically competitive and technologically sophisticated. They provide cleaner alternatives that help reduce the environmental effects linked to fossil fuels. Energy efficiency techniques and technical advancements, such as electric vehicles and smart grids, are also playing vital roles in decreasing dependence on non-renewable resources. However, despite their environmental advantages, renewable energy sources still face challenges related to cost and reliability. Non-renewable fuels, such as coal and natural gas, remain relatively cheaper and provide stable energy supply, which is crucial since solar energy is unavailable at night, and wind energy is intermittent.

To summarize, although non-renewable fuels have been crucial in driving global industrial and economic advancements, their negative impacts on the environment, public health, and economy make it imperative to transition towards more sustainable energy techniques. The limited availability of these resources, together with their substantial impact on environmental deterioration and climate change, emphasizes the pressing requirement for a shift towards renewable energy sources and a reconsideration of our energy consumption habits. Nevertheless, it must be acknowledged that while energy from non-renewable sources presents increasing challenges, it still ensures energy stability. Adopting sustainable energy solutions is crucial for both preserving the environment and guaranteeing long-term energy security and economic stability.

2.1. Effects of using non-renewable fuels

The consumption of fossil fuels has significant and undesirable effects on both the environment and human health [6]. Here are some of the harmful effects associated with the use of fossil fuels:

*Air pollution and health impacts

The combustion of fossil fuels releases various pollutants into the air, leading to significant environmental and health concerns. Key pollutants include particulate matter (PM2.5), sulfur dioxide (SO_2), and nitrogen oxides (NO_x), which contribute to air pollution, smog formation, and acid rain. These pollutants have severe effects on human health, particularly on the respiratory and cardiovascular

systems, increasing the risk of respiratory diseases, cardiovascular disorders, and even cancer. Long-term exposure to airborne pollutants from fossil fuel combustion is associated with chronic health conditions and poses a serious public health risk. Additionally, these emissions can harm ecosystems by acidifying water bodies and damaging vegetation [7-9].

*Greenhouse gas emissions:

Carbon Dioxide(CO_2): The primary source of greenhouse gas emissions is the combustion of fossil fuels, particularly carbon dioxide (CO_2). These gases trap heat in the Earth's atmosphere, causing global warming and climate change. Consequences include rising sea levels, extreme weather events, ecosystem disruption, and threats to biodiversity [10].

* Climate change:

Increased Greenhouse gas concentrations: The rise in greenhouse gas concentrations, primarily resulting from burning fossil fuels, is a key driver of climate change. This phenomenon has widespread effects on weather patterns, precipitation, and temperatures globally, impacting agriculture, water resources, and natural habitats [11].

* Ocean acidification:

CO_2 absorption: The absorption of excess CO_2 by the world's oceans leads to ocean acidification. This process harms marine life, especially organisms with calcium carbonate shells or skeletons, such as corals and mollusks. Disruption in marine ecosystems can have cascading effects on fisheries and the entire food chain [12].

* Oil spills:

Extraction, transportation, and refining: The extraction, transportation, and refining of fossil fuels, particularly oil, pose the risk of accidental spills. Oil spills can have detrimental effects on marine ecosystems, causing long-term harm to marine life, coastal habitats, and local economies dependent on fishing and tourism [13].

Addressing these adverse effects requires a shift to cleaner and more sustainable energy sources to reduce environmental and health risks associated with fossil fuel consumption. For this reason, the utilization of renewable fuels is of paramount importance.

3. RENEWABLE FUELS

They are energy resources derived from sustainable and naturally replenishing sources, designed to minimize environmental impact and contribute to a cleaner energy ecosystem. These fuels are typically generated through processes harnessing solar, wind, geothermal, hydro, or biomass energy. Examples include biofuels, such as ethanol and biodiesel, produced from organic materials, and biohydrogen. The distinguishing feature of renewable fuels lies in their capacity for continuous regeneration, offering a more sustainable alternative to traditional, finite fossil fuels. These sources play a pivotal role in global efforts to transition towards greener energy solutions, aiming to reduce carbon emissions and mitigate the environmental consequences associated with conventional energy production [14-16].

3.1. Types of renewable fuels

3.1.1. Biomass fuels

Biomass refers to organic materials such as plants, agricultural residues, and organic waste that can be converted into fuel (Fig. 1). Biomass fuels include bioethanol, biodiesel, and biogas. Bioethanol is produced through the fermentation of sugars found in crops like corn and sugarcane, while biodiesel is derived from plant oils or animal fats. Biogas is generated through anaerobic digestion of organic materials such as agricultural waste or sewage [17-19].

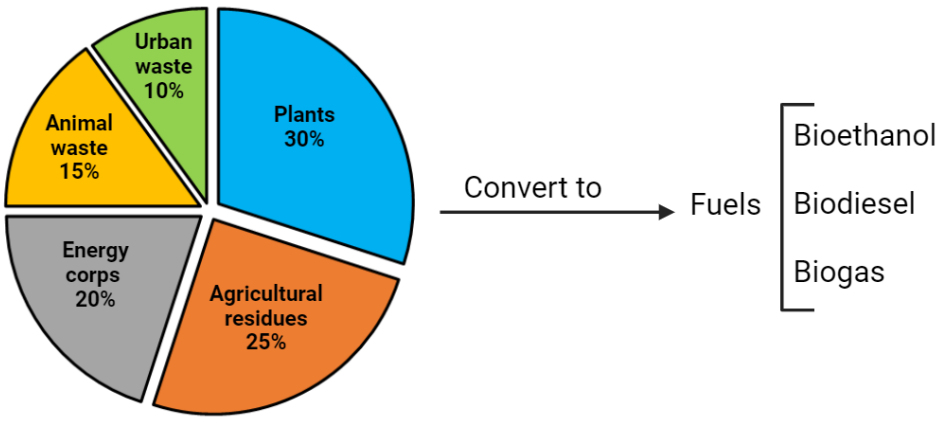

Fig. 1. Sources of biomass fuels

3.1.2. Solar energy

Solar fuels harness solar energy to generate electricity or produce direct fuel. Photovoltaic cells convert sunlight into electricity, and solar thermal systems use sunlight to generate steam for electricity production or facilitate chemical processes for fuel production. In particular, solar thermal systems can contribute to hydrogen production through high-temperature thermochemical water splitting or drive

reactions that generate synthetic fuels, such as syngas (a mixture of CO and H_2), which can be further processed into liquid fuels like methanol. However, Figure 3 illustrates a basic solar water heating system, which primarily provides thermal energy rather than directly producing a fuel. More advanced configurations of solar thermal systems would be required for actual fuel generation (Figs. 2 and 3] [20].

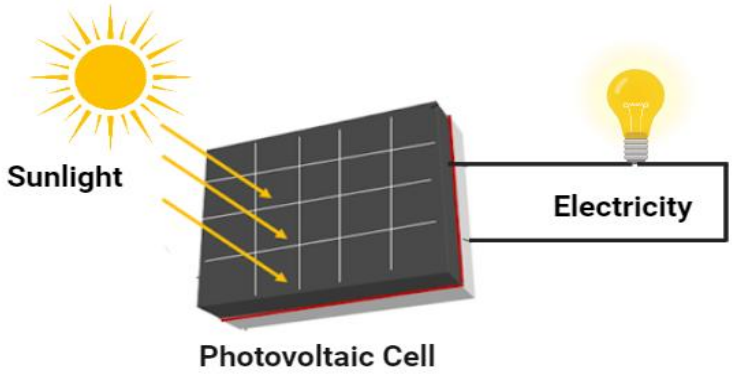

Fig. 2. Conversion of sunlight into electricity by photovoltaic cells

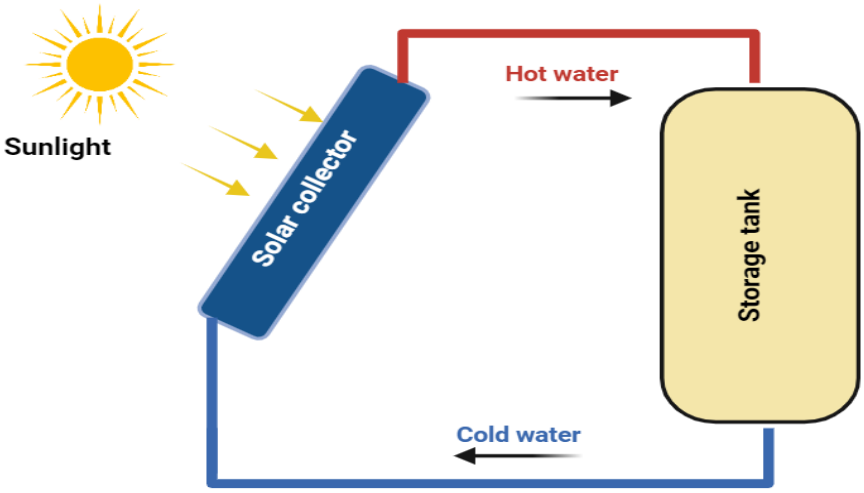

Fig. 3. Solar thermal systems: conversion of sunlight into steam for electricity

3.1.3. Wind energy

Wind power is harnessed through wind turbines to generate electricity. This electricity can be used directly or converted into other forms of renewable fuels, such as hydrogen, through processes like electrolysis, Fig. 4 [21].

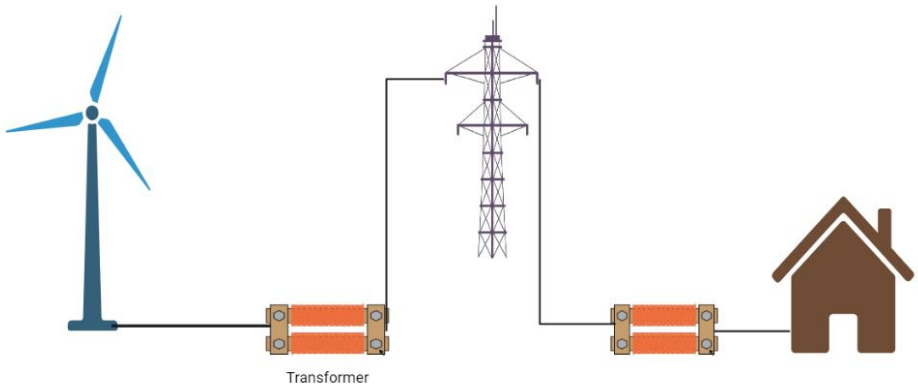

Fig. 4. Wind energy diagram

3.1.4. Hydropower

Hydropower utilizes the energy of flowing or falling water to generate electricity. This renewable energy source is derived from rivers, dams, or ocean tides. It provides a reliable and widely used form of clean energy, Fig. 5 [22].

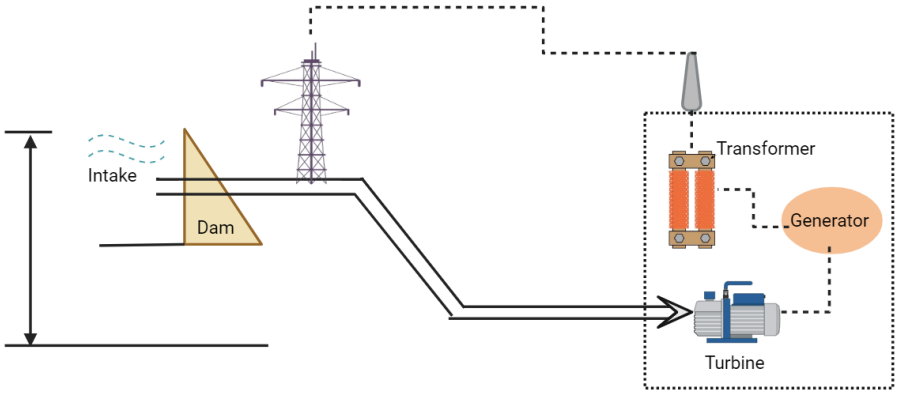

Fig. 5. The schematic of hydroelectric power plant.

3.1.5. Geothermal energy

Geothermal energy taps into the heat within the Earth for electricity generation or heating purposes. This includes harnessing geothermal reservoirs and capturing steam or hot water produced underground, Fig. 6 [23].

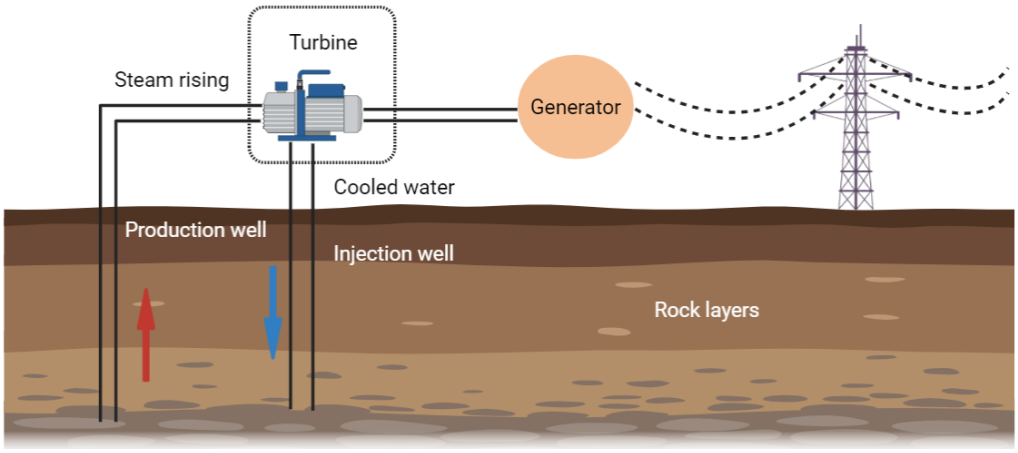

Fig. 6. Geothermal energy production

3.1.6. Hydrogen

Hydrogen can be produced through various renewable methods, including electrolysis using electricity generated from renewable sources. Hydrogen can be used directly as a fuel or converted into synthetic fuels like ammonia or methane. Hydrogen is classified into different colors based on its production method, ranging from green to white. Green hydrogen, produced through electrolysis powered by renewable energy sources, is the most sustainable option. White hydrogen refers to naturally occurring hydrogen found in underground deposits. Since this section focuses on renewable forms, emphasis is placed on green hydrogen as the cleanest and most viable alternative for a sustainable energy transition [24].

Beyond green and white hydrogen, several other classifications exist, primarily based on the energy sources and processes used in their production. Blue hydrogen is derived from natural gas or coal through steam methane reforming (SMR) or coal gasification, but the carbon dioxide generated during the process is captured and stored using carbon capture and storage (CCS) technologies, reducing its environmental impact. While it offers a lower carbon footprint compared to conventional fossil fuel-based hydrogen, it still relies on non-renewable resources. Gray hydrogen, on the other hand, is produced via the same SMR process but without carbon capture, making it one of the most environmentally harmful forms due to its significant CO_2 emissions. Brown and black hydrogen are also derived from coal gasification but result in even higher levels of greenhouse gas emissions, contributing substantially to climate change. A less conventional yet promising category is pink (or purple) hydrogen, which is produced via electrolysis powered by nuclear energy. This method has a low carbon footprint, yet its reliance on nuclear power presents its own challenges, including waste disposal and public perception issues. Although not yet widely extracted, white hydrogen exists naturally in underground reservoirs and could serve as a future source of hydrogen energy if cost-effective extraction methods are developed [25-27].

Among these types, green hydrogen remains the most sustainable and environmentally friendly option due to its reliance on renewable energy and the absence of carbon emissions during production.

3.1.7. Ocean energy

Ocean energy encompasses various technologies that capture energy from tides, waves, and temperature differences in the ocean. Technologies like tidal and wave energy converters aim to provide a continuous and reliable source of clean energy [28].

Each of these renewable fuel sources plays a crucial role in diversifying the energy landscape, reducing reliance on fossil fuels, and contributing to a more sustainable and environmentally friendly energy future [16, 29, 30].

3.2. Advantages of using renewable fuels

Using renewable fuels offers a broad spectrum of benefits that contribute to the outlook of a more sustainable and environmentally-friendly energy, such as, producing energy without emitting greenhouse gases from fossil fuels, thereby mitigating certain forms of air pollution. Broadening the energy supply sources and decreasing reliance on imported fuels. Stimulating economic growth and employment opportunities in various sectors, including manufacturing and installation. [31].

To conclude, renewable energy sources offer a comprehensive solution for simultaneously tackling ecological, economic, and societal issues. With ongoing technological progress and a global shift toward low-carbon energy systems, the strategic significance of renewables in ensuring a more sustainable energy future is projected to increase steadily. A comparative overview of the pros and cons associated with both renewable and non-renewable energy types is presented in Table 1.

Table 1**. The advantages and disadvantages of renewable and non-renewable energy**

Energy source	Advantages	Disadvantages
Renewable		
Biomass	Reduces waste Can be used continuously Less carbon emission compared to fossil fuels	Can lead to deforestation Requires significant land Emissions can still be significant
Solar energy	Abundant and sustainable Reduces electricity bills Low operating costs Low environmental impact	High initial costs Weather dependent Requires large areas for panels Energy storage is expensive
Wind energy	Clean and renewable Low operating costs Can be built on existing farms or ranches	Visual and noise pollution Impact on local wildlife Weather dependent High initial costs
Hydropower	Reliable and efficient Low emissions Provides water supply and recreational opportunities	Environmental impact on aquatic ecosystems High initial costs Risk of dam failure

Energy source	Advantages	Disadvantages
Geothermal	Reliable and efficient Low emissions Small land footprint	Location specific High initial costs Potential for depletion of geothermal resources
Hydrogen	High energy density Can be used in fuel cells for electricity Low emissions	High production costs Requires significant energy input to produce Storage and transportation challenges
Ocean energy	Vast resource Predictable energy source (tides) Low emissions	High initial costs Impact on marine ecosystems Technology still in development
Non-renewable		
Coal	Abundant supply Reliable and consistent power generation Low cost	High greenhouse gas emissions Environmental degradation Health hazards for workers and communities
Natural gas	Cleaner than coal and oil Efficient for heating and electricity Abundant supply	Methane emissions Risk of leaks and explosions Contributes to climate change
Oil	High energy density Easy to transport and store Crucial for transportation industry	High greenhouse gas emissions Oil spills and environmental disasters Finite resource
Overall		
Renewable	Sustainable Environmentally friendly Increasingly cost-effective with technology advances	Dependent on weather conditions High initial costs Land and resource intensive
Non-renewable	Currently more established Generally lower initial costs High energy density	Finite resources Significant environmental impact Health and safety risks

4. BIOMASS

Biomass refers to the renewable organic matter derived from plants and live or recently deceased organisms. Biomass can be combusted for thermal energy or transformed into liquid and gaseous fuels using several methodologies. The energy obtained by these creatures may be converted into usable energy through both direct and indirect methods. Biomass can be combusted for direct heat generation, transformed into electricity directly, or processed into biofuel indirectly [32].

Biomass sources for energy production include:

The Wood and Agricultural Products category includes many items such as logs, wood chips, agricultural leftovers, and other plant products. These sources are traditionally employed for the purpose of heating and generating energy.

Solid waste: The organic parts of municipal solid waste (MSW), such as leftover food and yard trash, are being used more and more to generate energy.

Animal waste, such as manure and other by-products from cattle, can be treated to generate biogas and other types of energy.

Industrial waste refers to any byproduct or residue generated during industrial processes. Co-products, on the other hand, are materials that are produced alongside the main product during manufacturing. By-products derived from the food, beverage, and wood processing sectors are very important biomass resources.

Energy crops, such as switchgrass, willow, and poplar, are developed expressly for the purpose of energy generation. These crops have the advantage of high yields and are typically produced on marginal soils that are not suited for growing food crops.

4.1. Biofuels

Biofuels typically denote liquid fuels and blending components derived from biomass resources known as feedstocks. Biofuels can encompass methane derived from landfill gas, biogas, and hydrogen derived from renewable resources. Biofuels primarily serve as transportation fuels; however, they may also be utilized for heating and energy production [33]. Several varieties of biofuels include:

Ethanol is an alcohol fuel that is mixed with petroleum gasoline to be used in cars.

Biodiesel is a type of biofuel that is often mixed with petroleum diesel for use.

Renewable diesel is a type of fuel that is chemically comparable to petroleum diesel fuel. It may be used as a drop-in fuel or blended with petroleum diesel.

4.1.1. Biogas

Biogas is a collection of gases produced by anaerobic bacteria from the decomposition and fermentation of garbage, animal and human waste, and plant waste in the absence of oxygen. Biogas consists of about 50-70% methane, 30-40% carbon dioxide, and small amounts of other gases [34]. The production of biogas occurs through anaerobic digestion, where microorganisms break down organic matter in an oxygen-free environment. This process leads to the release of methane (CH_4) and carbon dioxide (CO_2), making biogas a viable alternative to fossil fuels for energy generation. However, biogas requires combustion to release its energy, and while it offers a renewable energy source, it still produces carbon emissions upon use. The primary applications of biogas include electricity and heat generation, as well as its upgrading to biomethane for injection into natural gas grids or use as vehicle fuel [35, 36].

4.1.2. Biohydrogen

Biohydrogen is a form of hydrogen gas produced through biological processes, typically utilizing microorganisms or algae to generate hydrogen from organic compounds. This renewable form of hydrogen is derived from organic materials such as plant biomass, agricultural residues, or organic waste. The production of biohydrogen is considered a promising avenue for sustainable energy, offering a clean and environmentally friendly alternative to conventional methods reliant on fossil fuels [37, 38]. Unlike biogas, biohydrogen is produced through different biological pathways, such as dark fermentation, photo fermentation, and microbial electrolysis cells (MECs). These processes involve specific bacteria, algae, or other microorganisms that generate hydrogen gas without producing methane, making biohydrogen a more efficient and cleaner fuel option. Furthermore, biohydrogen can be directly utilized in fuel cells to generate electricity, offering a zero-carbon energy source that does not require combustion. Its primary advantages over biogas include higher energy efficiency, cleaner emissions, and its potential role in hydrogen-based energy systems, particularly in fuel cells and industrial applications [39-42].

4.1.2.1. Methods of biohydrogen production

Biohydrogen can be generated using different raw materials through thermochemical methods (steam reforming of biobased oils, pyrolysis, supercritical gasification of water, simple gasification, steam gasification), and biological processes. These methods encompass the following processes [43].

4.1.2.1.1. Thermochemical process

Thermochemical strategies for biohydrogen production involve the conversion of biomass into hydrogen gas by the application of heat and chemical processes. These technologies offer significant benefits since they are capable of processing a diverse range of biomass sources, including agricultural waste, wood chips, and even municipal solid waste. The main thermochemical methods are gasification, pyrolysis, and supercritical water gasification (SCWG). Gasification is the process of partly oxidizing biomass at high temperatures, often ranging from 800 to

1000°C, using a regulated amount of oxygen, steam, or air. This procedure transforms biomass into syngas, which is primarily a blend of H_2, CO, and CO_2 gases. Pyrolysis involves the heat degradation of organic molecules in the absence of oxygen, resulting in the production of several byproducts. This procedure involves the decomposition of biomass using heat, in the absence of oxygen, at temperatures ranging from 400 to 600°C. The outcome consists of bio-oil, syngas, and char [44, 45].

Supercritical water gasification (SCWG) is a high-efficiency process that utilizes supercritical water (above 374°C and 22 MPa) as a reaction medium to break down biomass into hydrogen-rich syngas. Under these conditions, water acts as both a solvent and a reactant, enhancing the solubility of organic materials while eliminating char and tar formation. SCWG enables the conversion of wet biomass, such as sewage sludge and algae, without requiring a drying step, making it particularly advantageous for processing high-moisture feedstocks. Additionally, the high reaction efficiency results in a higher hydrogen yield compared to conventional gasification methods (46, 47].

4.1.2.1.2. Biological processes

Microorganisms are employed in biological processes to convert organic materials into hydrogen gas for biohydrogen generation. Typically, these procedures are carried out under less extreme circumstances than thermochemical approaches, which makes them more ecologically sound and maybe more enduring. The main biological techniques for producing biohydrogen include bio photolysis, photo fermentation, and dark fermentation [48-50]

Bio photolysis is the enzymatic process by which specific photosynthetic microorganisms, such as cyanobacteria and green algae, utilize light energy to cleave water molecules into hydrogen and oxygen.

Photo fermentation is a process in which certain photosynthetic bacteria use light energy to transform organic substrates into hydrogen in the absence of oxygen. These bacteria, specifically *Rhodobacter* and *Rhodospirillum* species, are frequently employed in this procedure.

Dark fermentation is a biochemical process in which anaerobic bacteria transform organic substrates into hydrogen gas without the presence of light. Clostridium and Enterobacter species are frequently employed in the process of dark fermentation.

Biological technologies for biohydrogen synthesis provide encouraging and eco-friendly alternatives to thermochemical approaches. Bio photolysis, photo fermentation, and dark fermentation employ distinct microbes and metabolic processes to transform organic substances into hydrogen.

4.1.2.2. Feedstock of biohydrogen production

Feedstock for biohydrogen production refers to the organic materials or substrates used in the process to generate hydrogen through biological pathways. These materials serve as a source of

carbon for microorganisms or algae involved in the fermentation or photosynthesis processes that ultimately produce biohydrogen. The terms "first generation," "second generation," and "third generation" in the context of bioenergy and biofuel production are used to categorize different types of biomasses based on their origin, characteristics, and potential applications [51]. This classification is essential for distinguishing between traditional feedstocks derived from food crops and newer, more sustainable options. Here's a breakdown of each generation:

First generation feedstocks:

First-generation feedstocks are biomass materials sourced from traditional food crops or specific plant parts. These feedstocks have historically been utilized in the production of first-generation biofuels. Examples of common first-generation feedstocks include Corn (Maize), Sugarcane, and Soybean. These crops are well-established sources for bioethanol and biodiesel production [52].

Advanced feedstocks (second and third Generation):

Second and third-generation feedstocks represent more advanced and sustainable alternatives that go beyond the use of traditional food crops [53]. They include lignocellulosic biomass, algae, waste biomass [54]. These advanced feedstocks present several potential advantages, including enhanced sustainability, reduced competition with food crops, and improved environmental performance. Their development and utilization contribute to the evolution of more sustainable and environmentally friendly practices in the field of bioenergy [55]. The choice of feedstock depends on factors such as availability, cost, and the specific microorganisms or processes used in biohydrogen production. Utilizing diverse feedstocks contributes to the sustainability and flexibility of biohydrogen as a renewable energy source [53].

4.1.2.2.1. Lignocellulose

Among all the mentioned feedstocks, lignocellulosic biomass is an abundant and renewable source of hydrocarbons, which founded in hardwood, softwood, grasses, and agricultural residues. Global annual yields of lignocellulosic biomass residues surpass 220 billion tons, equivalent to approximately 60-80 billion tons of crude oil [56]. Comprising primarily glucose and xylose, lignocellulosic feedstocks necessitate microbial strains proficient in their degradation for the advancement of renewable H_2 production processes [57]. The direct conversion of lignocellulosic biomass to H_2 requires pretreatment to hydrolyze its intricate and crystalline structure [58, 59]. Consequently, lignocellulosic biomass stands as an appealing, cost-effective feedstock for H_2 production.

"Lignocellulose" is a term used to describe biomass derived from plants, consisting of three main components: cellulose, hemicellulose, and lignin. These complex organic polymers form the structural framework of plant cell walls [60]. Cellulose is a polysaccharide composed of linear sequences of glucose units connected through β-1,4-glycosidic linkages. These linear chains organize

into crystalline, rigid structures that contribute to the mechanical strength and firmness of plant cell walls. As the most prevalent organic substance on earth, cellulose plays a critical structural role in biomass. In contrast, hemicellulose consists of branched chains containing diverse sugar units such as glucose, xylose, and mannose. Its non-crystalline, irregular configuration functions as an adhesive matrix interlinking cellulose microfibrils, further supporting the integrity of plant cell walls. Lignin, another essential component, is an amorphous polymer comprised of phenolic subunits. It establishes a 3D network that fills the voids between cellulose and hemicellulose, enhancing the rigidity and microbial resistance of plant tissues [61-63].

Together, these three polymers cellulose, hemicellulose, and lignin constitute the complex structural framework of lignocellulosic biomass. Due to its high availability and structural richness, lignocellulosic biomass is widely recognized as a promising feedstock for biofuel generation via advanced conversion routes such as enzymatic hydrolysis and microbial fermentation [54]. The structure of lignocellulose biomass is shown in Fig. 7.

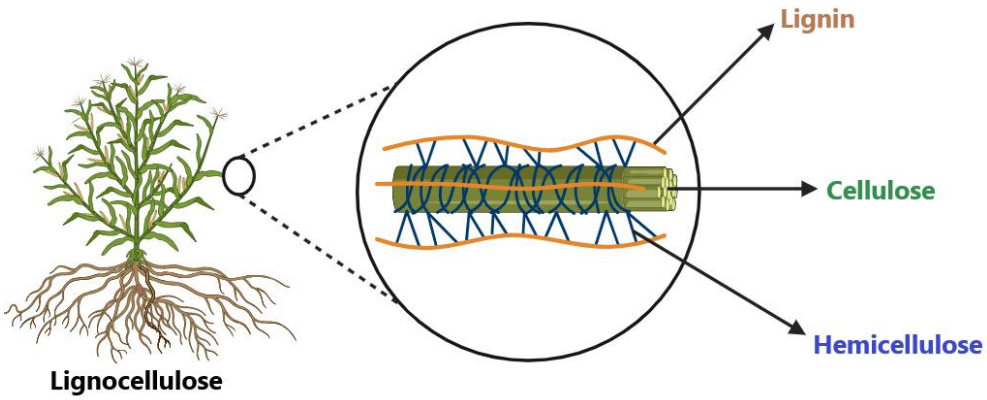

Fig. 7. The schematic of lignocellulose biomass

Lignocellulosic biomass plays a crucial role in the production of biofuels, offering significant advantages and contributing to the global shift towards sustainable energy sources. It is abundant and widely available, encompassing agricultural residues like crop straws and forestry residues such as wood chips, providing a readily accessible and sustainable feedstock for biofuel production. Unlike finite fossil fuels, lignocellulosic biomass is a renewable resource. Its utilization for biofuels helps reduce dependence on non-renewable energy sources, fostering a more sustainable and environmentally friendly energy sector. The use of lignocellulosic biomass for biofuels contributes to mitigating greenhouse gas emissions. Biofuels derived from biomass result in lower net carbon emissions when compared to traditional fossil fuels, aiding in the fight against climate change and reducing the overall environmental impact. Ongoing advancements in technology have improved the efficiency and cost-effectiveness of converting lignocellulosic biomass into biofuels. Innovations in biochemical and thermochemical processes have made it increasingly feasible to extract sugars and convert them into

biofuels like ethanol or biodiesel. Lignocellulosic biomass exhibits versatility in terms of feedstock options. Different types of biomasses can be utilized based on regional availability, climate conditions, and specific energy needs, providing flexibility in adapting biofuel production to diverse geographical and environmental contexts [64, 65]. In summary, the importance of lignocellulosic biomass for biofuels production lies in its renewable nature, environmental benefits, waste utilization, and its role in contributing to energy security and economic development. As technology continues to advance, lignocellulosic biomass is likely to play an increasingly significant role in shaping the future of sustainable bioenergy.

4.1.2.2.1.1. Pretreatment of lignocellulosic biomass

The production of biohydrogen from lignocellulosic biomass involves a series of steps aimed at breaking down the complex structure of biomass and extracting hydrogen gas. Here is an overview of the general process for biohydrogen production from lignocellulosic biomass.

The primary goal of pretreatment is to break down the complex structures present in lignocellulosic biomass. This includes the breakdown of lignin, cellulose, and hemicellulose to make these components more accessible for subsequent steps in the biohydrogen production process. The advantages of pretreatment can be highlighted as follows enhanced accessibility, increased enzymatic digestibility, and reduced inhibitors [66, 67].

Various pretreatment methods, including physical, chemical, physicochemical, and biological approaches, have been employed to reduce lignin content and enhance the availability of pentose and hexose sugars in lignocellulosic biomass [68, 69].

Physical pretreatment methods, such as milling (to decrease particle size), atmospheric and high-pressure microwave treatment, extrusion, and ultrasonication, have been utilized for biomass pretreatment [69].

Chemical methods, such as alkaline and acid hydrolysis, as well as organosolvent processes, have been explored by various research groups.

Alkaline hydrolysis pretreatment involves the use of substances like sodium hydroxide, calcium, potassium, and ammonium. These processes modify the lignin structure by breaking down ester and glycosidic side chains, resulting in swelling and decrystallization of cellulose. Additionally, they eliminate acetyl and various uronic acid substitutions on hemicelluloses, enhancing enzyme accessibility [70].

The acid hydrolysis pretreatment method involves the use of both organic and inorganic acids, including formic acid, maleic acid, sulfuric acid, hydrochloric acid, and phosphoric acid. Dilute acid hydrolysis has been demonstrated to induce swelling of biomass, leading to the formation of porous and distorted fibrils, as well as the development of exposed zones or hollow regions with pores. This process disrupts the structural connections between xylan and lignin. After pretreatment, the crystallinity index of biomass solids increases, indicating the exposure of the cellulose portion due to

the elimination of amorphous materials like lignin and xylan. As a result, the internal surface area becomes readily accessible to enzymes following acid pretreatment, facilitating the generation of more fermentable sugars [71].

Physicochemical pretreatment involves both physical and chemical transformations during the processing of lignocellulosic materials. The commonly utilized methods for such pretreatment include steam explosion (SE), ammonia fiber explosion (AFEX), liquid hot water (LHW), and supercritical fluid (SCF).

Steam explosion: This approach employs high-pressure saturated steam, leading to explosive decompression [72].

Ammonia fiber explosion: In this process, lignocellulosic material undergoes treatment with liquid ammonia at elevated temperatures and pressures ranging from 0.7 to 2.7 MPa. The conditions, coupled with the presence of ammonia, induce biomass structure swelling, resulting in increased specific surface area, hemicellulose solubilization, and alterations to the lignin structure [73].

Liquid hot water: Another physicochemical pretreatment method, it utilizes water at elevated temperatures and pressures for treating lignocellulosic material. This technique is environmentally friendly, as it does not involve the use of chemical catalysts [74].

Supercritical fluid: This technology is regarded as a promising alternative for lignocellulosic pretreatment. The elevated temperature and pressure of the fluid in a supercritical state enhance reaction performance by improving solvent penetration through enlarged fiber pores and defects [75].

Biological pretreatment approaches involve employing bacteria, fungi, and complete enzymes, such as lignin peroxidase, laccases, cellobiose dehydrogenase, and manganese peroxidase, capable of breaking down lignin. These enzymatic agents for degradation are categorized into lignin-degrading auxiliary enzymes (LDA) and lignin-modifying enzymes (LME) [76, 77]. Table 2 provided a summary of the methods of lignocellulose processing, along with the benefits and drawbacks of each method.

Table 2. **Summary of advantages and disadvantages of lignocellulose processing methods**

Methods of pretreatment	Advantages	Disadvantages
Physical		
Milling	Reduces particle size, increasing surface area Improves enzyme accessibility	Energy-intensive High operational costs
Atmospheric and High-Pressure Microwave Treatment	Rapid heating and disruption of lignocellulosic structure Enhances enzyme digestibility	High energy consumption Potential uneven heating
Extrusion	Continuous process Effective in breaking down lignocellulose structure	High energy requirement Equipment wears and tear
Ultrasonication	Cavitation effects improve enzyme penetration Can be combined with other pretreatments	Limited penetration depth Requires high power ultrasound devices
Chemical		
Acid pretreatment	High efficiency in hemicellulose removal Increases cellulose accessibility	Corrosive and hazardous chemicals Requires neutralization and handling of acid waste
Alkaline pretreatment	Effective in lignin removal Mild operational conditions	Long reaction times Generation of waste that needs disposal
Organosolvent pretreatment	Efficient lignin removal Solvents can be recycled	High cost of solvents Requires recovery and recycling of solvents
Biological		
Fungal pretreatment	Low energy requirement Environmentally friendly	Slow process Requires controlled conditions for microbial growth
Enzymatic pretreatment	Highly specific and efficient Mild operational conditions	High cost of enzymes Requires extensive optimization for different biomass types
Physico-chemical		
Steam explosion (SE)	Efficient in disrupting lignin structure Enhances enzyme digestibility	Requires high pressure and temperature Possible loss of hemicellulose
Ammonia fiber explosion (AFEX)	Effective in increasing enzyme accessibility No significant production of inhibitors	High ammonia recovery cost Requires high pressure
Liquid hot water (LHW)	Effective hemicellulose removal Does not produce toxic by-products	High water usage Requires subsequent drying steps
Supercritical fluid (SCF)	Efficient solubilization and fractionation of biomass Can operate at lower temperatures compared to traditional methods	High cost of equipment and operation Requires handling of supercritical fluids

4.1.1.2.1.2. Fermentation in biohydrogen production

Fermentation is a fundamental step in the biohydrogen production process, where sugars liberated from hydrolysis are converted into biohydrogen by specific microorganisms. The process of generating biohydrogen from lignocellulose can be categorized into three main groups: dark fermentation, photo fermentation, and the integration of dark and photo fermentation [78].

Dark fermentation

During dark fermentation, both obligate and facultative anaerobic bacteria such as Clostridium species convert sugars within lignocellulose biomass into hydrogen, carbon dioxide, and organic acids in the absence of light and oxygen. The efficiency of dark fermentation is significantly influenced by biomass pre-treatment, involving microorganisms, and sugar content [79]. The occurrence of a negative free energy in the reaction (Eq.1) signifies that the process proceeds spontaneously toward product formation without the need for external energy [80].

Eq.1. $C_6H_{12}O_6 + 2H_2O \rightarrow 2CH_3COOH + 2CO_2\uparrow + 4H_2\uparrow$ ($\Delta G° = -206$ KJ)

Photo fermentation

In photo fermentation, certain anoxygenic photosynthetic bacteria, particularly purple nonsulfur (PNS) bacteria, utilize light energy and oxidative power from the oxidation of low molecular weight organic compounds to convert hydrogen ions into hydrogen gas. Purple bacteria (photoheterotrophs) decompose organic acids in the presence of light to produce hydrogen and carbon dioxide (Eq.2) [81].

Eq.2. $CH_3COOH + 2H_2O + \text{light energy} \rightarrow 4H_2\uparrow + 2CO_2\uparrow$

Integrated dark and photo fermentation

Due to the relatively low efficiency of dark fermentation in hydrogen production, where only a portion of the substrate is converted and the effluent contains volatile fatty acids, purification is necessary before release into the environment. Alternatively, these effluents can be utilized in the photo fermentation process by PNS bacteria for hydrogen production. The integration of these two processes results in the production of 12 moles of hydrogen from each mole of glucose according to Eq.3 [82, 83]. Fig. 8. shows the biohydrogen production process by integrated dark and photo fermentation.

Eq.3. $C_6H_{12}O_6 + 6H_2O \rightarrow 12H_2 + 6CO_2$

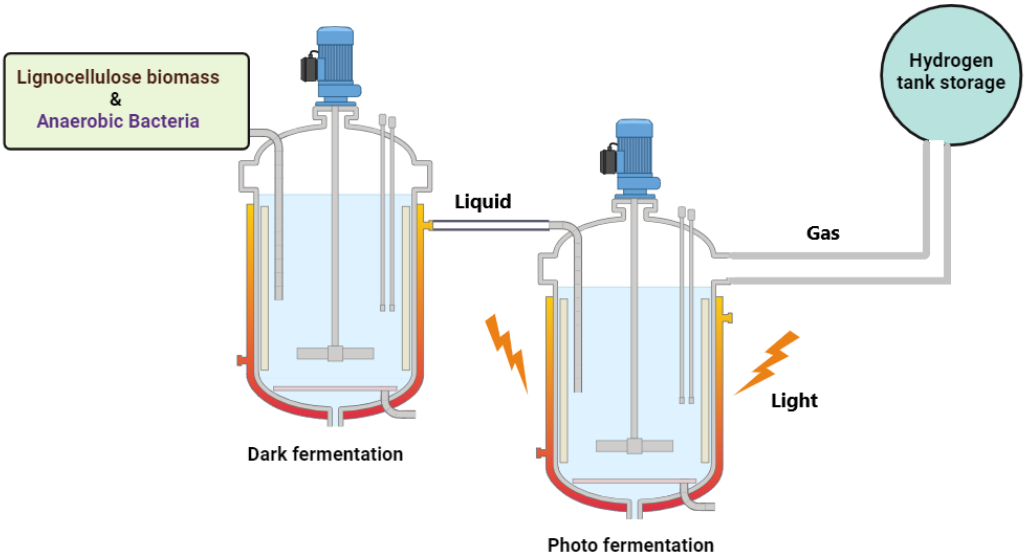

Fig. 8. Schematic of biohydrogen production by integrated dark and photo fermentation

4.1.2.2.1.3. Inhibitors of the fermentation process

As mentioned earlier, in the realm of lignocellulosic biomass hydrolysis and biohydrogen production, diverse inhibitors generated as byproducts during the decomposition of complex organic materials. These compounds can adversely affect the quality and quantity of the end product in both liquid and gaseous phases. Moreover, they may exhibit toxicity towards microorganisms involved in subsequent fermentation processes. Their detrimental effects encompass inhibiting cell growth, diminishing the efficiency of gaseous and liquid biofuel production, causing DNA damage, and impeding various enzymes crucial in glycolysis. These factors collectively contribute to a reduction in the yield of the final product in both liquid and gaseous phases [84]. Conversely, their toxicity extends to living organisms, disrupting ecosystems and posing a threat to human health, especially when the secondary derivative products are introduced into the environment [85, 86]. Furthermore, in accordance with the OECD 303a procedure [87], these chemicals exhibit non-biodegradability, implying their persistence in the environment for an extended period, thereby exacerbating their impact. Phenolic compounds, including Syringaldehyde, vanillin, and guaiacol, are released during the decomposition of lignin, a complex polymer in lignocellulosic biomass. These compounds have the potential to display toxic and inhibitory effects on fermenting microorganisms, impacting their metabolic activity and overall efficiency. Furfural (FF) and 5-Hydroxymethylfurfural (HMF) are formed through the dehydration of sugars (pentoses and hexoses) in acid-catalyzed hydrolysis. Both FF and HMF can disrupt cellular processes, acting as stressors for fermenting microorganisms. Formic acid and acetic acid are byproducts of hemicellulose hydrolysis, with formic acid also formed during sugar breakdown. These acids can reduce the pH of the fermentation broth, creating acidic conditions detrimental to microbial activity. Aliphatic acids, such as Levulinic Acid, result from the breakdown of sugars and other organic components during

hydrolysis. Elevated concentrations of aliphatic acids, including levulinic acid, can inhibit microbial fermentation. Lignin derivatives, such as syringyl lignin derivatives and vanillyl lignin derivatives, are released during lignin breakdown and can act as inhibitors, impacting the performance of fermenting microorganisms [88].

4.1.2.2.1.4. Methods of removing inhibitory compounds from hydrolysis of lignocellulosic biomass

The efficiency of bioconversion may be impacted by inhibitory compounds generated during pre-treatment, necessitating processing the broth primarily composed of hydrolysates for detoxification if required. Different lignocellulosic hydrolysates exhibit varying degrees of inhibition, and the tolerance of microorganisms to inhibition also varies. The selection of detoxification methods is contingent on the source of lignocellulosic hydrolysate and the microorganisms employed, leading to the categorization of detoxification methods into three groups: physical, physicochemical, and biological [89].

Classification based on chemical structures results in four groups of inhibitory compounds. Firstly, substances produced by hemicelluloses, such as acetic acid, serving as the source of xylan deacetylation. Secondly, compounds originating from lignin degradation, including phenolic compounds and other aromatic compounds. Thirdly, materials derived from the breakdown of pentoses [furan derivatives, FF) and hexoses (5-HMF). Lastly, metals leached from inorganic pollutants and/or equipment (copper, chromium, nickel, and iron). Individually or synergistically, these compounds can impact the physiology of fermenting microorganisms during bioconversion. Thus, it becomes imperative to remove or reduce the concentration of these compounds to enhance efficiency in the microbial fermentation process of biomass hydrolysates [90].

The management of post-fermentation broths is crucial, particularly considering that these broths may harbor not only the products of microbial metabolism but also remnants of the microbes involved in the bioconversion process. Consequently, the methods for purifying broths before and after fermentation are identical, and the relevant concepts are illustrated in Fig. 9. The advantages and disadvantages of each method are provided in table 3.

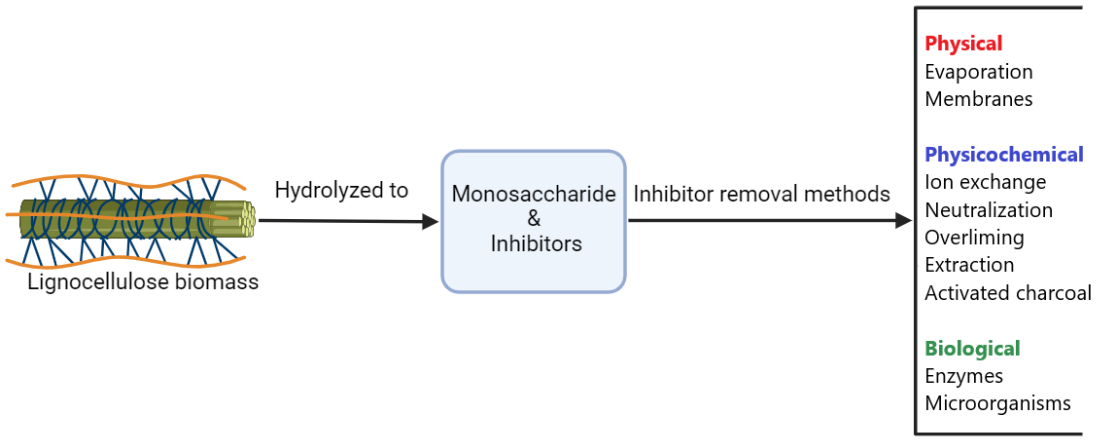

Fig. 9. Lignocellulose biomass detoxification methods for hydrolyzed broth

Physical methods

Evaporation

The evaporation process proves effective in eliminating toxic inhibitory compounds such as acetic acid, furfural, and vanillin. However, a drawback of this method is the potential increase in non-volatile toxic compounds, such as extractives [89]. Evaporation is particularly applicable for purifying post-fermentation broths, where elevated temperatures can impact the microbial structures in the broth. Increased temperature induces protein denaturation, facilitating the removal of proteins and microbial remnants from the post-fermentation broth, especially when combined with centrifugation and sediment separation.

Membranes

The membrane process serves as a detoxification method by preventing the mixing of the aqueous phase (hydrolysate) with the toxic organic phase (solvents), which can be harmful to microorganisms [91]. Each membrane features surface functional groups capable of removing inhibitory compounds, including acetic acid, 5-HMF, FF, formic acid, levulinic acid, and sulfuric acid, from hydrolysate solutions [92].

Physicochemical

Ion exchange

Ion exchange resins prove to be one of the most effective detoxification methods. This process efficiently removes inhibitory compounds from lignocellulose hydrolysis, including lignin, acetic acid, and furfural, thereby enhancing the fermentation process's efficiency [90]. An advantage of this method is the recoverability and reusability of the resins without compromising detoxification efficiency. However, drawbacks include an increased high-pressure drop across the bed during operation,

extended processing time due to slow pore diffusion, potential degradation of fragile biological product molecules, and the loss of a significant amount of fermentable sugars post-process [93].

Neutralization

Given the low pH after acid hydrolysis pretreatment, the pH neutralization process approximates fermentation conditions. In this method, inhibitory compounds (phenol and furfural) are removed through precipitation using chemical compounds like calcium hydroxide and sodium hydroxide. However, the calcium hydroxide neutralization method produces $CaSO_4$ precipitates that must be separated from the environment in the subsequent centrifugation step, posing potential challenges in the fermentation process [94].

Over liming

Reported as one of the most widely used detoxification methods, the $CaSO_4$ process is employed to raise the pH of acidic hydrolysis and subsequently lower it to the desired pH for fermentation. During the pH increase, toxic, inhibitory, and unstable compounds precipitate, particularly furan compounds. This method exhibits high efficiency in removing these compounds and is economically desirable [95, 96].

Activated charcoal

Activated charcoal is a cost-effective and efficient detoxification method widely utilized. This method primarily removes phenolic compounds without causing substantial changes in fermentable sugar levels. Key factors for enhancing this process include the ratio of activated carbon to hydrolysates, pH, temperature, and contact time [90, 97].

Extraction

Solvent extraction emerges as an efficient method for removing highly available toxic inhibitory compounds such as acetic acid, furfural, vanillin, hydroxybenzoic acid, and low molecular weight phenolics. Common solvents in this process include ethyl acetate, chloroform, and trichloroethylene [98].

Biological

Biological methods involve the use of specific enzymes and microorganisms to either eliminate or alter the composition of inhibitory compounds [89]. This approach offers several advantages, including reduced waste production, the potential for detoxification within the fermentation vessel, environmental friendliness, fewer side reactions, and lower energy requirements [99].

Despite these advantages, biological methods typically entail longer processing times. Enzymes such as laccase and peroxidase, derived from white-rot fungi, are employed to eliminate phenolic compounds from lignocellulose hydrolysates. The primary detoxification mechanism of these enzymes may involve the oxidative polymerization of low molecular weight phenolic compounds. White

rot fungi can be utilized in both pre-treatment and broth management steps, catalyzing the oxidation of alternative phenols, anilines, and aromatic thiols [100, 101]. However, enzymatic detoxification has drawbacks, including extended incubation times and high costs. Nevertheless, the method's advantage lies in its operation under mild environmental conditions, such as neutral pH and mesophilic temperature [102].

Microorganisms, such as yeasts, fungi, and bacteria, can absorb inhibitory and toxic compounds. Certain microorganisms release cellulose and hemicellulose during incubation, selectively decomposing lignin. This approach generates a lignocellulosic substrate capable of rapidly decomposing fermentable sugars under mild conditions [100, 102].

Table 3**. Summarizing the advantages and disadvantages of various inhibitor removal methods**

Detoxification method	Advantages	Disadvantages
Physical		
Evaporation	Simple and straightforward No chemical additives required	Energy-intensive Potential loss of volatile compounds
Membranes	High efficiency in separation No need for chemicals Can be specific to target inhibitors	High operational costs Membrane fouling and limited lifespan Requires pretreatment of feed
Physicochemical		
Ion exchange resins	High specificity and efficiency Regenerable Can handle large volumes	High cost of resins Requires periodic regeneration Disposal of spent resins
Neutralization	Simple and cost-effective Rapid process	Can produce large amounts of sludge Possible secondary contamination
Overlining	Cost-effective Effective for some inhibitors	May introduce excess salts Requires careful control of pH
Activated charcoal	High adsorption capacity Effective for a wide range of inhibitors	High cost of activated charcoal Requires periodic replacement or regeneration
Extraction	Can be highly selective Suitable for a wide range of inhibitors	Solvent recovery and disposal issues High operational and capital costs
Biological		
Enzymes	High specificity Can work under mild conditions Environmentally friendly	High cost of enzymes Enzyme denaturation and inhibition Limited availability of specific enzymes
Microorganisms	Cost-effective Can degrade a wide range of inhibitors Environmentally friendly	Requires controlled conditions Slow process compared to physical/chemical methods Potential for by-product formation

5. GREEN SOLVENTS

Green solvents are solvents that are usually obtained from renewable sources and are environmentally safe and sustainable. Among their most important features are low toxicity, biodegradability, and minimal impact on human health and the environment. Green solvents are designed to replace conventional and often dangerous solvents in order to reduce pollution and increase safety in industrial processes. Green solvents include ionic liquids, deep eutectic solvents [81], supercritical fluids, and bio-based solvents, all of which offer specific advantages in terms of sustainability and efficiency [103].

5.1. Liquid-liquid extraction (LLE)

To date, various methods, including chemical, physical, and biological approaches [91, 104-107], have been employed for the detoxification of biomass hydrolysates, as mentioned in Table 3. The majority of these techniques are intricate, expensive, time-consuming, generate by-products, and may result in the loss of sugars [104]. Among these technologies, liquid-liquid extraction (LLE) Fig. 10 stands out as one of the most appealing processes due to its simplicity, low energy usage, high production capacity, fast operation, and the potential for almost complete removal of fermentation inhibitors from hydrolysates [108, 109]

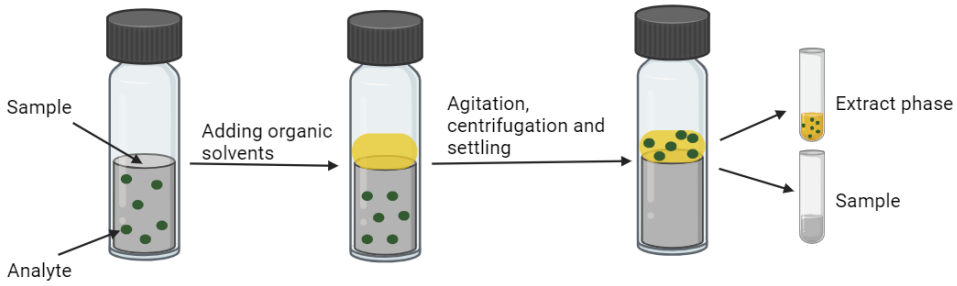

Fig. 10. The procedure of liquid-liquid extraction

The efficacy of the extraction process significantly depends on the choice of the extraction solvent. Ideal extraction solvents should exhibit a strong affinity for inhibitor compounds, low solubility, high stability in the aqueous phase, low viscosity, cost-effectiveness, non-toxicity, and should not dissolve sugars. Various commonly used extraction solvents include ethyl acetate, isobutyl acetate [110], octanol, isopropyl acetate, toluene [111], o-xylene, m-xylene, and ethylbenzene [112]. Despite the effectiveness of these solvents in extraction, their recovery is often challenging, requiring expensive and energy-intensive solvent recovery units. Additionally, many of these solvents are toxic. Hence, extensive research is focused on finding alternative extraction agents.

5.1.1. Deep eutectic solvents (DES)

In recent times, a novel category of "green solvents," known as deep eutectic solvents [81], has gained attention due to their physicochemical properties resembling ionic liquids, lower toxicity, cost-effective synthesis, and increased biodegradability. DESs are blends of two or more compounds capable of forming eutectic liquids through specific interactions between hydrogen bond donor (HBD) and hydrogen bond acceptor (HBA). Thus far, DESs have been successfully utilized in various applications such as fuel desulfurization [113], lignin removal from biomass [114], sample preparation [115-117], water treatment [118], carbon dioxide capture [119], biogas purification [120, 121], and as an electrolyte medium for solar cells [122], among others.

5.1.1.1. Classification of DES

DES are typically classified based on the nature of their components and the type of interactions involved in their formation. The most common types of them include [123, 124]:

Type I DES: These are composed of quaternary ammonium salts, such as choline chloride, combined with metal salts, often aluminum or zinc chloride. This combination results in a eutectic system with unique coordination chemistry, making them suitable for various chemical reactions and processes.

Type II DES: These consist of quaternary ammonium salts mixed with metal chlorides. Unlike type I, these DES are non-coordinating, which gives them distinct properties such as higher stability and different solvent capabilities.

Type III DES: This subclass involves quaternary ammonium salts combined with hydrogen bond donors like urea, carboxylic acids, or alcohols. The most well-known example of this type is the mixture of choline chloride and urea, which has been widely studied for its applications in biomass processing and chemical synthesis due to its favorable solvent properties.

Type IV DES: This category includes DES formed by mixing metal salts with hydrogen bond donors, excluding quaternary ammonium salts. These solvents have been less explored but show promise in specific catalytic and separation processes due to the unique metal-ligand interactions they provide.

Type V DES: These involve complexation between non-ionic species, such as molecular organic compounds, which form a eutectic mixture. This type is gaining interest for their potential in specialized extraction and separation processes, where traditional ionic solvents might not be effective.

Natural DES (NADES): Are composed of naturally occurring components such as sugars, amino acids, and organic acids. They are of particular interest due to their biocompatibility and potential applications in pharmaceuticals, food, and cosmetics. While traditional DESs are categorized into Types I-V based on their components and interactions, the classification of NADES remains a subject

of debate, and it is not yet clear whether they should be assigned to Type V, Type VI, or considered a separate category. Their natural origin, however, distinguishes them from synthetic DESs and contributes to their enhanced biocompatibility and environmental benefits.

5.1.1.2. New class of DES

Recently, scientists have developed a new class of DES. This new class includes DESs with additional capabilities or tailored properties, such as hydrophobicity, magnetism, or thermal stability.

Hydrophobic deep eutectic solvents (HDESs) have emerged as a novel solvent class with outstanding features, including low toxicity, high selectivity, and impressive solubility for various organic compounds [125, 126]. These solvents have proven effective in the extraction and separation of diverse organic compounds, such as phenols, alcohols, and aldehydes [115, 127]. Moreover, they show promise in removing inhibitor compounds from hydrolyzed broths after hydrolysis [108].

Hydrophobic magnetic deep eutectic solvents (HMDESs) represent a distinct type of superhydrophobic deep eutectic solvents that have gained increasing attention. These solvents combine the properties of super hydrophobicity and magnetism, achieved by incorporating magnetic nanoparticles (MNPs) into a mixture of two or more eutectic components [128]. The introduction of MNPs not only imparts magnetic characteristics but also enhances the hydrophobic nature of the solvent, resulting in superhydrophobic behavior. The dual properties of magnetic and hydrophobic behavior make HMDESs versatile for applications like separation, extraction, and catalysis [129-133]. Additionally, HMDESs can be easily separated from the matrix using an external magnet, eliminating the need for centrifugation, filtration, or column packing [134].

Iron oxides, particularly magnetite (Fe_2O_3) and maghemite (g-Fe_3O_4), are commonly employed MNPs due to their ferromagnetic or superparamagnetic properties, small size, high surface area, biocompatibility, and ease of preparation. Among these, Fe_3O_4 MNPs are prevalent for their specific surface area, superparamagnetic properties, straightforward synthesis, and cost-effectiveness. Fig. 11 is shown how HMDES is easily prepared and uncomplicated to make. Despite the commonality of the HDES, it exhibited the ability to efficiently remove phenolic inhibitors without the need for an overly specialized removal reagent, showcasing its versatility and practicality [135].

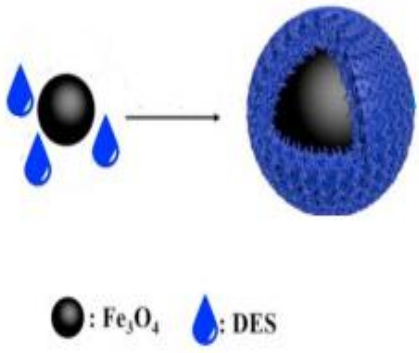

Fig. 11. The formation process of HMDES

5.1.2. Applications of DES in bioprocessing

DES have been extensively studied for their role in various bioprocessing applications, particularly in the pretreatment and fractionation of lignocellulosic biomass. Their ability to dissolve and extract lignin, hemicellulose, and cellulose makes them valuable in the production of biofuels and biochemicals. Furthermore, DES have shown promise in the enzymatic hydrolysis of biomass, where they can improve the accessibility of cellulose to enzymes, thereby enhancing sugar yields [136-139].

5.1.3. Application of DES for removing inhibitor compounds

One of the critical challenges in bioprocessing, especially after the hydrolysis and fermentation of biomass, is the presence of inhibitor compounds such as 5-hydroxymethylfurfural (HMF), furfural (FF), hydroquinone (HQ), and vanillin (VAN). These compounds can significantly hinder microbial growth and fermentation efficiency, thus reducing the overall yield of desired products [54].

Recent studies have explored the use of hydrophobic deep eutectic solvents (HMDES) as a solution for the selective removal of these inhibitory compounds from fermentation broths. HMDES are a subclass of DES characterized by their low polarity and hydrophobic nature, which makes them particularly suitable for extracting hydrophobic inhibitors from aqueous solutions. The use of HMDES in this context not only helps in detoxifying the broth but also enhances the recovery of valuable compounds from the fermentation process [140].

Other DES types, depending on their composition and properties, may also be suitable for this application. For instance, DES based on choline chloride and phenolic compounds have shown potential in the extraction of aromatic inhibitors like vanillin due to their strong hydrogen-bonding interactions. Similarly, DES that incorporate organic acids or alcohols may offer effective means of selectively removing inhibitors like HMF and FF [141-145].

5.2. Supramolecular deep eutectic solvents (SUPRADES)

In recent years, the convergence of supramolecular chemistry with the realm of deep eutectic solvents [81] has led to the emergence of a fascinating class of materials known as SUPRADES [146, 147]. These innovative solvents, characterized by their ability to form intricate supramolecular assemblies within the solvent matrix, represent a significant leap forward in the quest for advanced and versatile solvent systems. The integration of supramolecular principles into DESs has unlocked a wealth of possibilities for designing solvent systems with enhanced performance and functionality [148]. By harnessing a myriad of non-covalent interactions such as hydrogen bonding, π-π stacking, host-guest interactions, and electrostatic forces, SUPRADESs offer unique advantages over conventional DESs, including increased solvation power, tunable physicochemical properties, and responsiveness to external stimuli [149, 150].

The unique supramolecular nature of SUPRADESs stems from their unconventional structure, primarily governed by the inclusion of cyclodextrins. Cyclodextrins, a pivotal component in SUPRADESs, are cyclic oligosaccharides derived from the enzymatic degradation of starch. These macrocyclic molecules are characterized by their truncated cone shape, which arises from the arrangement of D-glucopyranose units linked by α-(1-4) bonds. Typically, cyclodextrins occur in three main forms: α-CD (six glycosyl units), β-CD (seven glycosyl units), and γ-CD (eight glycosyl units), each with a varying number of glucopyranose units, resulting in distinct cavity sizes within their structures [151-153].

The remarkable property of cyclodextrins lies in their ability to form inclusion complexes with guest molecules. This property arises from the hydrophilic exterior and relatively hydrophobic cavity of cyclodextrins, which allows them to encapsulate guest molecules of appropriate size and hydrophobicity. In aqueous solutions, cyclodextrins can form inclusion complexes with a wide range of guest molecules, facilitating non-covalent host-guest interactions [154-156].

In SUPRADESs, cyclodextrins serve as the cornerstone of the non-standard structure, dictating the solvent's supramolecular properties. By incorporating cyclodextrins into the solvent matrix, SUPRADESs exhibit enhanced solvation capabilities and responsiveness to external stimuli. The ability of cyclodextrins to form inclusion complexes within SUPRADESs enables tailored interactions with guest molecules, leading to versatile functionalities and applications in diverse fields of science and technology. Thus, cyclodextrins play a crucial role in defining the unique characteristics and potential of SUPRADESs as advanced solvent systems [149].

The application of SUPRADES, or Supramolecular Deep Eutectic Solvents, spans a wide range of fields, each benefiting from the unique properties and functionalities offered by these advanced solvent systems. Through the integration of supramolecular chemistry principles with deep eutectic solvents, SUPRADESs exhibit enhanced solvation capabilities, tunable physicochemical properties, and responsiveness to external stimuli, making them versatile and adaptable to various applications.

SUPRADES, find applications in catalysis [157], extraction [158], absorbent [159], drug delivery [160], and electrochemistry [150].

6. NEW TYPES OF SORBENTS

One of the other potential avenue promising is using Metal-Organic Frameworks (MOFs). MOFs have garnered increased attention in the field of water remediation due to their proven effectiveness [161]. These crystal materials find extensive application as adsorbents for the removal of hazardous substances through adsorption. These materials, characterized as structured crystalline metal clusters with exceptional porosity (>90%), consist of metal-oxide clusters and organic linkers. With an incredibly large surface area (up to 10,000 m^2g^{-1}), MOFs are versatile for various applications, including the adsorption of MPs [162, 163]. The adjustment of pore size, volume, and functionality for specific applications is achievable by altering metal oxides and organic linkers. The properties of MOFs are predominantly influenced by the chosen inorganic and organic nodes, ligands, and their connectivity [164]. Notably, MOFs are easily synthesized and modified, making them highly suitable for water treatment applications. Their stable structures and high adsorption capacity make them effective in removing both inorganic and organic pollutants from water [165]. Furthermore, MOFs exhibit outstanding performance in recycling and large-scale filtration experiments. Therefore, this is attributed to their favorable characteristics, including diverse compositions and structural types, tunable pore size, exceptionally high porosity, substantial surface area, and metal regions with coordinated unsaturation or saturation that allow the regulation of adsorption capabilities [166-171].

6.1. Integration of DES and MOFs

The integration of DES and MOFs represents a promising approach in the field of materials science and chemistry. DES, known for its environmentally friendly characteristics, and MOFs, a class of crystal materials with unique properties, are combined to leverage their individual advantages for specific applications. The integration of DES and MOFs involves combining these two materials to create hybrid structures with enhanced functionalities. This integration aims to capitalize on the synergies between the unique characteristics of DES and the porous structure of MOFs. By functionalizing MOFs with DES, researchers seek to achieve improved adsorption and separation capabilities, higher recovery rates, and enhanced reusability. The integration of DES and MOFs holds promise in various applications, including the removal of inhibitory compounds from hydrolysis reactions in biomass processing. The combination of these materials offers a comprehensive solution for selectively extracting inhibitory compounds, showcasing the potential for advancements in the field of materials science and green chemistry. Ongoing research in this area focuses on refining the integration process and exploring novel applications for DES-MOF hybrid materials [166, 167, 172-174].

7. SUMMARY OF NEW METHODS FOR REMOVING INHIBITORS FROM FERMENTATION BROTH

In the fermentation industry, one of the key challenges is the presence of inhibitory compounds in the fermentation broth, which can hinder microbial activity and reduce the efficiency of the fermentation process. To address this, several innovative methods have been developed to remove these inhibitors effectively. Among these methods, the use of hydrophobic magnetic DES (HMDES), Supramolecular DES (SUPRADES), and Metal-Organic Frameworks combined with pseudo-DES (MOF@ pseudo-DES) has shown great promise.

7.1. Hydrophobic Magnetic DES (HMDES)

DES are a type of solvent created by mixing two or more components, usually a hydrogen bond donor and a hydrogen bond acceptor. They are known for their tunable properties, low toxicity, and ease of preparation. DES have been used to selectively extract inhibitors such as FF, HMF, and phenolic compounds from fermentation broth. Their effectiveness comes from the ability to tailor their polarity and solubility to target specific inhibitors without negatively affecting the desired products in the broth.

7.2. Supramolecular DES (SUPRADES)

SUPRADES are an advanced form of DES that incorporate supramolecular chemistry principles. They are designed to have a more complex structure that allows for the selective capture of specific inhibitors through host-guest interactions. This means that SUPRADES can be customized to have a higher affinity for particular inhibitory compounds, making them even more effective at removing these unwanted substances from fermentation broths. The specificity of SUPRADES makes them a powerful tool in enhancing the efficiency of the fermentation process.

7.3. Metal-Organic Frameworks combined with pseudo-DES (MOF@DES)

MOF@ pseudo-DES represents a hybrid approach that combines the high surface area and tunable pore structure of Metal-Organic Frameworks (MOFs) with the solvent properties of DES. MOFs are porous materials made from metal ions and organic linkers, and they can be engineered to capture and hold specific molecules. When combined with DES, MOF@ pseudo-DES systems provide a dual-function approach where the MOF structure can trap inhibitors while the DES component helps in dissolving and removing these compounds. This hybrid method is particularly effective for dealing with a wide range of inhibitors in complex fermentation broths.

8. THE GOAL OF THE WORK

The main goal of this doctoral dissertation is to develop and evaluate advanced, green, and sustainable extraction methods for removing inhibitory compounds from the fermentation broth derived from lignocellulosic biomass hydrolysates, particularly in the context of biohydrogen production. These inhibitors, such as FF, HMF, HQ and VAN, severely impact microbial activity and hydrogen yield, necessitating efficient and environmentally friendly removal strategies.

To achieve this goal, the following tasks were undertaken:

*Comprehensive literature review on the formation of inhibitors during biomass hydrolysis and their impact on fermentation efficiency.

*Synthesis of novel green solvents, including hydrophobic magnetic deep eutectic solvents (HMDES), SUPRADES, and MOF-based pseudo-DES.

* Physicochemical characterization of the developed systems using techniques such as FTIR, XRD, SEM, BET, and TGA for pseudo-DES@MOF, and density, viscosity, and surface tension measurements for SUPRADES.

*Optimization of extraction conditions for maximum inhibitor removal using statistical models like Plackett-Burman and Box-Behnken designs.

*Comparison of performance between the proposed green solvents and conventional methods in terms of efficiency, selectivity, and reusability.

*Application of the optimized systems to real fermentation broths to validate performance under practical conditions.

*Evaluation of biohydrogen production improvement after detoxification, confirming the positive impact of inhibitor removal on microbial hydrogen generation.

9. MATERIALS AND METHODS

In this study, a comprehensive analytical approach was employed, integrating chromatographic, spectroscopic, microscopic, and thermal analysis techniques to characterize the synthesized materials. These methodologies were systematically selected to assess their chemical composition, structural integrity, morphological features, surface properties, and thermal stability, providing a detailed insight into their physicochemical behavior and potential applications. The following sections outline the specific instruments and methodologies utilized in this investigation.

9.1. Apparatus

9.1.1. High-performance liquid chromatography (HPLC)

To analyze phenolic inhibitors chromatographically, a Merck Hitachi HPLC system from Germany, equipped with a diode array detector (Beckman Coulter, model DAD 166, USA), was utilized. The HPLC system featured an analytical column with C18 packing material, measuring 250 mm × 4.6 mm with a particle size of 3 µm. Prior to analysis, the samples were prepared by filtration through a syringe filter containing a 0.22 µm Nylon membrane to ensure removal of any particulate matter that could interfere with the chromatographic process or damage the column. Following filtration, 30 µL of the liquid sample was injected into the HPLC system for analysis. The mobile phase used for the chromatographic separation consisted of a mixture of water, methanol, and acetonitrile in the ratio of 88:4:8 v/v%. The separation was carried out under isocratic conditions, meaning the composition of the mobile phase remained constant throughout the run. The flow rate of the mobile phase was set at 0.6 $mL.min^{-1}$. Detection of the phenolic inhibitors was performed using the diode array detector set to an analytical wavelength of 284 nm, which is suitable for identifying phenolic compounds based on their absorbance characteristics. Throughout the analysis, the column temperature was maintained at room temperature to ensure consistent performance and reproducibility of the chromatographic results. HPLC analysis was conducted for all detoxification methods investigated in this study, including HMDES, SUPRADES, and MOF@pseudo-DES. The chromatographic parameters such as mobile phase composition, flow rate, detection wavelength, and column specifications were kept constant throughout all analyses to ensure comparability and consistency in evaluating the phenolic inhibitor concentrations.

9.1.2. Fourier-transform infrared spectroscopy (FT-IR)

FT-IR characterizations of the surface functional groups of metal-organic frameworks (MOFs) and MOF-deep eutectic solvent (MOF-DES) nanomaterials were conducted using a Thermo Scientific Nicolet iS50 FTIR Spectrometer.

Molecules within the sample absorb specific wavelengths of the IR light, causing vibrations that are characteristic of the bonds and functional groups present in the material. The Nicolet iS50 FTIR Spectrometer uses a Fourier transform to convert the raw data into an IR spectrum, which is a plot of absorbance (or transmittance) versus wavelength (or wavenumber).

The FT-IR spectra for the MOF and MOF-DES nanomaterials were collected at room temperature, ensuring that the thermal environment did not affect the vibrational states of the molecules. The analysis was performed over a wavelength range of 650-4000 cm^{-1}. This range is broad and encompasses the most significant vibrational modes for organic and inorganic materials, including:

4000-2500 cm^{-1}: Stretching vibrations of N-H, O-H, and C-H bonds.

2500-2000 cm^{-1}: Triple bond regions (C≡C and C≡N).

2000-1500 cm^{-1}: Double bond regions (C=C, C=O, and C=N).

1500-650 cm^{-1}: Fingerprint region, which is highly specific to the molecular structure and is used for identifying different functional groups and molecular configurations.

The Thermo Scientific Nicolet iS50 FTIR Spectrometer provides high spectral resolution (better than 0.09 cm^{-1}) and broad infrared coverage (from 4000 to 400 cm^{-1} in the mid-IR region, extendable to the near-IR and far-IR with additional modules), allowing for precise identification of even subtle changes in the chemical structure of the materials. This information is crucial for understanding the interactions between the MOF and the DES, the stability of the functional groups, and the overall properties of the nanomaterials.

9.1.3. Powder X-ray diffraction (PXRD)

PXRD data were collected using a MiniFlex 600 Benchtop X-ray diffractometer, which is a compact and versatile instrument suitable for a wide range of applications in materials science and chemistry. This diffractometer was equipped with a copper (Cu) Kα radiation source, which emits X-rays with a wavelength of 0.154 nm. This specific wavelength is commonly used in X-ray diffraction due to its suitability for investigating crystal structures.

In the PXRD analysis, the powdered sample is exposed to the X-ray beam. As the X-rays interact with the crystal lattice of the material, they are diffracted in various directions. By measuring the angles and intensities of these diffracted beams, one can obtain information about the atomic structure of the sample. The diffractometer records this information as a diffraction pattern, which is essentially a plot of the intensity of the diffracted X-rays versus the diffraction angle (2θ).

The diffraction data were collected over a range of 2θ angles from 2° to 40°. This range is selected to cover the most significant diffraction peaks that provide valuable information about the crystal structure. The step size, or the increment at which data points are collected, was set at 1° per

minute. This means that the diffractometer measured the intensity of the diffracted X-rays at every degree within the selected range, ensuring a detailed and high-resolution diffraction pattern.

In this study, PXRD analysis was specifically performed to characterize the structure of NH_2-UiO-66@pseudo-DES, which was employed as one of the novel sorbents for removing fermentation inhibitors from lignocellulosic hydrolysates.

9.1.4. Field-emission scanning electron microscopy (FE-SEM)

FE-SEM was employed to investigate the morphology of the produced powders using an FEI Quanta FEG 250 scanning electron microscope. This advanced imaging technique provides high-resolution and high-magnification images of the sample surface, allowing for detailed analysis of the material's microstructure.

The FEI Quanta FEG 250 is a versatile and powerful SEM equipped with a field emission gun, making it suitable for a wide range of applications in materials science, nanotechnology, and other fields. It allows for both high-vacuum and low-vacuum operations, accommodating different types of samples, including non-conductive materials without the need for extensive preparation. The FEI Quanta FEG 250 is coupled with an energy dispersive X-ray spectroscope (EDX), specifically the EDAX Genesis APEX 2i. EDX is a complementary technique used alongside FE-SEM to provide elemental composition analysis of the sample.

The sample is placed in the FE-SEM chamber, and the electron beam is focused on the sample surface. Secondary electron images are collected to reveal the morphology. For elemental analysis, the electron beam is directed at specific areas of interest on the sample. The EDX detector captures the emitted X-rays and generates an elemental spectrum. The application of FE-SEM with the FEI Quanta FEG 250, coupled with EDX, provides a powerful toolset for investigating the morphology and elemental composition of the produced powders.

In this work, FE-SEM and EDX analyses were specifically conducted to characterize the surface morphology and elemental distribution of the MOF@pseudo-DES composite, one of the developed materials for removing fermentation inhibitors from lignocellulosic hydrolysates.

9.1.5. Brunauer-Emmett-Teller (BET)

BET method was employed to determine the specific surface area and pore sizes of the samples using a Micromeritics Gemini V200 Shimadzu analyzer. This method is widely used for characterizing the surface area and porosity of materials, providing critical information about their textural properties. The BET method is based on the physical adsorption of gas molecules on the surface of a material. It extends the Langmuir adsorption theory to multilayer adsorption, which is more representative of the actual adsorption process in porous materials.

The sample is degassed to remove any adsorbed contaminants, such as moisture or organic residues, which might affect the accuracy of the measurements. Then the prepared sample is exposed to nitrogen gas at liquid nitrogen temperature (-196 °C). The amount of gas adsorbed on the surface of the sample is measured at different relative pressures. Adsorption data are collected over the relative pressure range of 0.05-0.3. This range is chosen because it includes the linear portion of the BET plot, which is critical for accurate surface area determination. The adsorption data are plotted according to the BET equation, resulting in a linear plot from which the specific surface area can be calculated.

The BET equation is given by:

$$\frac{1}{W\left(\frac{p}{p_0}\right)-1} = \frac{C}{W_m C} \times \frac{\mathrm{p}}{p_0} + \frac{1}{W_m C} \quad \text{(Eq.4)}$$

where:

W is the amount of gas adsorbed at a relative pressure $\frac{p}{p_0}$

Wm is the amount of gas required to form a monolayer on the surface

C is the BET constant, related to the energy of adsorption

By plotting $\frac{1}{W\left(\frac{p}{p_0}\right)-1}$ against $\frac{p}{p_0}$, a straight line is obtained. From the slope and intercept of this line, Wm and C can be determined, and consequently, the specific surface area S can be calculated using:

$$S = \frac{W_m \times N_A \sigma}{M}$$

(Eq.5)

where:

NA is Avogadro's number

σ is the cross-sectional area of the adsorbate molecule (for nitrogen, typically 0.162 nm^2)

M is the molar volume of the adsorbate gas.

In this study, the BET analysis was performed specifically on the NH_2-UiO-66@pseudo-DES composite to assess its surface area and porosity, which are essential characteristics influencing its performance as a sorbent for removing fermentation inhibitors from lignocellulosic hydrolysates.

9.1.6. Thermogravimetric analysis (TGA)

TGA was utilized to investigate the thermal stabilities of the samples using a Mettler Toledo TGA2 instrument. This analytical technique measures the change in mass of a sample as it is heated, providing valuable information about its thermal stability, composition, and decomposition behavior.

In this procedure a small amount of the sample (typically a few milligrams) was placed in a crucible on the balance inside the TGA instrument. The sample was heated from room temperature to 800 °C at a controlled rate of 10 °C per minute. The nitrogen atmosphere ensures an inert environment, preventing reactions such as oxidation. As the temperature increases, the instrument continuously was measured the mass of the sample. The data collected include the mass of the sample as a function of temperature and time.

The primary output of TGA is a thermogravimetric curve, which plots the sample mass (y-axis) against temperature or time (x-axis). This curve shows the mass loss at various temperatures, indicating decomposition, volatilization, or other thermal events. The derivative thermogravimetry (DTG) curve is derived from the TGA data and represents the rate of mass loss (dm/dt) as a function of temperature. Peaks in the DTG curve correspond to the temperatures at which the most significant mass loss rates occur, providing more precise information about thermal events.

The Mettler Toledo TGA2 instrument is supported by STARe Software, which facilitates the analysis and interpretation of TGA data. The software allows for the generation of both TGA and DTG curves, providing a comprehensive understanding of the thermal behavior of the sample.

The software assists in identifying key thermal events, calculating the onset and endset temperatures of decomposition phases, and quantifying the mass loss associated with each phase.

The thermogravimetric analysis using the Mettler Toledo TGA2 instrument provides detailed information about the thermal stability and composition of materials. The use of a nitrogen atmosphere prevents unwanted reactions, ensuring accurate measurement of thermal decomposition. The combination of TGA and DTG curves, facilitated by STARe Software, enables precise analysis of mass loss rates and decomposition stages, contributing to a thorough understanding of the material's thermal properties.

In this study, TGA was specifically applied to evaluate the thermal decomposition behavior of the MOF@pseudo-DES composite, developed as an innovative sorbent for removing fermentation inhibitors from biomass hydrolysates.

9.1.7. Gas Chromatography-Thermal Conductivity Detector and Flame Ionization Detector (GC-TCD-FID)

GC-TCD-FID was employed to perform quantitative and qualitative analysis of the gaseous products generated during dark fermentation. This analytical technique was chosen due to its high sensitivity and selectivity in identifying and quantifying gaseous components such as hydrogen (H_2), carbon dioxide (CO_2), methane (CH_4), and other volatile organic compounds. The GC-TCD-FID system was operated under optimized conditions to ensure accurate and reproducible measurements. The GC oven temperature program was set as follows: initially maintained at 50°C for 6 minutes, followed by a temperature ramp of 10°C min^{-1} up to 180°C, held for 10 minutes, and then further ramped at 5°C min-

^{1} to reach a final temperature of 200°C, maintained for an additional 10 minutes. This stepwise temperature gradient allowed for the efficient separation of gaseous components with different volatilities. For detection, two independent detectors were utilized. The flame ionization detector (FID) was primarily used for hydrocarbon-based gases, ensuring high sensitivity in detecting methane and other organic compounds. The FID was operated at 220°C, with hydrogen and air supplied at flow rates of 45 mL min^{-1} and 450 mL min^{-1}, respectively. The thermal conductivity detector (TCD) was employed for non-hydrocarbon gases, including hydrogen and carbon dioxide. The TCD was maintained at 180°C, with argon as the carrier gas at a flow rate of 20 mL min^{-1}, ensuring reliable thermal conductivity-based detection. The injection port temperature was set at 100°C to facilitate sample vaporization and efficient introduction into the chromatographic column. Each sample was injected with a fixed volume of 500 µL to maintain consistency across measurements. The integration of TCD and FID detection provided a comprehensive analysis of both hydrocarbon and non-hydrocarbon gaseous fermentation products, ensuring precise quantification and identification. The optimized GC conditions allowed for a high-resolution separation of dark fermentation gaseous products, facilitating a detailed understanding of the metabolic pathways and gas composition in the fermentation process.

This technique was specifically applied to evaluate biohydrogen production before and after the application of SUPRADES, one of the developed sorbents for removing fermentation inhibitors from lignocellulosic hydrolysates. The aim was to assess the impact of detoxification on hydrogen yield and gas composition.

9.2. Methods

9.2.1. Preparation of HMDES

A hydrophobic deep eutectic solvent (HDES) was synthesized by combining menthol as a hydrogen bond acceptor (HBA) and nonanoic acid as a hydrogen bond donor (HBD) in a 2:1 molar ratio. The blend was vigorously stirred at 800 rpm for 30 minutes until it transformed into a clear liquid. Subsequently, 25 g of magnetite nanoparticles (Fe_3O_4-NP) were introduced into 100 g of the HDES and subjected to sonication for around 30 minutes, leading to the creation of a stable ferrofluid [175]. Figure 12 illustrates the diagram of HMDES preparation.

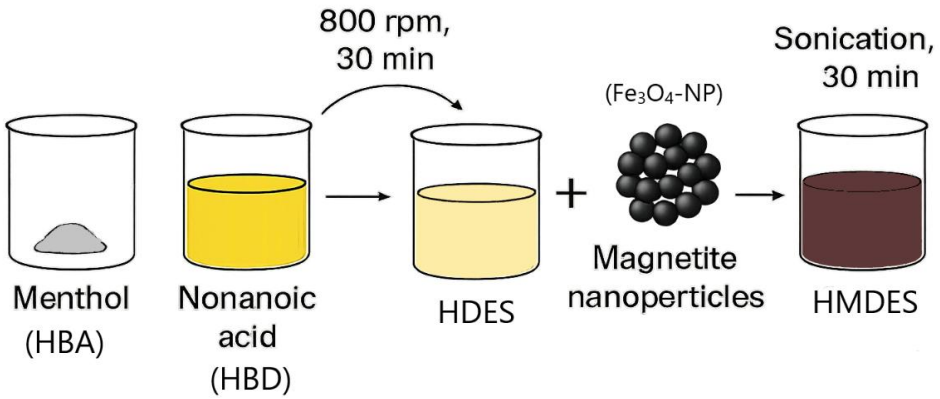

Fig. 12. Schematic of preparation of HMDES.

9.2.2. Synthesis of NH_2-UiO-66@pseudo-DES

The synthesis of NH_2-UiO-66 was carried out following the methodology outlined by Li et al. [176], with some modifications. Initially, 1.7 mmol of zirconium tetrachloride ($ZrCl_4$) was dissolved in 50 mL of dimethylformamide (DMF) within a 250 mL glass container. The solution was stirred at a temperature of 50-60°C for 10 minutes. Next, an equimolar amount (1.7 mmol) of 2-amino terephthalic acid was introduced into the reaction medium, and stirring continued for another 10 minutes. The resulting mixture was then subjected to thermal treatment at 120°C for 24 hours in an oven. After completion of the reaction, the system was allowed to cool naturally to ambient temperature, and the precipitated solid was recovered via filtration. The collected material was subsequently rinsed twice with DMF, followed by four washes with ethanol. To ensure complete drying, the product was subjected to vacuum drying at 90°C for three hours, yielding $Zr_6O_4(OH)_4$(benzene-1,4-dicarboxylate (terephthalate)-$NH_2)_6$.

To eliminate residual guest molecules, the obtained MOF was immersed in ethanol three times, each cycle utilizing 10 mL of solvent. The material was then separated by decantation, and the resulting powder underwent overnight heating at 150°C under vacuum to remove any remaining solvent and moisture.

For the preparation of NH_2-UiO-66@pseudo-DES, a modified version of the method described by Akbarian et al. [177] was employed. In this approach, 50 mg of the synthesized MOF and 31 mg of choline chloride (ChCl) were mixed in a test tube and subjected to continuous magnetic stirring at 80°C for four hours. Upon completion of this process, the reaction mixture was cooled to ambient temperature, leading to the formation of a dark yellow solid. Figure 13 shows the schematic representation of the NH_2-UiO-66@pseudo-DES synthesis process.

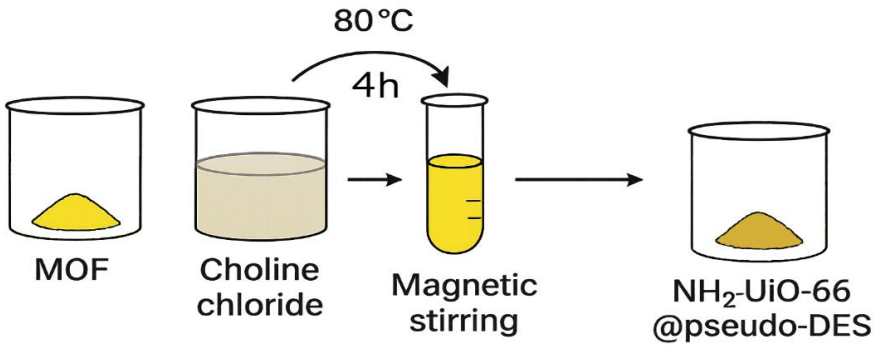

Fig. 13. Preparation scheme of NH_2-UiO-66@pseudo-DES

To confirm the structural and physicochemical characteristics of the synthesized NH_2-UiO-66@pseudo-DES, a series of analytical techniques were employed, including FTIR, PXRD, FE-SEM, BET, and TGA.

9.2.3. Preparation of SUPRADES

A hydrophobic deep eutectic solvent (HDES) was synthesized by combining menthol, serving as the HBA, with nonanoic acid, acting as the HBD, in a molar ratio of 2:1. The components were thoroughly mixed and subjected to stirring at 800 rpm for 30 minutes to ensure complete homogenization. Following this, a precisely measured quantity of methyl β-cyclodextrin (MβCD) was introduced into the HDES. The resulting mixture was continuously stirred at 80 ℃ for a duration of 3 hours to facilitate the dissolution and incorporation of MβCD, ultimately yielding a solutions with a CD concentration of 5-10% (by mass) within the HDES system [158]. Figure 14 depicts the step-by-step procedure for preparing SUPRADES.

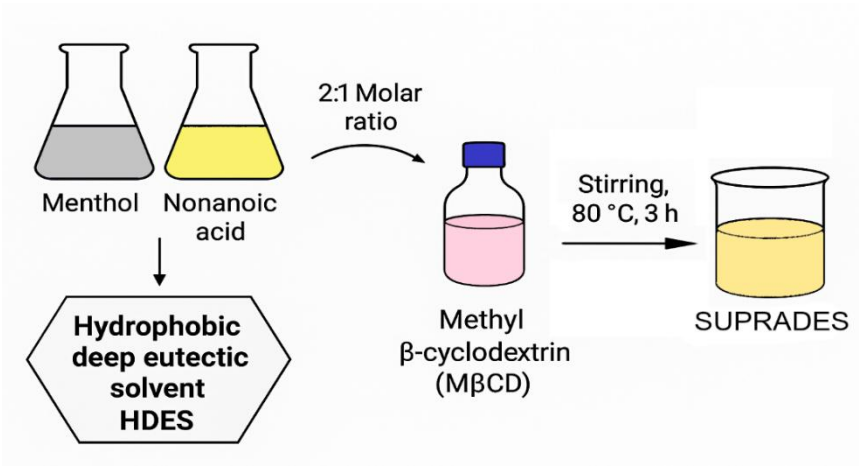

Fig. 14. Synthesis pathway of SUPRADES

9.2.4. Real sample preparation for removing inhibitor compounds by HMDES and NH_2-UiO-66@pseudo-DES

To evaluate the performance of HMDES and NH_2-UiO-66@pseudo-DES under realistic process conditions, a wide range of real biomass-derived samples was prepared and analyzed. These included hydrolysates obtained from a hardwood blend (comprising beech, energetic willow, and poplar), starch and lignocellulose-rich residues from potato processing, and leachates from composted biomass were first dried in a laboratory oven at 105°C for approximately 2-3 days. Depending on the sample type, some materials were used directly, while others underwent additional chemical pre-treatment.

For the hydrolysis-based samples, 3.0 g of dried biomass was treated with 20 mL of sulfuric acid (5% or 30%), sodium hydroxide (0.5 M or 1.5 M), or hydrogen peroxide (5% or 30%) to facilitate lignocellulosic breakdown and sugar release. Reactions were carried out in sealed containers at 60 °C with agitation (100 rpm) for 40 hours. After hydrolysis, the mixtures were centrifuged to remove solid residues and filtered using 0.45 µm PTFE syringe filters. The clear hydrolysates were stored at -80 °C and subsequently treated with HMDES and NH_2-UiO-66@pseudo-DES to assess the extraction efficiency of inhibitor compounds (HQ, HMF, FF, and VAN).

For fermentation-based samples, lignocellulosic hydrolysates served as substrates for dark, alcoholic, and photo fermentation processes using various microorganisms such as *Klebsiella aerogenes, Pichia stipitis, Saccharomyces cerevisiae, and Rhodospirillum rubrum*. The broths obtained after fermentation were collected, centrifuged, and filtered as described above. These clarified fermentation supernatants were then subjected to sorption using HMDES and NH_2-UiO-66@pseudo-DES to evaluate post-fermentation removal of remaining inhibitor compounds. Comprehensive analytical data on inhibitor concentrations before and after treatment, along with removal efficiencies, are presented in Figs 30, 31 and 39.

9.2.5. Real sample preparation for removing inhibitor compounds by SUPRADES

The biomass consisted of decayed wood fragments and bio-waste previously exposed to rot fungi. To facilitate hydrolysis, the material was treated with a 5% acetic acid solution. The biomass was combined with the acid and subjected to continuous stirring at 100 rpm in a thermoreactor, maintaining a steady temperature of 40°C for five days. Once the hydrolysis process was completed, the mixture underwent filtration using a glass filter funnel flask to separate the liquid phase from solid residues. The filtered solution was then refrigerated at 4°C for preservation. For subsequent analysis, two 200 mL portions of the hydrolyzed solution were extracted and adjusted to the desired pH.

*9.2.**6**. Inoculum preparation*

The inoculum for the dark fermentation process was derived from cryopreserved *Enterobacter aerogenes (ATCC 13048)* and prepared in a nutrient solution containing 20 mL of buffered peptone water, both with and without casein, at a concentration of 29 gL^{-1}. The bacterial culture was incubated under controlled conditions at 37°C with continuous shaking at 100 rpm for 24 hours to promote microbial growth. Prior to introducing the bacterial strain, all samples were subjected to sterilization in an autoclave at 126°C for 11 minutes, ensuring that the internal pressure did not exceed 2 bars. Additionally, the inoculum was used to cultivate bacterial colonies on agar plates, enabling fermentation to be carried out with a single microbial colony. The fermentation experiments, including diagnostics, were conducted using a 100 mL inoculum prepared following the same procedure.

9.2.7. Dark fermentation process

Dark fermentation experiments were carried out using two laboratory-scale bioreactors (1 L working volume), each equipped for anaerobic operation and real-time monitoring. Both systems were fitted with a Pt100 temperature sensor (Endress+Hauser, Germany), digital pH electrode (Mettler Toledo, FiveEasy F20), and dissolved oxygen probe (Eutech Instruments DO 2700). A gas flow meter (Ritter drum-type, Germany) was used to monitor cumulative gas volume, and data were continuously recorded using the Kamush® DAQ system. Stirring was maintained via a magnetic heating stirrer (IKA C-MAG HS 7), and nitrogen gas was flushed for 30 minutes prior to inoculation to ensure anaerobic conditions.

Each bioreactor received 100 mL of Enterobacter aerogenes inoculum, with the growth medium adjusted depending on the experimental cycle. One bioreactor was fed with hydrolysate extracted via 5% acetic acid, while the second used detoxified hydrolysate obtained using SUPRADES. Both media were based on buffered peptone water (29 gL^{-1}), with casein added to the SUPRADES group to support microbial growth.

Fermentation was conducted at 37 °C and pH 5.5, automatically controlled by a peristaltic pump (Ismatec Reglo Digital) for NaOH dosing. The experiment proceeded in three successive cycles, with each new batch seeded using biomass from the previous one. A glucose-only fermentation test served as the control for evaluating the effect of inhibitor removal on hydrogen production.

Dark fermentation experiments were conducted in three consecutive cycles to assess the impact of SUPRADES-treated hydrolysate on hydrogen production, in comparison with untreated hydrolysate and a glucose-based control. Two bioreactors were operated in parallel, each receiving distinct types of feedstocks and hydrolysate across the cycles. Buffered peptone water served as the base medium in all experiments, with casein added to the SUPRADES group to enhance nutrient availability.

In the glucose control test, neither bioreactor received hydrolysate; both were inoculated with freshly cultured *Enterobacter aerogenes* (1-day-old), and differed only in the addition of casein to the second bioreactor. In Cycle 1, the first bioreactor was fed with hydrolysate derived from bio-waste treated with 5% acetic acid, while the second received SUPRADES detoxified hydrolysate. The same bacterial culture and medium composition were used as in the control setup.

In Cycles 2 and 3, the feeding conditions remained unchanged; however, the bacterial inoculum was replaced with adapted cultures aged 8 and 15 days, respectively, obtained from the previous fermentation cycles. This approach enabled the evaluation of microbial adaptation over time.

This setup enabled a comprehensive evaluation of both the immediate and long-term effects of inhibitor removal via SUPRADES on microbial activity and hydrogen production efficiency under semi-continuous operation.

9.2.8. Sorption process by using HMDES

To eliminate inhibitors such as HMF, FF, HQ, and VAN, the pH of 10.0 mL of the sample solutions was adjusted to 8.0. Subsequently, 5.0 mL of HMDES was introduced, and the mixture was stirred at 1200 rpm at room temperature for 15 minutes. Afterward, utilizing an external magnet, the HMDES containing adsorbed analytes was separated from the mixture and discarded. A volume of 30 µL of the remaining solution was then injected into an HPLC to quantify the concentrations of the inhibitors that remained. These results were compared with the initial concentrations, and the removal efficiency (RE) was obtained by Eq.6.

$$\mathrm{RE}\ (\%) = \frac{C_i - C_f}{C_i} \times 100 \qquad \text{(Eq.6)}$$

Here, C_i represents the initial concentration, and C_f denotes the residual concentration of inhibitors both measured (mgL^{-1}) respectively.

The distribution ratio (K) was calculated using Eq.7:

$$K = \frac{C_{DES}}{C_{hyd}} \qquad \text{(Eq.7)}$$

where C_{DES} denotes the concentration of inhibitor compounds in the DES phase (mgL^{-1}), and C_{hyd} represents the concentration of inhibitor compounds in the hydrolysates after removal (mgL^{-1}).

9.2.9. Sorption process by using NH_2-UiO-66@pseudo-DES

To facilitate the removal of HMF, FF, HQ, and VAN, the pH of 2 mL sample solutions was first adjusted to 4. Afterward, 8 mg of NH_2-UiO-66@pseudo-DES was added to the solution, and the mixture was subjected to vortex agitation for 15 minutes to ensure thorough interaction. Before proceeding with the analysis, the treated samples were passed through a syringe filter equipped with a 0.22 µm Nylon

membrane to eliminate any remaining particulates. Following filtration, a 30 µL of the purified solution was injected into the HPLC system for further examination. The detected concentrations were then compared with the initial values to assess the extent of removal, and the adsorption efficiency was subsequently calculated according to Eq.6.

9.2.10. Sorption process by using SUPRADES

In the initial stage of this study, a Plackett–Burman experimental design was adopted to identify the key variables influencing the extraction efficiency of fermentation inhibitors, specifically HQ, HMF, FF, and VAN, from lignocellulosic biomass hydrolysates. A total of 12 experimental runs were conducted and statistically analyzed using Minitab 20 (Minitab, LLC, USA) to determine the significance of various process parameters.

Seven independent variables were considered in the design. The pH of the aqueous solution was adjusted within the range of 6 to 9, and the concentration of inhibitors varied between 1 and 30 mgL^{-1}. To formulate the SUPRADES phase, the content of methyl-β-cyclodextrin (MβCD) was set between 5% and 10% by weight. Operational parameters were also studied, including stirring speed, ranging from 400 to 1200 rpm, and extraction time, examined at both short (10 min) and extended (60 min) durations. Additionally, the volume of the aqueous sample and the volume of the SUPRADES phase were each varied between 5 and 20 mL to evaluate the impact of phase ratio.

Based on the statistical results, the optimal extraction conditions were identified as follows: a 5 mL aqueous sample containing 30 mgL^{-1} of each target inhibitor at pH 9, extracted with 5 mL of SUPRADES composed of 5 wt% MβCD. The mixture was stirred at 1200 rpm at ambient temperature for 60 minutes. After extraction, the phases were separated via centrifugation at 1000 rpm for 5 minutes, followed by filtration through a 0.22 µm Nylon membrane syringe filter. Subsequently, 30 µL of the clear supernatant was injected into the HPLC system for analysis.

To assess the extraction performance, inhibitor concentrations were determined before and after treatment with SUPRADES. The same procedure was then applied to real biomass hydrolysate samples, and extraction efficiency was calculated using Eq.6.

9.3. Reagents

Menthol (purity ≥ 98%), nonanoic acid (purity ≥ 97%), Choline chloride (ChCl) (purity ≥98%), $ZrCl_4$ (purity ≥99%), 2-aminabenzene-1,4-dicarboxylic acid (purity ≥99%), dimethylformamide (DMF) (purity ≥99%), 2-aminoterephthalic acid (purity ≥99%) acetic acid (purity ≥98%), ethanol (purity ≥98%), HCl (purity ≥38%), and NaOH (purity ≥99%) were obtained from Sigma-Aldrich (MO, USA). methyl-β-cyclodextrin (purity ≥ 98%), 5-Hydroxymethylfurfural (purity ≥99%), furfural (purity ≥99%), hydroquinone (purity ≥99%), and vanillin (purity ≥99%) were purchased from Chemat (Poland). Fe_3O_4 magnetic

nanoparticles (purity ≥99.55%, size 14-29 nm) was supplied by Nanografi Nano Teknoloji A.S. Türkiye (Turkey).

10. RESULTS OF USING HMDES FOR REMOVING INHIBITOR COMPOUNDS

To enhance the sorption efficiency of HMDES for removing fermentation inhibitors, a detailed optimization study was conducted considering multiple operational parameters. This included solution temperature, stirring speed, volume of HMDES, sample volume, pH, initial concentration of inhibitors, and contact time. Each variable was systematically varied across defined ranges to determine its influence on extraction performance.

The temperature of the extraction medium was explored within the range of 15 to 60 °C, with the optimum sorption occurring at 20 °C. Stirring speed was adjusted between 600 and 1500 rpm, with 1200 rpm identified as the most effective for maintaining uniform dispersion. The volume of HMDES added ranged from 1 to 15 mL, and 5 mL was found to be optimal. Likewise, the sample volume was tested between 5 and 30 mL, with 10 mL delivering the best balance between concentration and recovery.

The pH of the solution was varied from 5 to 10, and a pH of 8 maximized the interaction between the sorbent and the target compounds. Inhibitor concentrations were studied in the range of 1-50 mgL^{-1}, with 40 mgL^{-1} yielding the highest removal efficiency without saturation. Finally, contact time was investigated between 5 and 20 minutes, and 15 minutes was identified as sufficient to reach equilibrium.

These optimized conditions provided the foundation for subsequent experiments on real lignocellulosic hydrolysates. The full optimization details were previously reported in Honarmandrad et al., 2024 [140].

10.1. Effect of pH

The influence of pH on the removal efficiency of inhibitors using HMDES was assessed by adjusting the pH of a 40 mgL^{-1} standard solution from 5.0 to 10.0. The results (Fig. 15) showed that the sorption efficiency declined under both strongly acidic and highly alkaline conditions. At low pH, the ionized form of inhibitors reduces their affinity toward non-ionic solvents [178]. Conversely, at pH levels above 8, partial precipitation occurs due to interactions between hydroxide ions and the coordinated metals in HMDES, leading to phase separation and reduced magnetic recovery [141].

The best performance was observed at pH 8.0, where both the stability of the solvent and the balance of interaction forces supported effective extraction.

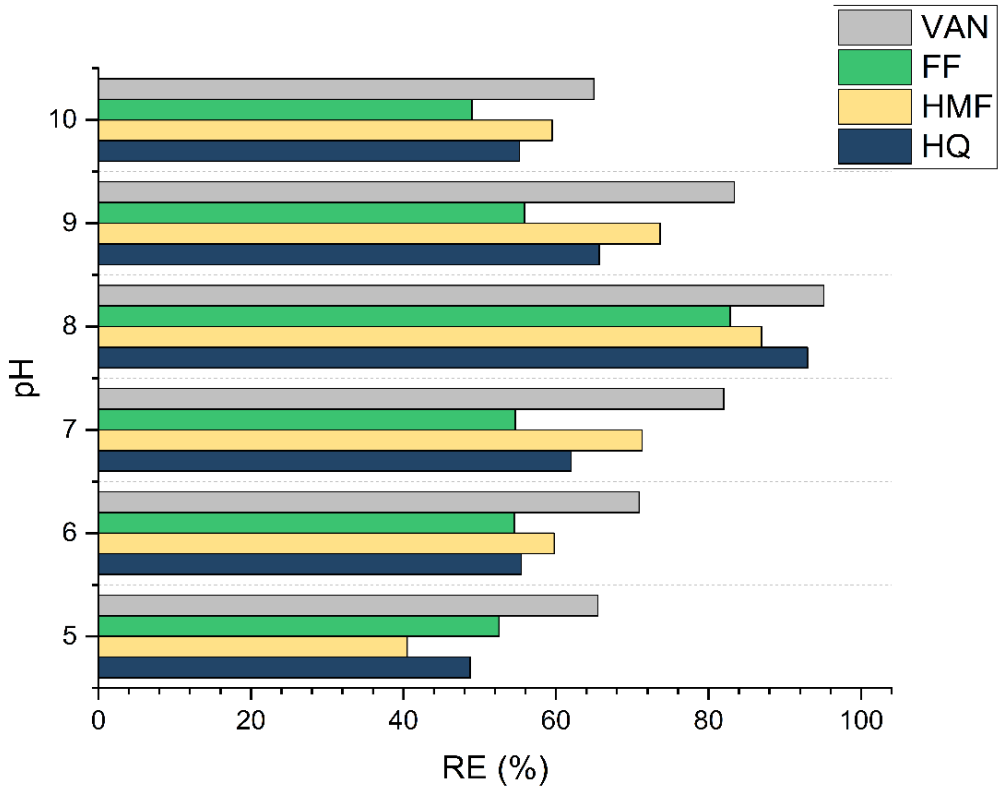

Fig. 15. Impact of pH on the efficiency of inhibitor sorption using HMDES under optimum condition [140].

10.2. Effect of temperature

Temperature notably influences the sorption performance of HMDES by altering its viscosity, phase behavior, and molecular interactions [113, 128]. Experiments conducted across a range of 15-60 °C (Fig. 16) showed that removal efficiency (RE) increased from 15 to 20 °C due to improved mass transfer as viscosity decreased. However, further heating led to a gradual decline in RE, likely caused by weakening of hydrogen bonding and disruption in the balance between HBA and HBD components [126, 179, 180]. Elevated temperatures may also reduce sorption capacity due to the exothermic nature of interactions between HMDES and inhibitors, as explained by Van't Hoff's principle. Additionally, thermal degradation of sugars at high temperatures could negatively affect downstream biohydrogen production [181].

The highest removal efficiencies were achieved at 20 °C, reaching 92.97% for HQ, 86.72% for HMF, 82.86% for FF, and 95.12% for VAN, confirming this temperature as optimal for balancing energy use and sorption effectiveness.

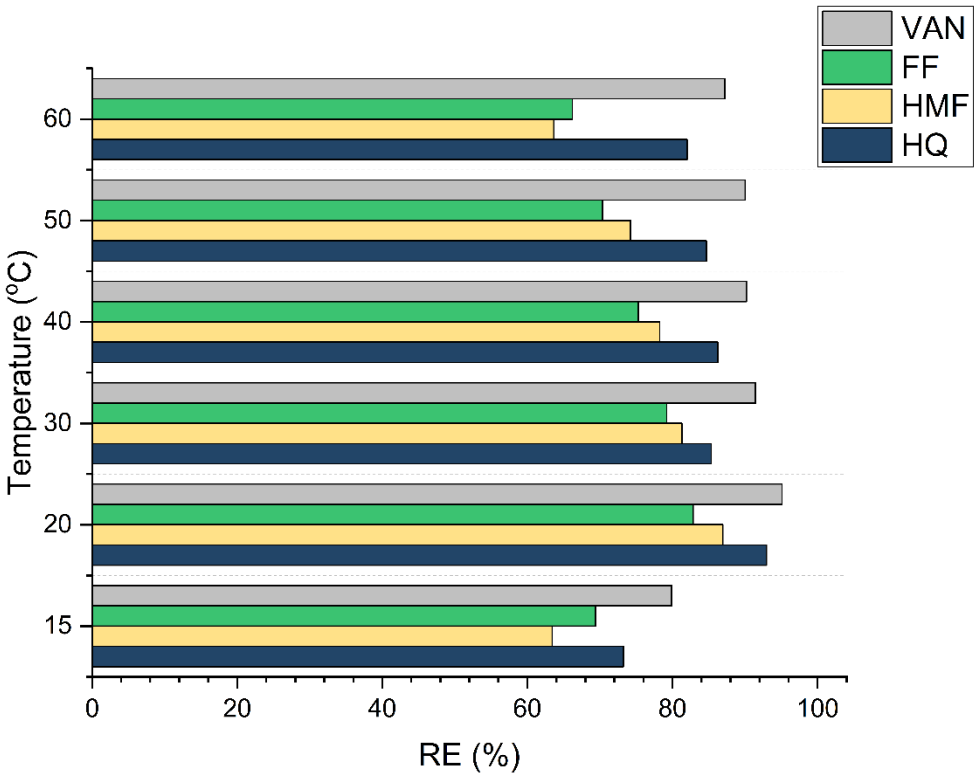

Fig. 16. Impact of temperature on the efficiency of inhibitor sorption using HMDES under optimum condition [140].

10.3. Effect of initial concentration of inhibitors

The influence of initial inhibitor concentration (1-50 mgL^{-1}) on RE is shown in Fig. 17. The results indicate that RE increases with concentration, particularly up to 40 mgL^{-1}. This improvement is attributed to enhanced interactions between HMDES and inhibitors, facilitated by the greater availability of target molecules. At lower concentrations, reduced efficiency is likely due to the dominant role of water-inhibitor interactions, which can hinder access to sorption sites in HMDES [182, 183].

Beyond 40 mgL^{-1}, the RE curve levels off, suggesting that HMDES operates efficiently without reaching saturation. This plateau implies that the active sites are effectively utilized, and further increases in concentration do not significantly impact removal performance [127, 182]. These findings highlight the importance of optimizing initial concentrations to maximize sorption while maintaining system efficiency.

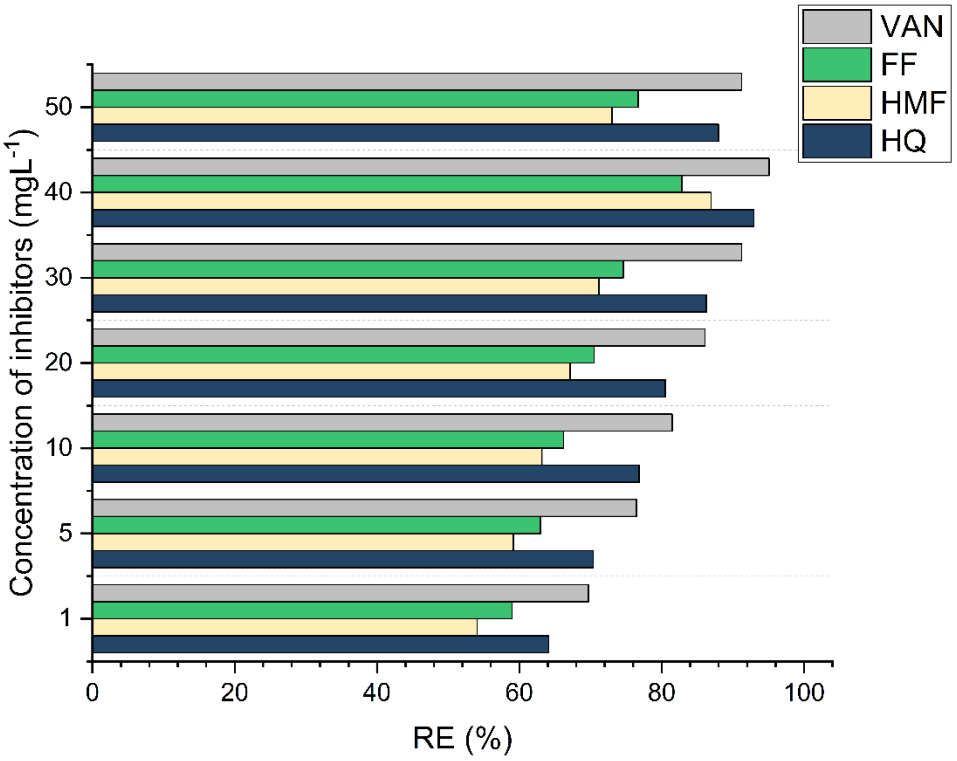

Fig. 17. Impact of concentration of inhibitors on the efficiency of inhibitor sorption using HMDES under optimum condition [140].

10.4. Effect of analyte volume

The effect of analyte volume on inhibitor removal was evaluated over a range of 5 to 30 mL (Fig. 18). Increasing the volume from 5 to 10 mL enhanced the removal efficiency, indicating that the system could accommodate more solution without saturation. At 10 mL, maximum efficiencies were observed for all tested compounds.

Beyond this point, further increases in volume led to a gradual decline in performance, suggesting that the binding capacity of HMDES approached its limit. As a result, not all inhibitors present in larger volumes could be effectively extracted [184]. These findings emphasize the need to balance analyte volume to avoid overloading the sorbent and to maintain high extraction efficiency.

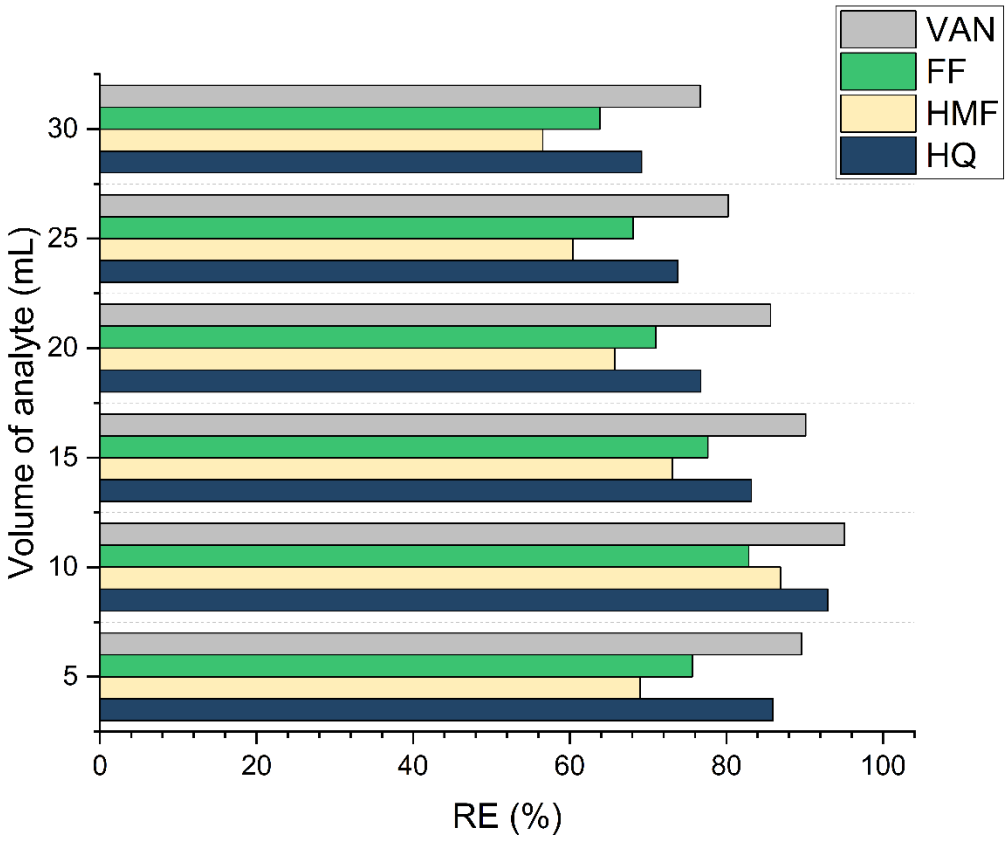

Fig. 18. Impact of volume of analyte on the efficiency of inhibitor sorption using HMDES under optimum condition [140].

10.5. Effect of volume of HMDES

The removal efficiency (RE) of HQ, HMF, FF, and VAN was studied by varying the volume of HMDES between 1 and 15 mL (Fig. 19). Increasing the volume from 1 to 5 mL improved RE, reflecting a greater availability of sorption sites. However, further increases beyond 5 mL led to a slight decline and eventual stabilization of RE, indicating system saturation. At this stage, additional solvent no longer enhanced removal, and in some cases, may have diluted the analyte, slightly reducing performance [108, 185, 186].

From both technical and economic perspectives, 5 mL was identified as the optimal volume. According to Eq.7, partition coefficient (K) values at this condition were calculated as 18.88% (HQ), 29.37% (HMF), 26.3% (FF), and 69.42% (VAN). The observed sorption behavior suggests non-conventional interactions may be involved. To improve efficiency, future strategies might include multi-step extraction using smaller solvent portions instead of a single high-volume extraction step.

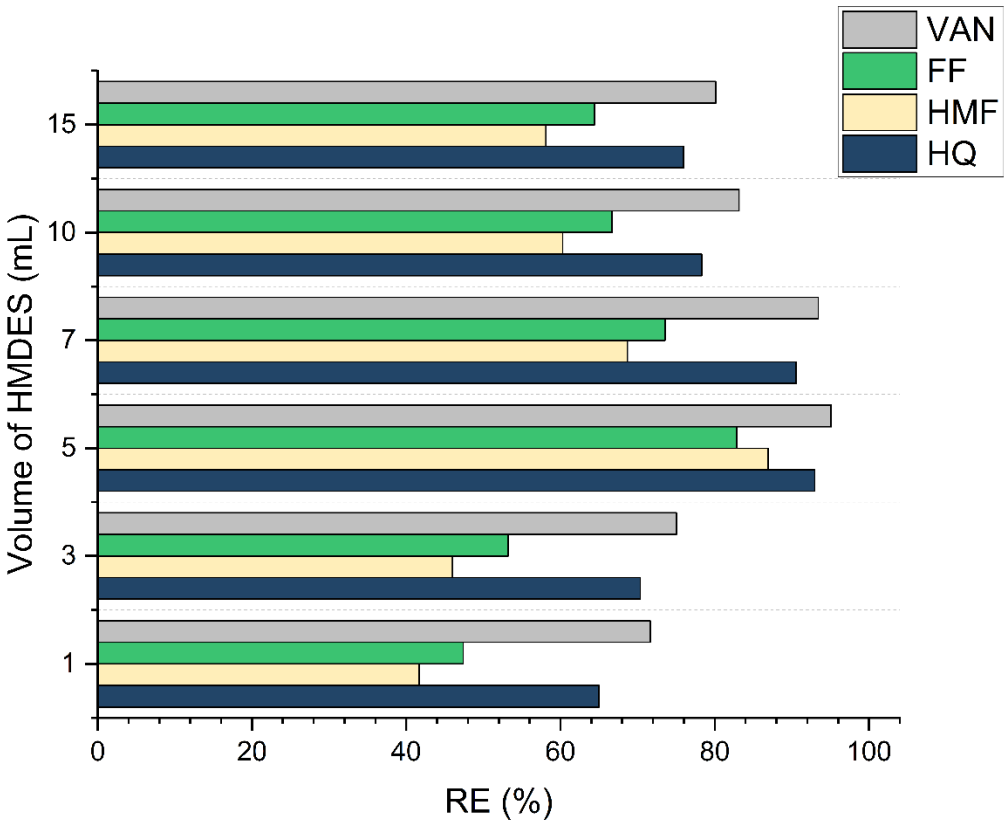

Fig. 19. Impact of volume of HMDES on the efficiency of inhibitor sorption using HMDES under optimum condition [140].

10.6. Effect of stirring speed

The impact of stirring speed (600-1500 rpm) on the efficiency of inhibitor removal using HMDES is shown in Fig. 20. As agitation increased, improved mixing facilitated greater contact between analytes and HMDES, enhancing mass transfer and sorption. The optimal performance was recorded at 1200 rpm, where maximum interaction and uptake occurred. Further increases beyond this speed yielded minimal gains, indicating that the system had reached kinetic equilibrium and additional mixing was no longer beneficial. Therefore, 1200 rpm was selected as the ideal stirring rate, balancing high efficiency with reasonable energy consumption.

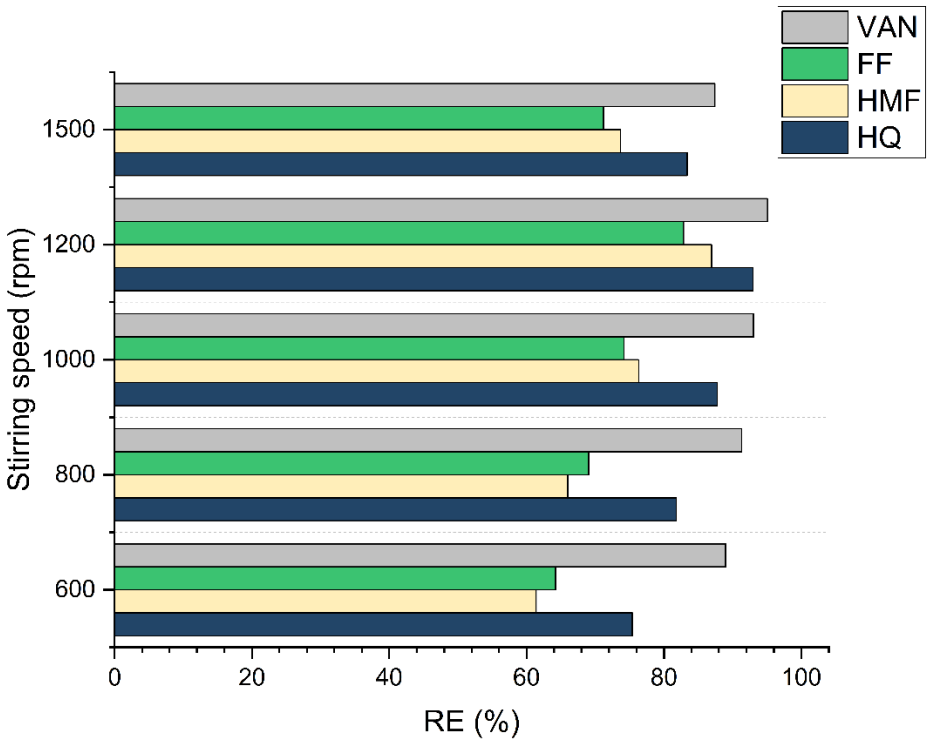

Fig. 20. Impact of stirring speed on the efficiency of inhibitor sorption using HMDES under optimum condition [140].

10.7. Effect of contact time

The duration of contact between HMDES and inhibitor compounds significantly influences removal efficiency. As shown in Fig. 21, RE increased with time, reaching a maximum at 15 minutes indicating sufficient mass transfer and system equilibrium. Shorter durations led to incomplete extraction, likely due to limited analyte diffusion [187]. Extending contact time beyond 15 minutes did not improve RE and caused a slight decline, possibly due to minor structural effects on HMDES during prolonged exposure [180, 186]. Therefore, 15 minutes was selected as the optimal contact time, balancing efficiency, stability, and practicality.

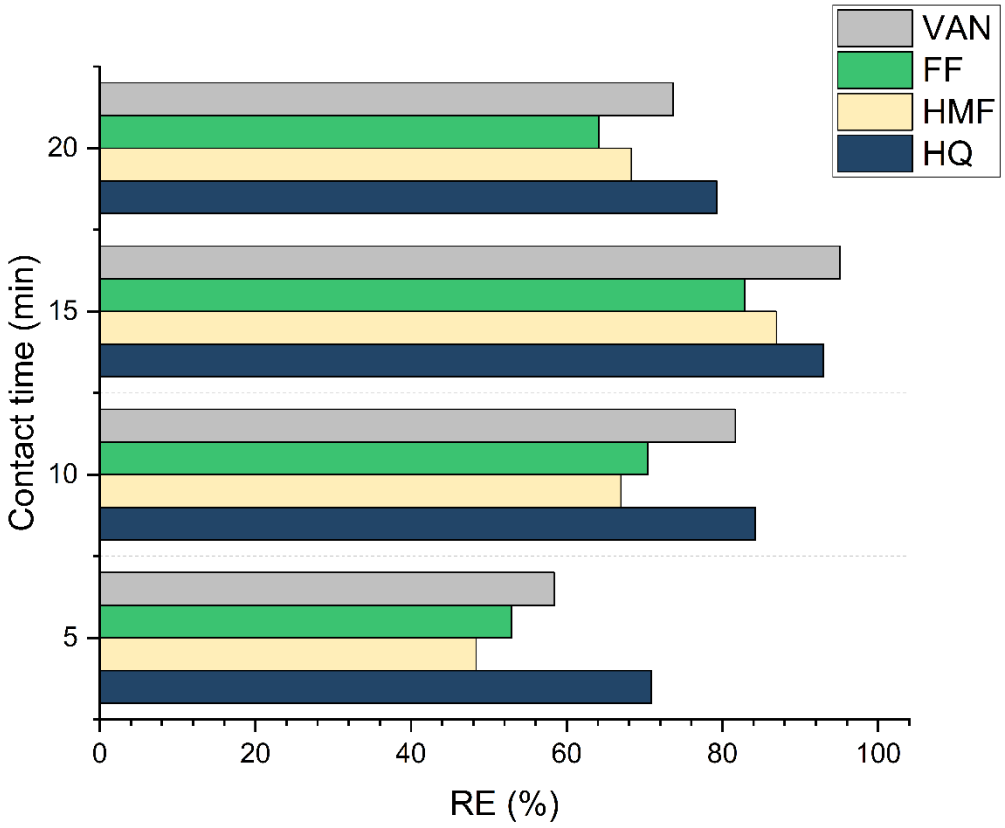

Fig. 21. Impact of contact time on the efficiency of inhibitor sorption using HMDES under optimum condition [140].

10.8. Regeneration and reusability of HMDES

To assess the reusability of HMDES, regeneration tests were performed over 13 consecutive cycles using activated carbon as a purifying agent. After each extraction, HMDES was mixed with activated carbon for 30 minutes, followed by centrifugation and filtration to recover the regenerated phase. FTIR analyses were conducted after selected cycles (3, 5, 7, and 13) to monitor possible structural changes.

Results (Fig. 22) showed minor spectral shifts, primarily in the -OH stretching region, attributed to gradual water uptake. No further shifts were observed beyond the fifth cycle, suggesting structural stabilization. As depicted in Fig. 23, after 13 cycles, RE values for HQ, HMF, FF, and VAN remained above 77%, with minimal loss compared to the fresh solvent.

These findings confirm that HMDES can be efficiently regenerated and reused multiple times without significant degradation in performance, supporting its application as a cost-effective and sustainable extraction medium.

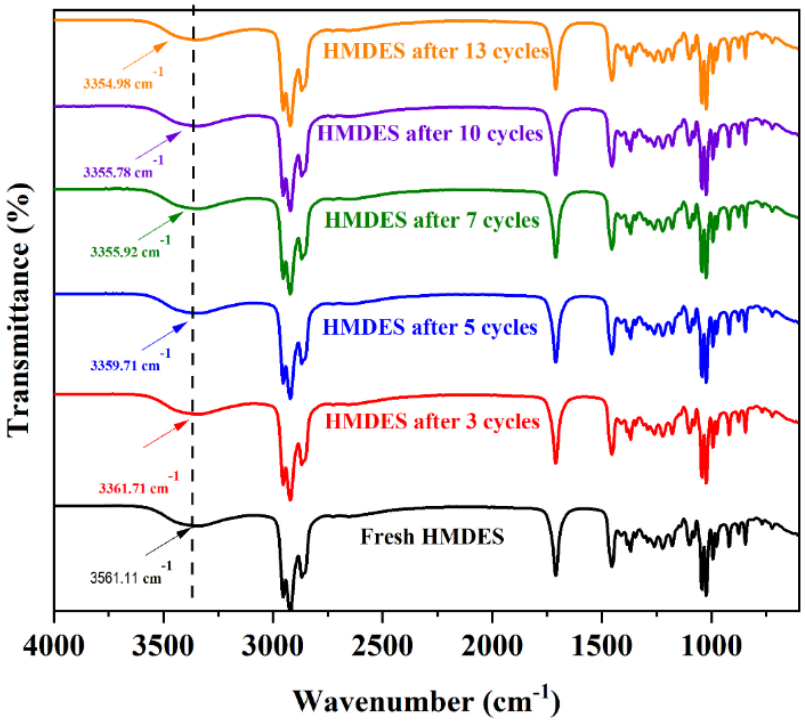

Fig. 22. FT-IR spectra comparison between fresh and regenerated HMDES [140].

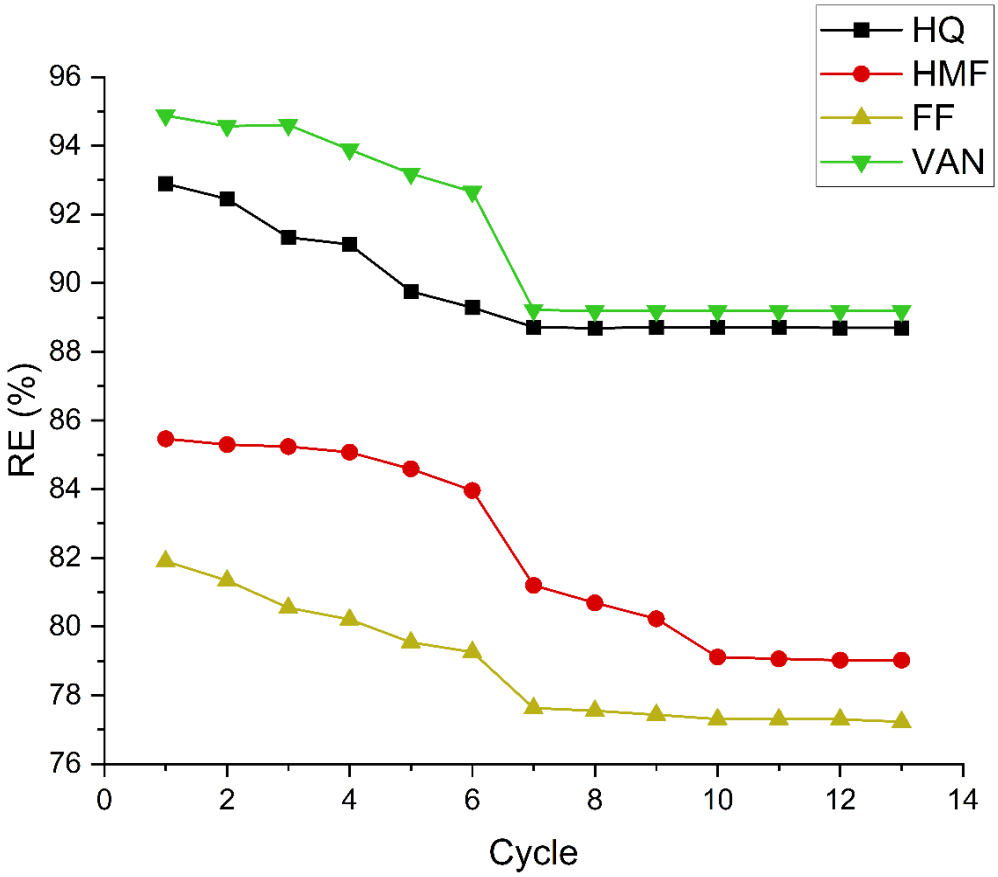

Fig. 23. Effect of multiple regeneration cycles on the removal efficiency of inhibitory compounds [140].

10.9. Structural stability of HMDES under acidic, alkaline, and neutral conditions

To evaluate the robustness of HMDES under diverse chemical environments, its stability was tested by introducing three representative pH-modifying agents: NaOH (alkaline), H_2SO_4 (acidic), and Na_2HPO_4 (neutral), at concentrations of 0.1 M and 1 M. As shown in Fig. 24, the FTIR spectra exhibited only minimal shifts in peak positions compared to those of pristine HMDES, indicating that its structure remains largely unchanged even in varied pH environments.

This observation confirms that HMDES retains its structural integrity across acidic, alkaline, and neutral conditions, which is essential for its versatility in a wide array of chemical and industrial applications. Such stability ensures that HMDES can be reliably deployed in settings like wastewater treatment, chemical processing, and environmental remediation where exposure to differing pH levels is common without compromising its sorption efficiency or necessitating frequent regeneration.

In summary, the demonstrated resilience of HMDES under these conditions supports its utility as a durable and dependable sorbent material, capable of maintaining high performance and cost-effectiveness even under fluctuating or extreme pH scenarios.

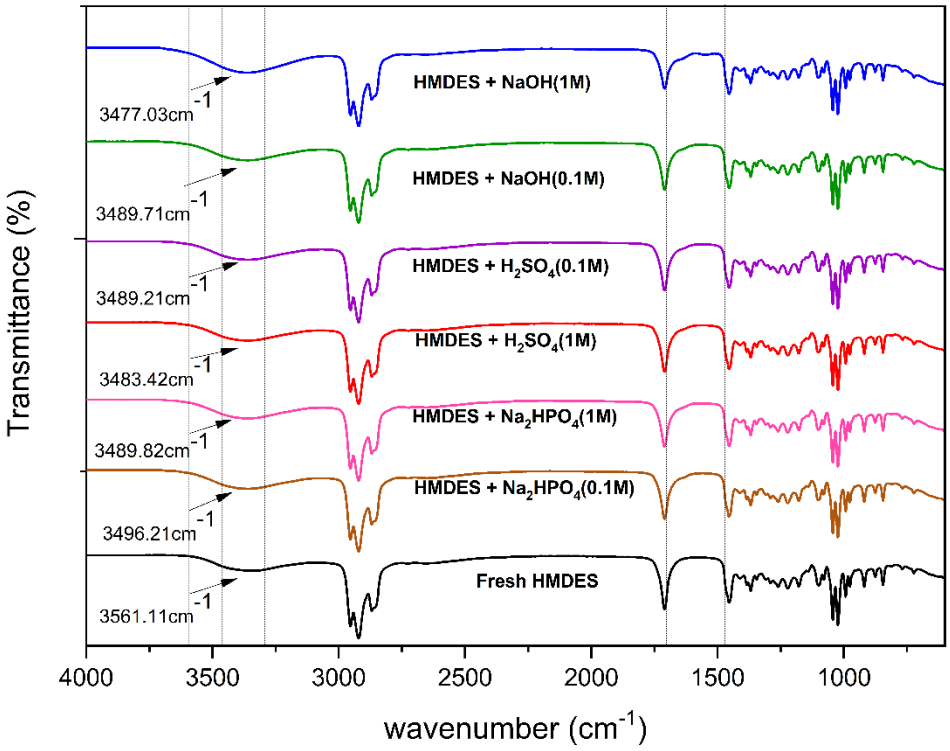

Fig. 24. Effect of pH-modifying agents (NaOH, H_2SO_4, Na_2HPO_4) on the structural stability of HMDES as evaluated by FTIR analysis [140].

10.10. Mechanism of extraction

To gain insights into the extraction mechanism of HMF, FF, HQ, and VAN using HMDES, FTIR spectroscopy was employed to analyze the structural interactions involved in the sorption process. The FTIR spectrum of the Ment:NA@Fe_3O_4 composite was examined, identifying peaks corresponding to key functional groups in HMDES. Upon introducing the inhibitor compounds (HQ, HMF, FF, and VAN), noticeable shifts in spectral bands were observed, indicating structural modifications in HMDES due to interactions with the inhibitors.

As illustrated in Figs. 25-28, the FTIR spectrum of menthol exhibited prominent peaks in the 3398.16-3694.33 cm^{-1} range, corresponding to OH stretching vibrations, which suggest the involvement of hydroxyl groups in hydrogen bonding. Additionally, sharp peaks in the 2939.85-3027.96 cm^{-1} range were associated with CH_3 stretching vibrations. The FTIR spectrum of nonanoic acid revealed distinct peaks indicative of carboxylic acid (COOH) groups, with a strong absorption band in the 1603.30-

1851.99 cm^{-1} range attributed to C=O stretching vibrations. Other notable bands included C-H stretching vibrations (3045.01-2937.01 cm^{-1}) and C-O stretching vibrations (1063.99-1405.05 cm^{-1}).

The functional groups in the inhibitor compounds were found to interact with HMDES functional groups through hydrogen bonding and other intermolecular forces. The carbonyl (C=O) groups present in HMF and FF facilitated hydrogen bonding with the OH group of menthol or the COOH group of nonanoic acid. Similarly, HQ, which contains hydroxyl (OH) groups, could establish hydrogen bonds with the OH or COOH groups in HMDES. In the case of vanillin, both carbonyl (C=O) and hydroxyl (OH) groups enabled multiple interaction modes with HMDES, contributing to its extraction efficiency.

Post-extraction FTIR spectra (Figs. 24-27) revealed a significant shift in the -OH absorption band, which became more intense and shifted to lower wavenumbers following the removal of the inhibitors. Specifically, for HQ, HMF, FF, and VAN, the OH peak shifted from 3561.11 cm^{-1} to 3450.74 cm^{-1}, 3406.95 cm^{-1}, 3470.63 cm^{-1}, and 3561.11 cm^{-1}, respectively. The more pronounced peak shifts observed for HQ and vanillin, compared to HMF and FF, indicate stronger hydrogen bonding interactions between these inhibitors and HMDES, correlating with their higher removal efficiencies.

These results suggest that hydrogen bonding serves as the primary extraction mechanism, facilitating the interaction between the functional groups of the inhibitors and HMDES. The strength of these interactions plays a crucial role in determining the effectiveness of the removal process, where stronger hydrogen bonds lead to higher extraction efficiencies.

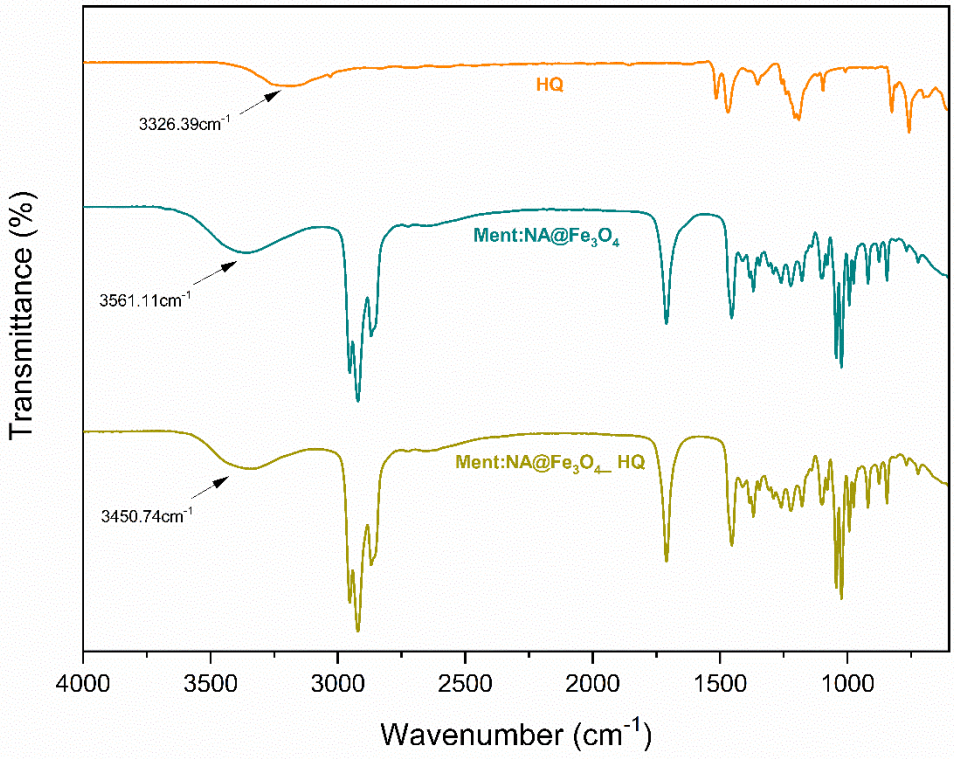

Fig. 25. FT-IR spectra of pure HQ, synthesized Ment:NA@Fe_3O_4 sorbent, and Ment:NA@Fe_3O_4 after HQ adsorption [140].

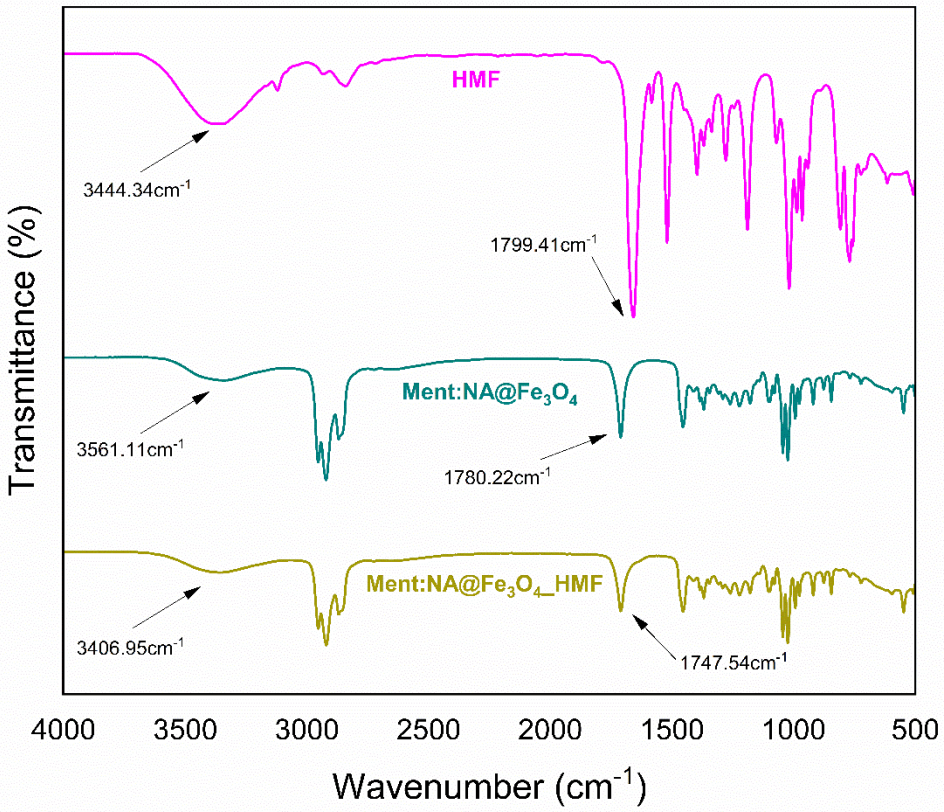

Fig. 26. FT-IR spectra of pure HMF, synthesized Ment:NA@Fe_3O_4 sorbent, and Ment:NA@Fe_3O_4 after HMF adsorption [140].

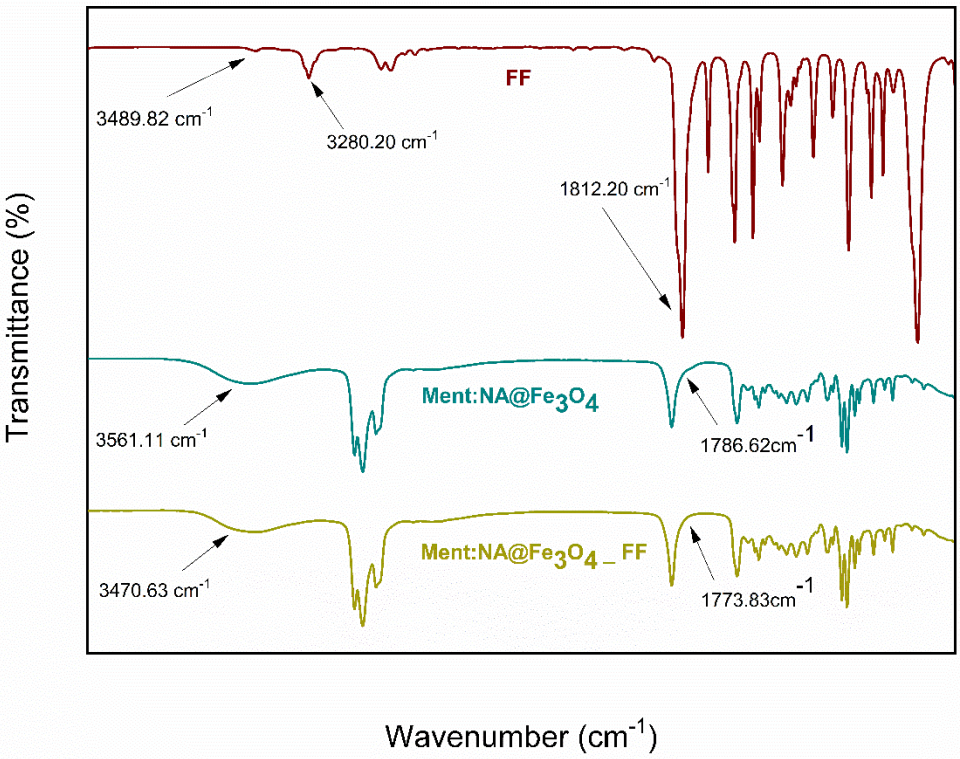

Fig. 27. FT-IR spectra of pure FF, synthesized Ment:NA@Fe_3O_4 sorbent, and Ment:NA@Fe_3O_4 after FF adsorption [140].

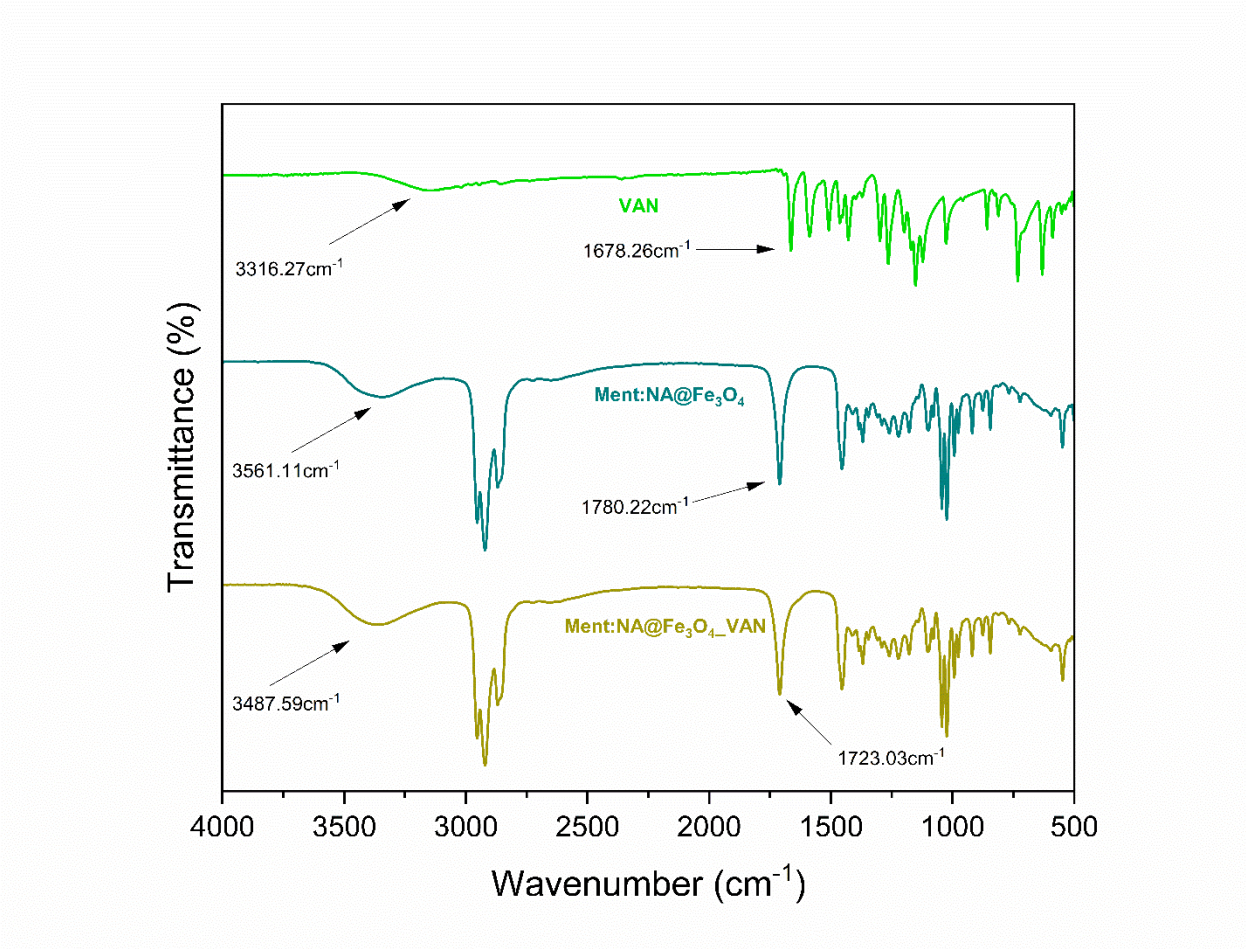

Fig. 28. FT-IR spectra of pure VAN, synthesized Ment:NA@Fe_3O_4 sorbent, and Ment:NA@Fe_3O_4 after VAN adsorption [140].

10.11. Comparison of HMDES with ordinary DES

The performance of HMDES was compared to that of conventional DES lacking magnetic nanoparticles (Fig. 29). Results revealed that HMDES achieved significantly higher RE, owing to its magnetic separability, hydrophobic nature, and enhanced interaction with inhibitory compounds. The presence of MNPs improved surface area and mass transfer, while the hydrophobicity reduced water interference, both contributing to stronger sorption.

In contrast, ordinary DES showed reduced efficiency, likely due to weaker retention and the absence of magnetic recovery. Additionally, HMDES maintained its performance over repeated use, demonstrating superior reusability and operational stability. These advantages position HMDES as a more efficient, selective, and sustainable extraction system compared to traditional DES formulations.

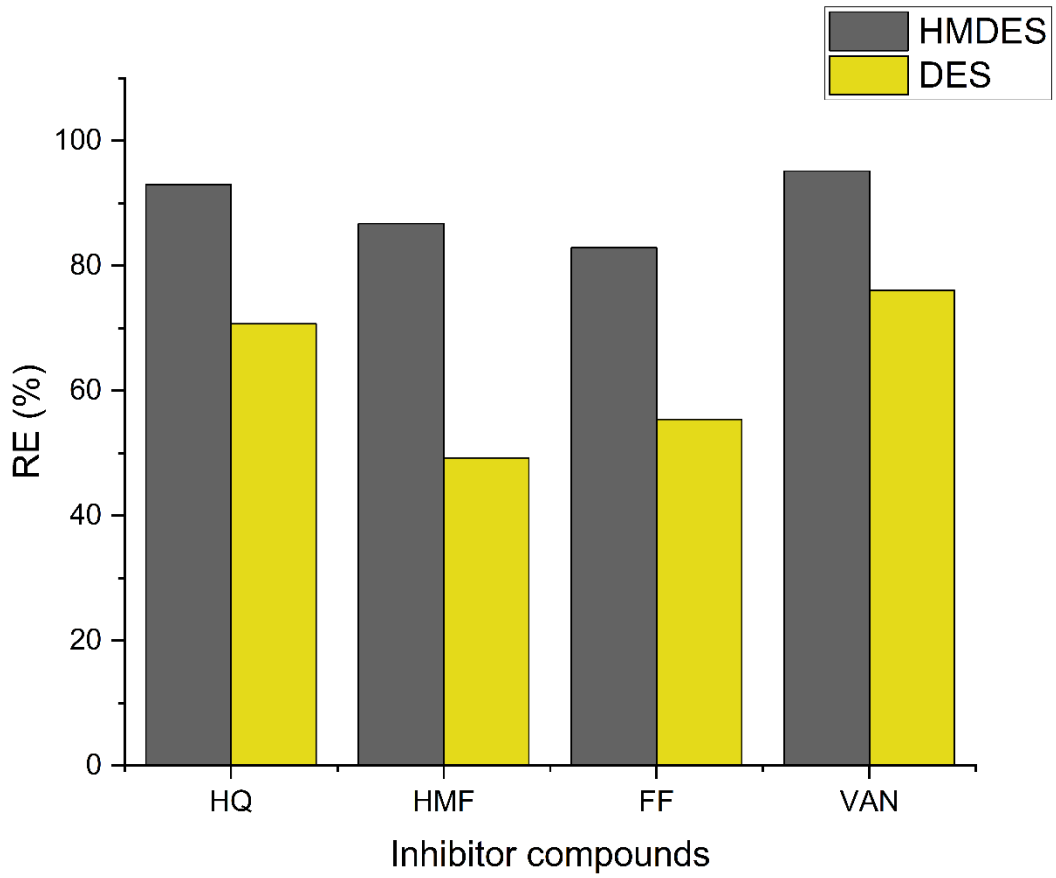

Fig. 29. Comparison of inhibitory compound removal efficiency between HMDES and DES under optimal conditions [140].

10.12. Real samples and effects of matrix

In order to evaluate the effectiveness of the newly developed method, removal tests were performed under optimized conditions on real samples obtained after hydrolysis and fermentation. The REs for these real samples is presented in Fig. 30, demonstrating RE values of 83.3%, 71.42%, 69.99%, and 76.80% for HQ, HMF, FF, and VAN, respectively. These results confirm the capability of the Meth:NA@Fe_3O_4 based system in efficiently extracting inhibitory compounds from hydrolysis and fermentation processes. The real samples analyzed in this study comprised a diverse set of hydrolysates and fermentation broths, including hardwood blends pretreated with varying concentrations of H_2SO_4, NaOH, and H_2O_2; starch and lignocellulose-based hydrolysates from potato processing and biofraction leachates; as well as fermentation broths derived from dark, alcoholic, and photo-fermentation using various microbial strains. The full descriptions corresponding to each sample code (e.g., 1.1-1.11) are summarized in Table 4. When comparing the removal performance in real samples to that in synthetic solutions, a noticeable decrease in RE was observed, which aligns with

expectations. Real samples often consist of complex matrices containing diverse organic components, which can interfere with the sorption process by competing for active sites or modifying the chemical interactions between the inhibitors and the removal agent. In contrast, synthetic solutions are generally designed with controlled compositions, allowing for optimized removal conditions with minimal external interference.

A key factor contributing to the lower RE in real samples is the presence of additional substances containing hydroxyl [-OH) and carboxyl (-COOH) functional groups, which can interact with HMDES through hydrogen bonding or van der Waals forces [108, 128, 141]. these interactions can partially block the active sites in HMDES, thereby reducing its capacity to extract HQ, HMF, FF, and VAN efficiently. Despite these challenges, the removal efficiencies in real samples remained remarkably high, reinforcing the robustness and practicality of the developed extraction method for industrial applications.

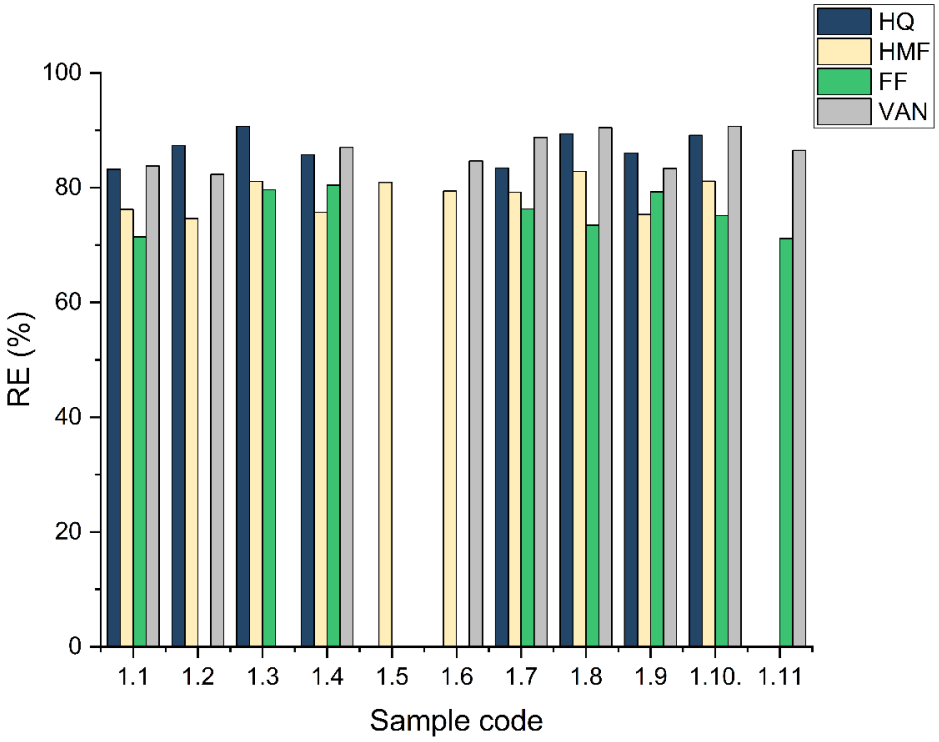

Fig. 30. Removal efficiency of inhibitor compounds from real post-hydrolysis sample using HMDES [140].

Table 4. Description of real sample codes

Sample code	Description
1.1	Hardwood blend after pre-treatment with 5% H_2SO_4
1.2	Hardwood blend after pre-treatment with 30% H_2SO_4
1.3	Hardwood blend after pre-treatment with 0.5M NaOH
1.4	Hardwood blend after pre-treatment with 1.5M NaOH
1.5	Hardwood blend after pre-treatment with 5% H_2O_2
1.6	Hardwood blend after pre-treatment with 30% H_2O_2
1.7	Starch and lignocellulose hydrolysate from potato processing after centrifugation (industrial by-product)
1.8	Starch and lignocellulose hydrolysate from potato processing additionally pre-treated with 5%H_2SO_4
1.9	Starch and lignocellulose hydrolysate from potato processing additionally pre-treated with 0.5 M NaOH
1.10	Starch and lignocellulose hydrolysate from potato processing additionally pre-treated with 5% H_2O_2
1.11	Starch and lignocellulose hydrolysate from bio fraction leachate obtained from biomass composter

11. CONCLUSIONS ON HMDES

The application of hydrophobic magnetic deep eutectic solvents (HMDES) for the removal of phenolic inhibitory compounds from fermentation broths demonstrated excellent efficiency under both synthetic and real conditions. Through systematic optimization, the highest removal efficiencies were achieved at pH 8.0, a contact time of 15 minutes, stirring speed of 1200 rpm, ambient temperature (20 °C), 5 mL HMDES and 10 mL of hydrolysate. Under these conditions, HMDES achieved removal efficiencies of 92.97% for HQ, 86.72% for HMF, 82.86% for FF, and 95.12% for VAN in model solutions.

When applied to actual hydrolysates derived from lignocellulosic biomass, the system maintained a high removal performance, with efficiencies of 83.3%, 71.42%, 69.99%, and 76.80% for HQ, HMF, FF, and VAN, respectively. Although slightly reduced compared to synthetic matrices, these values confirm the robustness of HMDES in complex real hydrolysate environments. The lower performance in real matrices is attributed to matrix interferences and competitive interactions that limit inhibitor availability for extraction.

Mechanistic insights obtained via FTIR spectroscopy revealed that hydrogen bonding and van der Waals forces govern the interaction between HMDES and inhibitor molecules. Shifts in the -OH and C=O absorption bands after extraction confirmed strong specific interactions between functional groups of menthol and nonanoic acid in the solvent and those of the inhibitor compounds. More pronounced shifts for HQ and vanillin suggest stronger binding, consistent with their higher removal efficiencies.

In comparison with conventional solvent-based techniques including toluene, isobutyl acetate, and ionic liquids HMDES showed superior operational advantages. It enabled high removal

efficiency within only 15 minutes (compared to 30-240 minutes in other methods), functioned effectively at room temperature without the need for heating or cooling, used lower solvent volumes, and allowed for rapid magnetic separation without centrifugation. Moreover, regeneration experiments confirmed the stability of HMDES over 13 consecutive cycles with negligible efficiency loss.

In addition to its technical merits, HMDES is non-toxic, biodegradable, and environmentally benign, making it a sustainable alternative to conventional solvents. Its cost-effective reusability, rapid action, and ease of separation render it highly suitable for industrial bioprocesses, especially in the context of lignocellulosic biomass valorization. Taken together, these findings position HMDES as a highly promising, scalable, and green solution for the selective removal of fermentation inhibitors.

12. RESULTS OF USING MOF@PSEUDO-DES FOR REMOVING INHIBITOR COMPOUNDS

12.1. Box–Behnken optimization of MOF@pseudo-DES for efficient inhibitor removal

To achieve optimal conditions for removing fermentation inhibitors (HQ, HMF, FF, and VAN), a Box–Behnken Design (BBD) was employed to systematically evaluate four variables: vortex time (X1), pH (X2), analyte concentration (X3), and MOF@pseudo-DES dosage (X4). Each variable was assessed at three levels, requiring 27 experimental runs. The tested range and recognized optimal values for each parameter are summarized in Fig. 31.

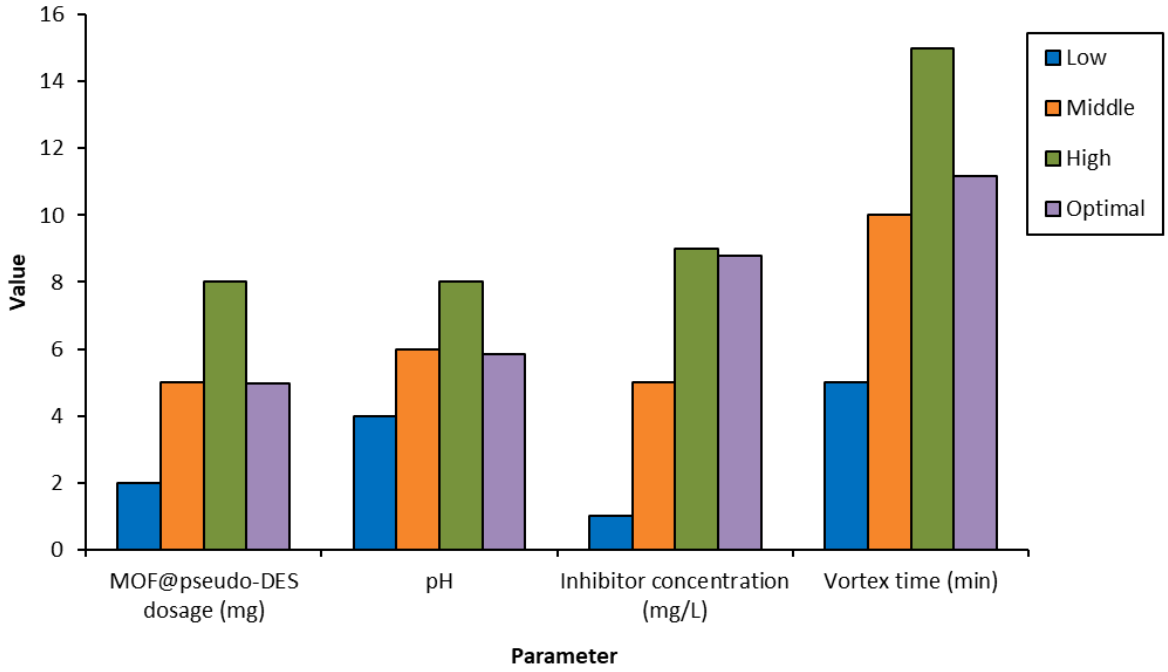

Fig. 31. Range of tested levels for the four variables in the Box–Behnken optimization of MOF@pseudo-DES dosage.

ANOVA analysis revealed that sorbent dosage (X4) had a statistically significant effect on VAN and overall removal ($p < 0.05$). Key interaction terms, such as X1·X3 and X2·X4, also played a notable role in influencing removal efficiency. Quadratic polynomial equations were generated to predict individual and total removal efficiencies (Y_HMF, Y_FF, Y_HQ, Y_VAN, and Y), with high determination coefficients (R^2 ranging from 0.79 to 0.93), indicating excellent model accuracy.

The optimal conditions identified for universal removal were: 11.16 min vortex time, pH 5.86, 8.77 mg L^{-1} inhibitor concentration, and 4.97 mg MOF@pseudo-DES. These conditions were validated using real lignocellulosic hydrolysate and post-fermentation broth samples. The model maintained strong predictive power across diverse feedstocks, with removal efficiencies for individual compounds

reaching up to 64% and universal removal (Y) averaging around 60%, depending on sample composition.

In practice, HQ removal was more challenging in samples with initially high concentrations, while HMF and VAN were efficiently removed even in complex matrices. Starch-derived samples showed lower RE due to the presence of interfering organics. These findings confirm the suitability of BBD-based optimization for tuning MOF@pseudo-DES dosage and pH to different waste streams in real-world applications.

12.2. Characterization of the NH_2-UiO-66@pseudo-DES

Through a solvothermal synthesis approach, a zirconium-based NH_2-UiO-66 MOF was successfully fabricated, followed by the incorporation of ChCl to enhance its structural and functional properties. This modification aimed to enhance the functional properties of the MOF, optimizing its potential for sorption / extraction applications involving target compounds. The successful synthesis and modification of NH_2-UiO-66@pseudo-DES were systematically confirmed through comprehensive physicochemical characterization techniques, which are detailed in the following sections.

12.2.1. X-ray diffraction (XRD)

The successful formation of the NH_2-UiO-66 structure was validated through powder X-ray diffraction (PXRD) analysis, with the corresponding diffraction patterns depicted in Fig.32. The XRD investigation presented in Fig.32, provides crucial insights into the crystallinity and structural integrity of both NH_2-UiO-66 and its choline chloride-modified counterpart (ChCl@NH_2-UiO-66). The XRD patterns exhibit characteristic peaks at 7.2°, 8.3°, 11.8°, 13.9°, 14.6°, 16.8°, 18.4°, 18.9°, 20.7°, 22.0°, 25.0°, 25.5°, and 30.5°, which correspond to the (111), (200), (220), (311), (222), (400), (331), (420), (422), (511), (531), (600), and (711) Bragg reflections associated with the octahedral crystal structure of NH_2-UiO-66. These diffraction patterns are consistent with previously documented data for NH_2-UiO-66 (COD - 4348132), further confirming the successful synthesis and structural fidelity of the material [176, 177, 188]. The sharpness and intensity of the diffraction peaks are indicative of a high degree of crystallinity and a well-ordered crystal lattice, which are critical factors influencing the performance of MOFs in various applications. Notably, the XRD patterns of NH_2-UiO-66@pseudo-DES exhibited no significant shifts or variations in peak intensity, verifying that the structural framework of NH_2-UiO-66 remained intact following post-synthetic modification. These findings suggest that the incorporation of choline chloride did not alter the fundamental crystalline architecture of the MOF, further demonstrating its stability and suitability for adsorption and extraction applications.

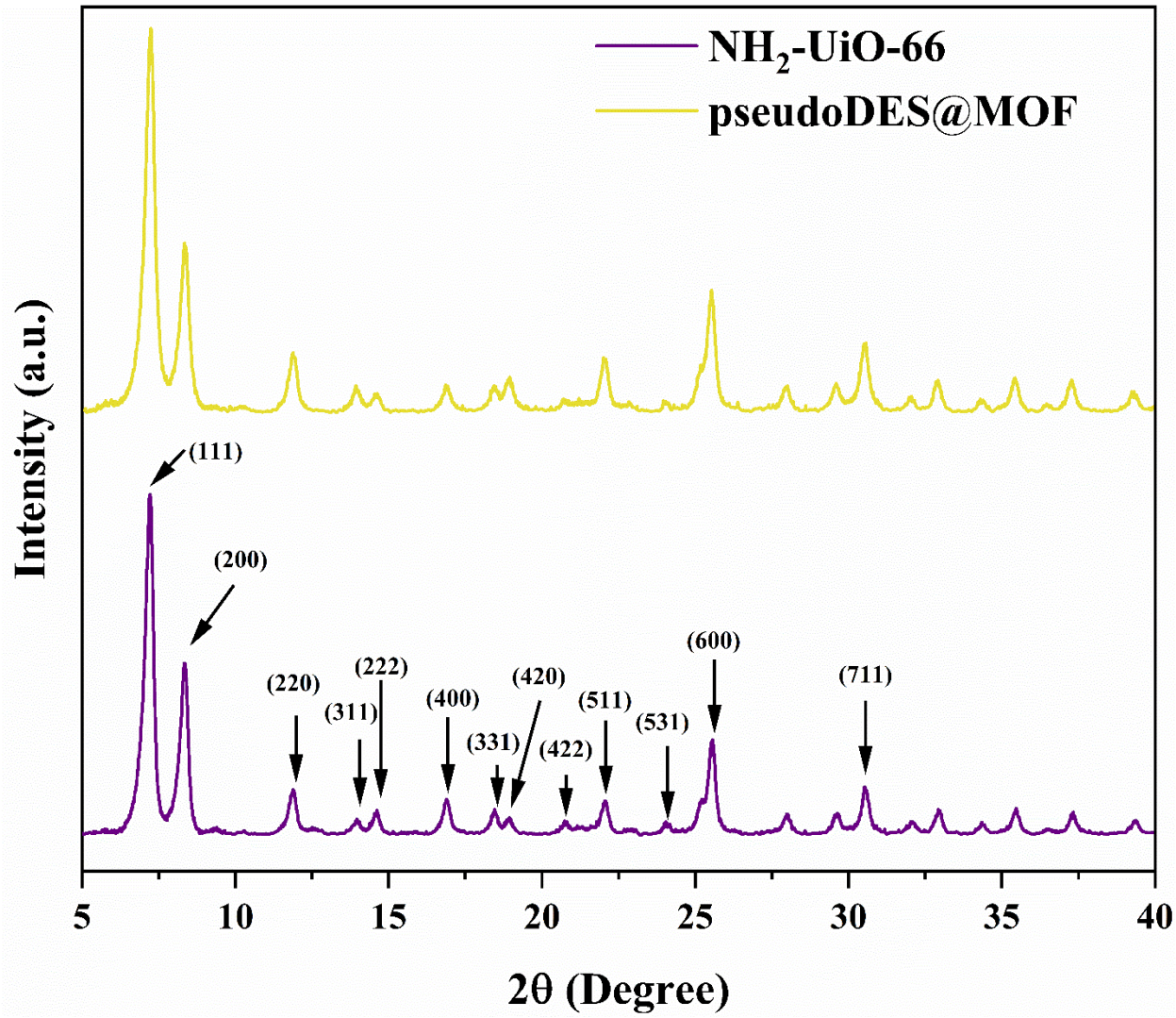

Fig. 32. Experimental PXRD pattern comparison between NH_2-UiO-66 and NH_2-UiO-66@pseudo-DES [189]

12.2.2. Fourier transform infrared spectroscopy (FTIR)

FTIR analysis confirmed structural modifications in NH_2-UiO-66 after functionalization with pseudo-DES (Fig.33). Characteristic N-H stretching vibrations appeared at 3482 and 3387 cm^{-1}, while a band at 764 cm^{-1} supported the presence of amine groups. Peaks at 1695, 1579, and 1494 cm^{-1} were attributed to C=O, carboxylate, and aromatic C–N vibrations, typical of the MOF's organic linker [176, 177]. A signal at 664 cm^{-1} indicated the Zr-O-Zr framework [190].

After ChCl modification, new bands emerged at 3012, 1156, 1180, and 865 cm^{-1}, corresponding to -OH bending, CCO stretching, CH_2 rocking, and NCH_3 vibrations, confirming ChCl incorporation [191]. A shift in N-H stretching from 3287 to 3419 cm^{-1}, along with broadening, indicated strong hydrogen bonding between the MOF and ChCl [192]. These spectral changes confirm the successful

formation of NH_2-UiO-66@pseudo-DES and the presence of key functional groups from both components.

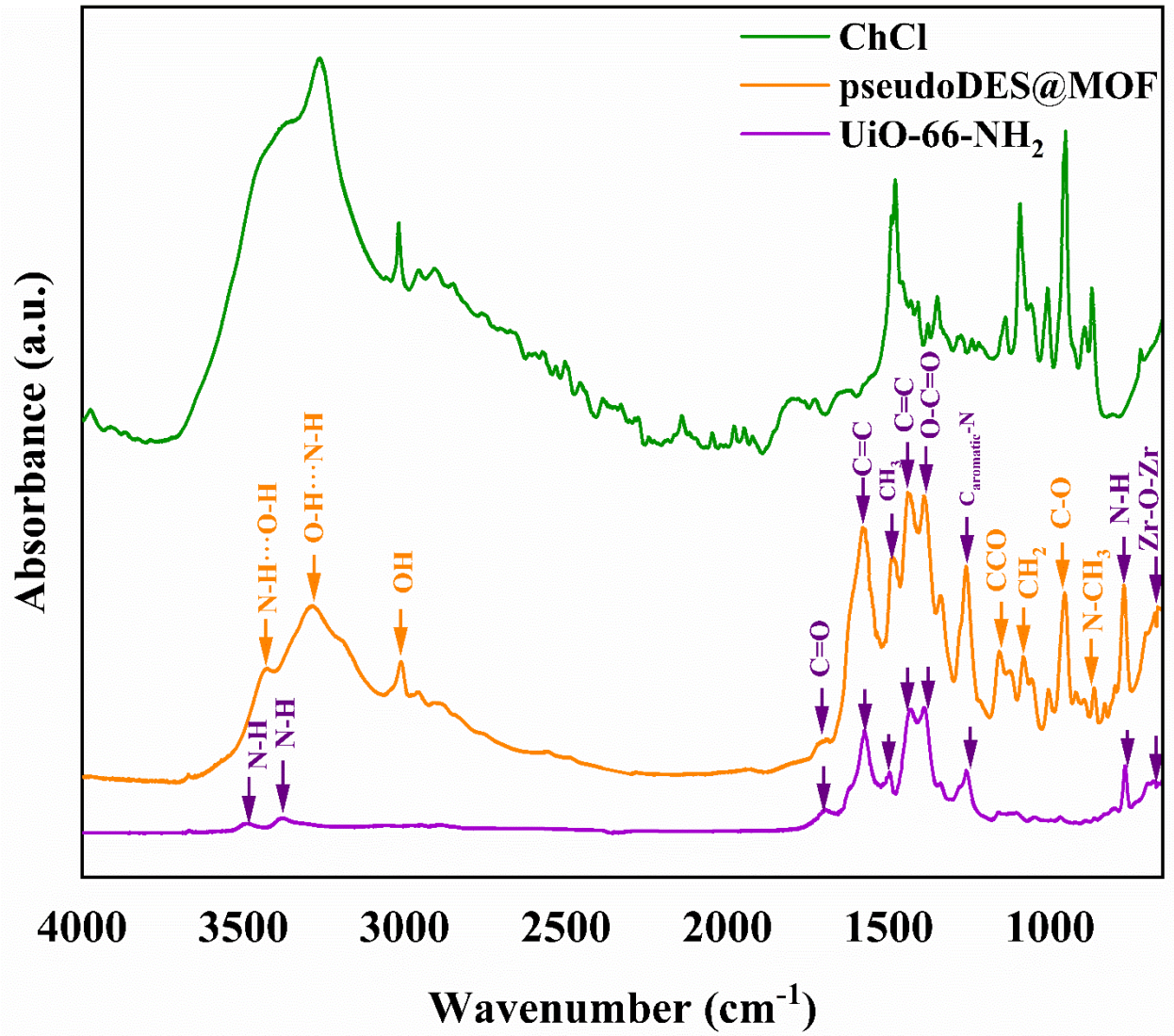

Fig. 33. FTIR spectral comparison of NH_2-UiO-66 and NH_2-UiO-66@pseudo-DES [189].

12.2.3. Scanning electron microscopy (SEM)

SEM imaging (Fig. 34a–f) revealed that NH_2-UiO-66 displays uniform octahedral crystals (100–200 nm), characteristic of its crystalline ZrO_6-node framework structure [193]. After functionalization with ChCl, NH_2-UiO-66@pseudo-DES retained this morphology, but a superficial pseudo-DES layer and slight changes in particle aggregation were observed, indicating surface modification [177]. EDX analysis confirmed the elemental composition before and after modification. For NH_2-UiO-66: N (22.10 wt%), O (42.34 wt%), and Zr (35.56 wt%) were present. In NH_2-UiO-66@pseudo-DES, Cl appeared (6.65 wt%), while other elements N (14.66 wt%), O (22.25 wt%), Zr (14.12 wt%) decreased due to coverage by the ChCl layer. Elemental mapping (Fig. 35) showed uniform Cl distribution,

supporting successful incorporation of ChCl without compromising MOF structure. These results confirm the formation of NH_2-UiO-66@pseudo-DES with preserved morphology and integrated ChCl, suggesting improved surface functionality for enhanced interactions with target compounds.

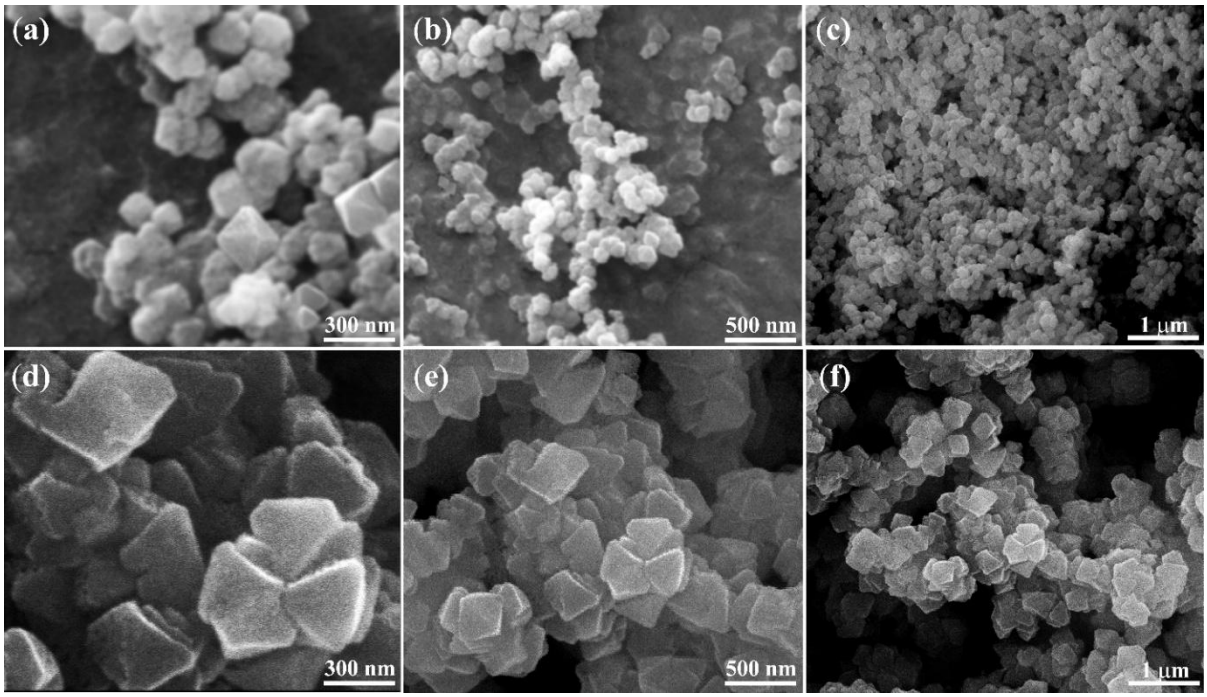

Fig. 34. SEM micrographs of NH_2-UiO-66 (a-c] and NH_2-UiO-66@pseudo-DES (d-f) [189].

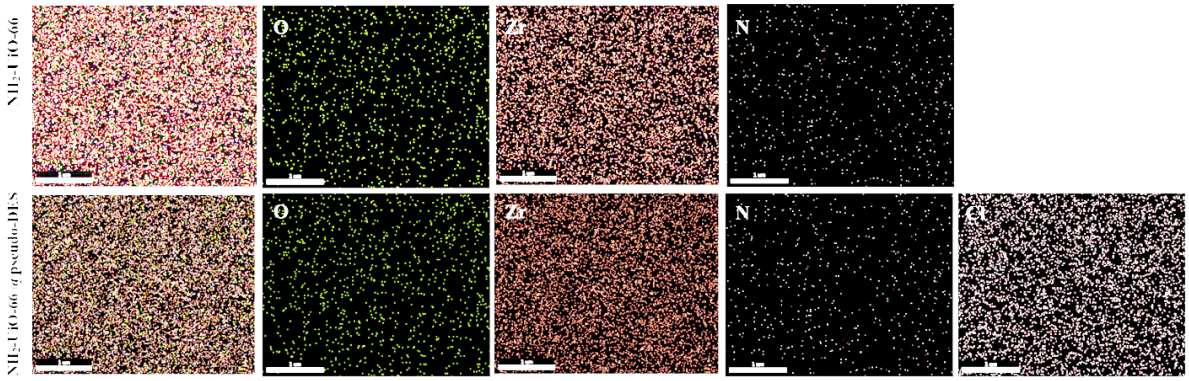

Fig. 35. Elemental mapping images obtained from energy-dispersive X-ray spectroscopy (EDX) for NH_2-UiO-66 and NH_2-UiO-66@pseudo-DES [189].

12.2.4. Thermogravimetric analysis (TGA)

TGA analysis [Fig. 36) revealed distinct thermal behaviors for NH_2-UiO-66 and NH_2-UiO-66@pseudo-DES. An initial mass loss below 150 °C in both samples was attributed to desorption of water and residual DMF. For pristine NH_2-UiO-66, a 20% weight reduction between 200-380 °C corresponded to dihydroxylation of Zr_6 clusters, followed by degradation of the organic linker and collapse of the framework up to 550 °C. In NH_2-UiO-66@pseudo-DES, two main degradation stages were observed: 35% mass loss at 200–260 °C due to Zr_6 cluster dehydroxylation, and 42% loss from 260-550 °C linked to decomposition of the pseudo-DES and MOF framework [177]. The presence of ChCl altered the degradation profile, especially in the 260-360 °C range, indicating its lower thermal stability and influence on MOF behavior. Pure ChCl exhibited decomposition beginning at ~300 °C, producing volatile compounds like ammonia, trimethylamine, HCl, and hydrocarbons. Its integration into the MOF accelerated breakdown processes via hydrogen bonding, leading to increased mass loss and a modified thermal response [194].

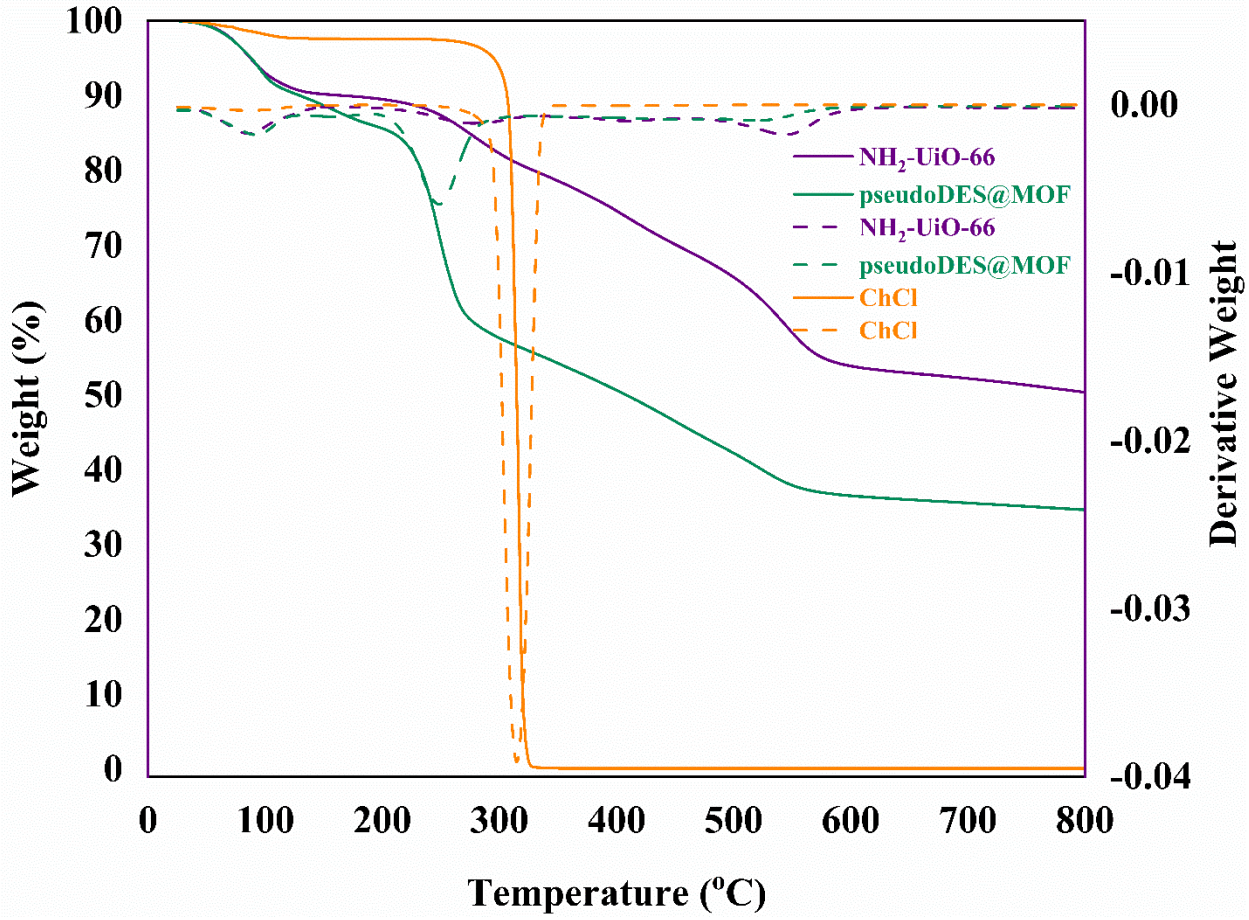

Fig. 36. Thermogravimetric analysis of NH_2-UiO-66 and NH_2-UiO-66@pseudo-DES [189].

12.2.5. Surface area (BET)

The evaluation of specific surface area confirmed that NH_2-UiO-66@pseudo-DES maintains a highly porous structure, exhibiting a Brunauer-Emmett-Teller (BET) surface area of 344 m^2g^{-1}, as shown in Fig. 37. A notable reduction in surface area was observed, decreasing from 778 m^2g^{-1} for NH_2-UiO-66 to 344 m^2g^{-1} for NH_2-UiO-66@pseudo-DES. This decline can be attributed to the formation of hydrogen bonds between the amine (-NH_2) functional groups of NH_2-UiO-66 and the hydroxyl (-OH) groups of choline chloride (ChCl), which plays a key role in the synthesis of NH_2-UiO-66@pseudo-DES.Furthermore, the decrease in BET surface area is closely linked to pore blockage caused by ChCl molecules during the composite formation process. The incorporation of ChCl within the MOF framework partially restricts access to the internal pores, leading to a reduction in available surface area while simultaneously contributing to the structural modification of the material. Despite this decline, the remaining porosity ensures that NH_2-UiO-66@pseudo-DES retains sufficient surface characteristics for efficient sorption and extraction applications [177, 195].

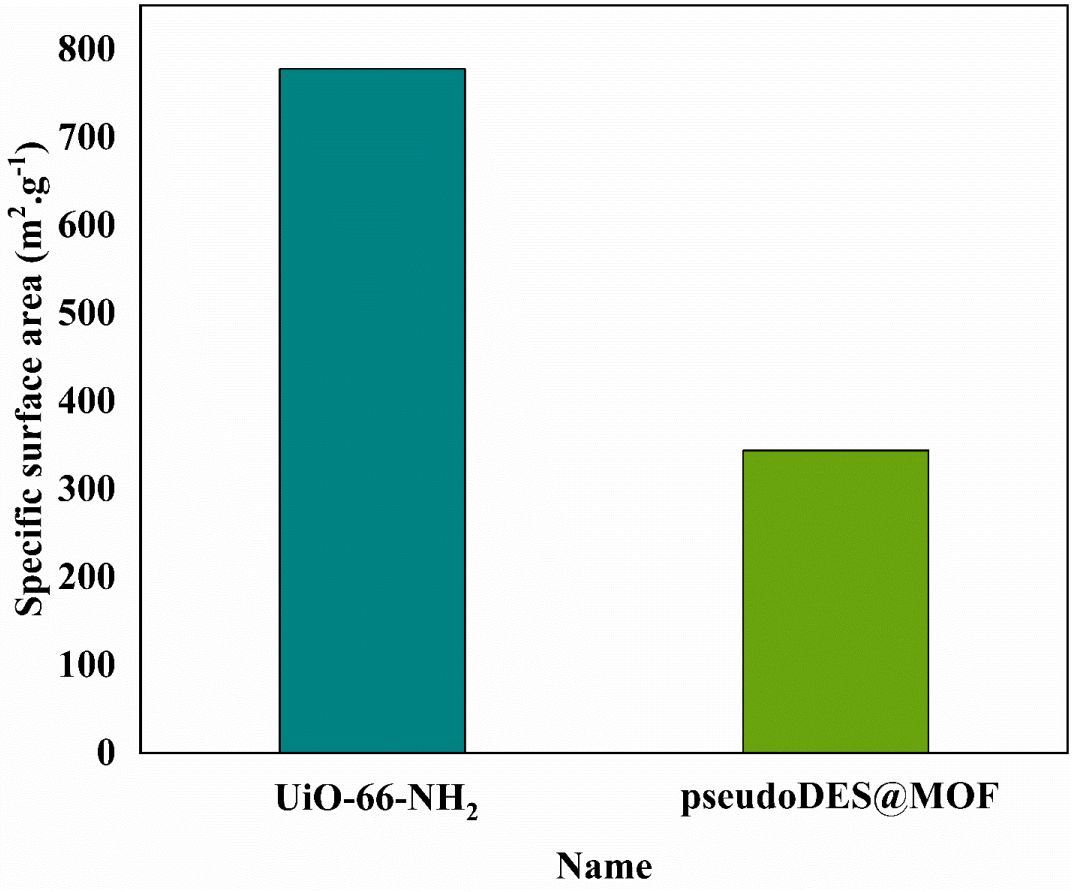

Fig. 37. BET specific surface area analysis of pristine NH_2-UiO-66 and choline chloride-functionalized NH_2-UiO-66 (NH_2-UiO-66@pseudo-DES) [189].

12.3. Effects of matrix composition in real samples treatment

To evaluate the performance of the newly developed approach, removal experiments were conducted under optimized conditions using real samples obtained following hydrolysis and fermentation. The outcomes of these experiments are summarized in Fig.38, which presents the RE of inhibitory compounds in real matrices. The full description of each sample code (1.1–2.5) is provided in Table 5 to aid clarity and interpretation. In these samples, the RE for HQ, HMF, FF, and VAN exceeded 51.73%, 53.21%, 42.69%, and 37.59%, respectively, indicating the capability of NH_2-UiO-66@pseudo-DES to extract inhibitory compounds even from complex real matrices.

The lower removal efficiencies observed in real hydrolysates and fermentation broths, compared to synthetic model solutions, can be attributed to matrix complexity. Real samples contain diverse organic species that may compete for sorption sites, decreasing the material's selectivity and capacity. Moreover, abundant hydroxyl (-OH) and carboxyl (-COOH) groups in the matrices may form hydrogen bonds or van der Waals interactions with NH_2-UiO-66@pseudo-DES [108, 128, 140, 141], potentially blocking active sites and reducing the effective adsorption of target inhibitors.

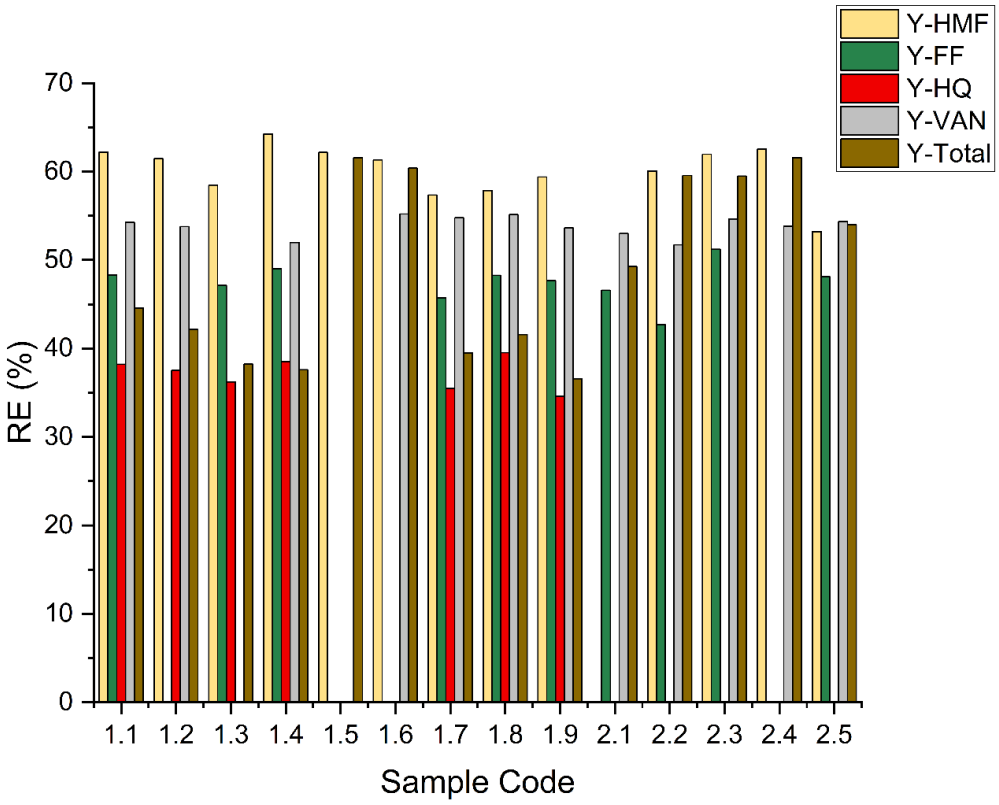

Fig. 38. Removal efficiency of inhibitory compounds across real samples [189].

.

Table 5. Description of real sample codes

Sample Code	Description
1.1	Hardwood blend after pre-treatment with 5% H_2SO_4
1.2	Hardwood blend after pre-treatment with 30% H_2SO_4
1.3	Hardwood blend after pre-treatment with 0.5M NaOH
1.4	Hardwood blend after pre-treatment with 1.5M NaOH
1.5	Hardwood blend after pre-treatment with 5% H_2O_2
1.6	Hardwood blend after pre-treatment with 30% H_2O_2
1.7	Starch and lignocellulose hydrolysate from potato processing. after centrifugation (industrial by-product)
1.8	Starch and lignocellulose hydrolysate from potato processing additionally pre-treated with 5%H_2SO_4
1.9	Starch and lignocellulose hydrolysate from potato processing additionally pre-treated with 0.5 M NaOH
2.1	Lignocellulosic biomass (corn cobs acidic hydrolysis (1.1))
2.2	Lignocellulosic biomass (corn cobs alkaline hydrolysis)
2.3	Lignocellulosic biomass (corn cobs alkaline hydrolysis)
2.4	Lignocellulosic biomass after oxidative pre-treatment (1.5)
2.5	Lignocellulosic biomass after alkaline pre-treatment (1.3)

12.4. Comparison of ChCl@NH_2-UiO-66 with NH_2-UiO-66

A comparative analysis of RE between NH_2-UiO-66@pseudo-DES and NH_2-UiO-66 for inhibitory compounds such as HQ, HMF, FF, and VAN highlights a notable performance disparity, as illustrated in Fig. 39. The results demonstrate that NH_2-UiO-66@pseudo-DES exhibits a substantially higher RE across all tested inhibitors compared to NH_2-UiO-66. For instance, HQ removal efficiency using NH_2-UiO-66@pseudo-DES reaches 55.16%, whereas NH_2-UiO-66 achieves only 27.98%. Similarly, for VAN, the RE of NH_2-UiO-66@pseudo-DES is 71.91%, significantly surpassing the 50.46% achieved by NH_2-UiO-66. This distinct improvement stems from chemical and structural modifications introduced through ChCl incorporation into the MOF structure, which facilitates the formation of a thin pseudo-DES layer enriched with NH_2 groups and additional hydroxyl (-OH) and chloride (Cl^-) functionalities features absent in NH_2-UiO-66.

The presence of pseudo-DES between ChCl and NH_2 within NH_2-UiO-66@pseudo-DES significantly enhances its surface chemistry, fostering stronger interactions with inhibitory compounds via hydrogen bonding and electrostatic attractions. These interactions play a crucial role in the efficient adsorption of polar inhibitors, which rely on strong polar interactions for effective sequestration. The incorporation of hydroxyl and chloride groups further strengthens sorption selectivity and efficiency, providing an advantage over NH_2-UiO-66, which lacks these functional groups.

Additionally, the inclusion of ChCl increases the hydrophilic nature of the material, thereby improving its affinity for polar compounds. This enhanced hydrophilicity contributes to the superior RE observed for HMF and FF when using NH_2-UiO-66@pseudo-DES, as depicted in Fig. 40. In contrast, the lower hydrophilicity of NH_2-UiO-66 restricts its ability to effectively capture polar molecules, leading

to diminished adsorption performance. Moreover, the synergistic combination of ChCl and NH_2 functionalities within NH_2-UiO-66@pseudo-DES leverages the MOF's intrinsic porosity, large surface area, and the newly introduced functional groups, significantly enhancing its stability and selectivity for inhibitory compounds [196].

The superior efficiency of NH_2-UiO-66@pseudo-DES over NH_2-UiO-66 can thus be attributed to the formation of a pseudo-DES layer, which not only optimizes surface chemistry but also increases hydrophilicity and induces synergistic effects that enhance stability, selectivity, and adsorption efficiency. These combined factors position NH_2-UiO-66@pseudo-DES as a highly efficient and versatile adsorbent, capable of significantly improving the removal of inhibitory compounds from hydrolysates, making it a promising solution for practical sorption applications.

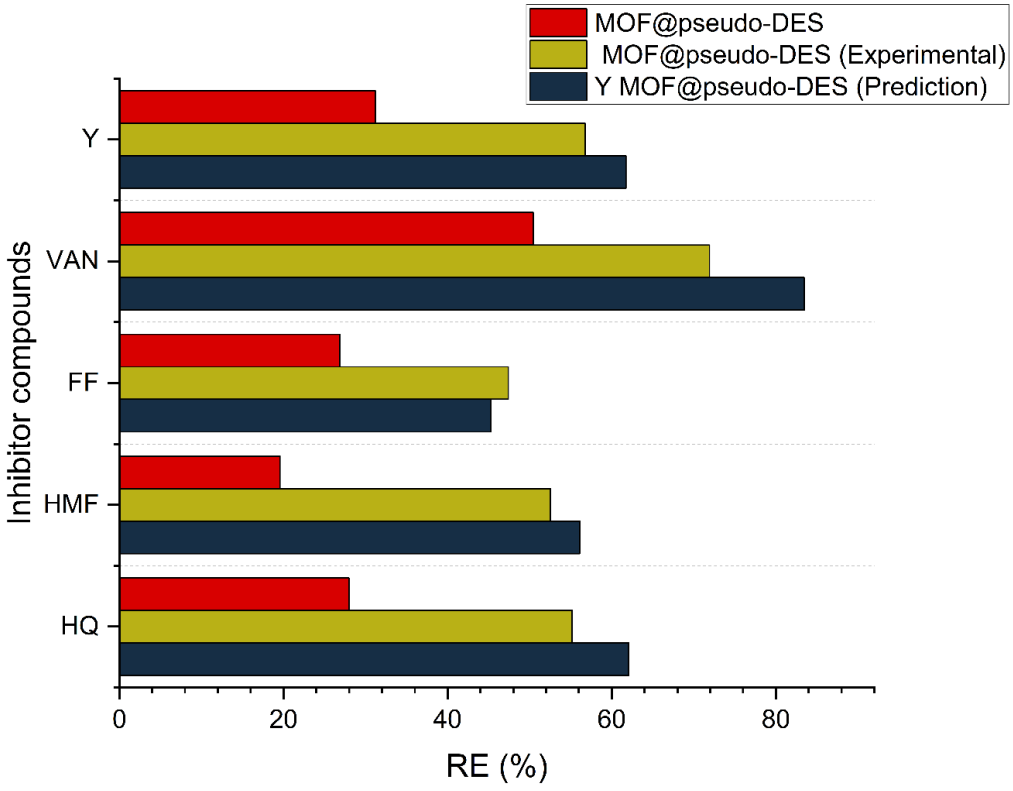

Fig. 39. Removal efficiency comparison between ChCl@NH_2-UiO-66 and NH_2-UiO-66, (pH 6, analyst concentration 9 mgL^{-1}, sorbent amount 5mg, vortex time 11 min) [189].

12.5. Reusability

Ensuring the reusability of NH_2-UiO-66@pseudo-DES while preserving its original structural and functional integrity is essential for both resource efficiency and cost-effectiveness. Under optimized conditions, as illustrated in Fig. 40, NH_2-UiO-66@pseudo-DES exhibits stable performance over four

consecutive cycles without a significant decline in the RE of inhibitory compounds. This observation suggests that the material retains its sorption capability and functional properties through multiple reuses.

However, beyond the fourth regeneration cycle, a gradual reduction in RE becomes evident, indicating a decrease in the material's adsorption capacity for inhibitory compounds. This decline suggests that prolonged use may lead to partial deactivation of active sites, limiting the efficiency of NH_2-UiO-66@pseudo-DES in capturing inhibitors. Despite this, the initial high reusability and performance stability highlight its potential as a robust and efficient sorbent for inhibitory compound removal. The findings reinforce the practical applicability of NH_2-UiO-66@pseudo-DES, demonstrating its ability to operate effectively over multiple cycles, thus contributing to sustainable and economically viable sorption processes.

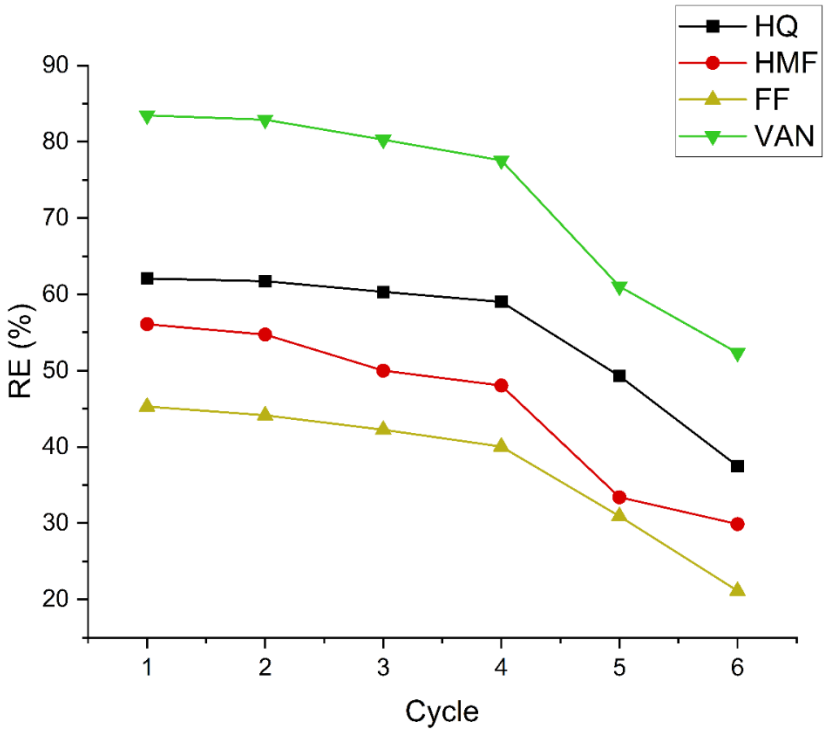

Fig. 40. Effect of reusability cycles on the removal efficiency of inhibitory compounds [189].

12.6. Mechanism of sorption

Analysis of the FTIR spectrum of NH_2-UiO-66@pseudo-DES provides crucial insights into its chemical structure and functional groups. A broad absorption band appearing between 3041 cm^{-1} and 3633 cm^{-1} corresponds to N-H symmetric and asymmetric stretching vibrations, indicative of hydrogen bonding interactions associated with amine functionalities. Additionally, a prominent peak at 2889 cm^{-1} is attributed to aliphatic C-H stretching vibrations, confirming the presence of alkyl chains from ChCl.

Another distinct feature is the strong absorption band at 1645 cm^{-1}, assigned to C=O stretching vibrations, which are characteristic of carboxylate groups coordinating with zirconium clusters in NH_2-UiO-66. Furthermore, a peak at 1508 cm^{-1} corresponds to N-H bending vibrations, confirming the presence of amino functionalities derived from the 2-amino terephthalate ligand. These functional groups play a key role in enhancing the adsorption efficiency of NH_2-UiO-66@pseudo-DES, facilitating strong interactions with HQ, HMF, FF, and VAN.

The adsorption mechanism is governed by specific interactions between the inhibitors and the functional groups of NH_2-UiO-66@pseudo-DES. HQ binds predominantly through hydrogen bonding with N-H groups, while its carboxylate groups contribute to electrostatic interactions and van der Waals forces, including π-π stacking with the aromatic rings of the MOF framework. HMF, which contains aldehyde and hydroxyl groups, establishes hydrogen bonds with N-H and carboxylate groups, in addition to engaging in van der Waals interactions with aliphatic C-H groups. FF, possessing an aldehyde functional group and a furan ring, interacts via hydrogen bonding with N-H and carboxylate groups, while also forming π-π stacking interactions through its aromatic furan ring. Similarly, VAN, with aldehyde, hydroxyl, and methoxy groups, forms hydrogen bonds with N-H groups, engages in electrostatic interactions with carboxylate groups, and undergoes van der Waals forces with aliphatic C-H and methoxy groups, in addition to π-π stacking due to its aromatic ring.

Post-adsorption FTIR spectra reveal shifts in wavenumbers alongside intensification of absorption bands, confirming the effective interaction of the inhibitors with NH_2-UiO-66@pseudo-DES. A significant downshift of the N-H peak further substantiates the adsorption process. Specifically, for HQ, HMF, FF, and VAN, the N-H peak shifts to 3450.74 cm^{-1}, 3278.77 cm^{-1}, 3406.95 cm^{-1}, 3214.63 cm^{-1}, and 3251.77 cm^{-1}, respectively, as illustrated in Figs. 41-45.

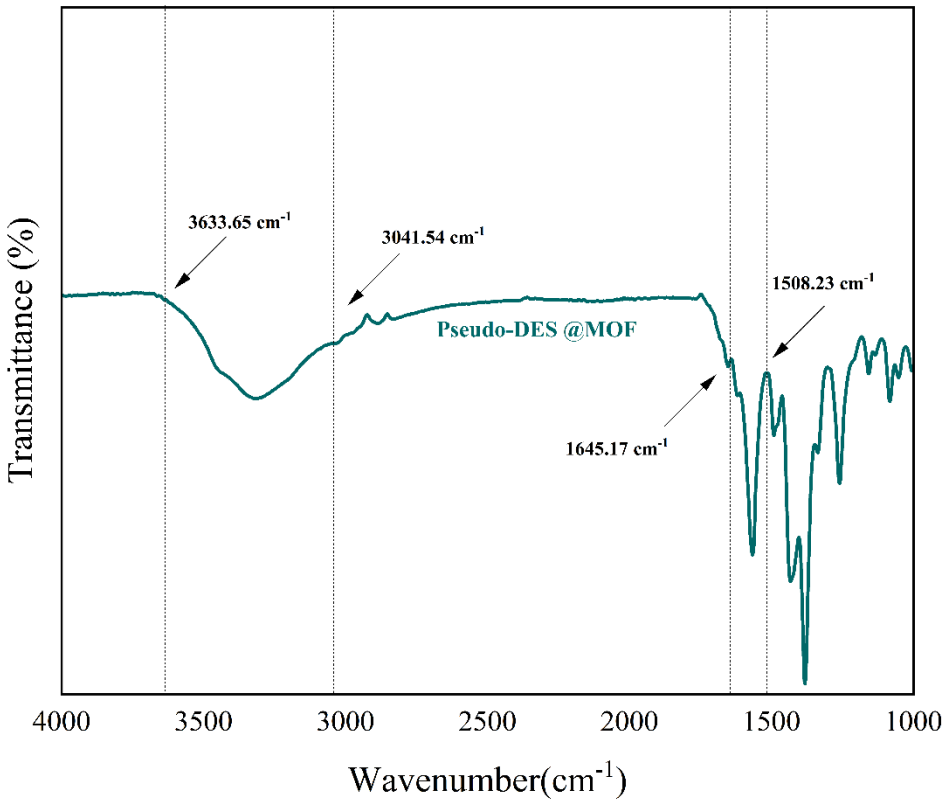

Fig. 41. FT-IR spectrum of the synthesized MOF@pseudo-DES [189].

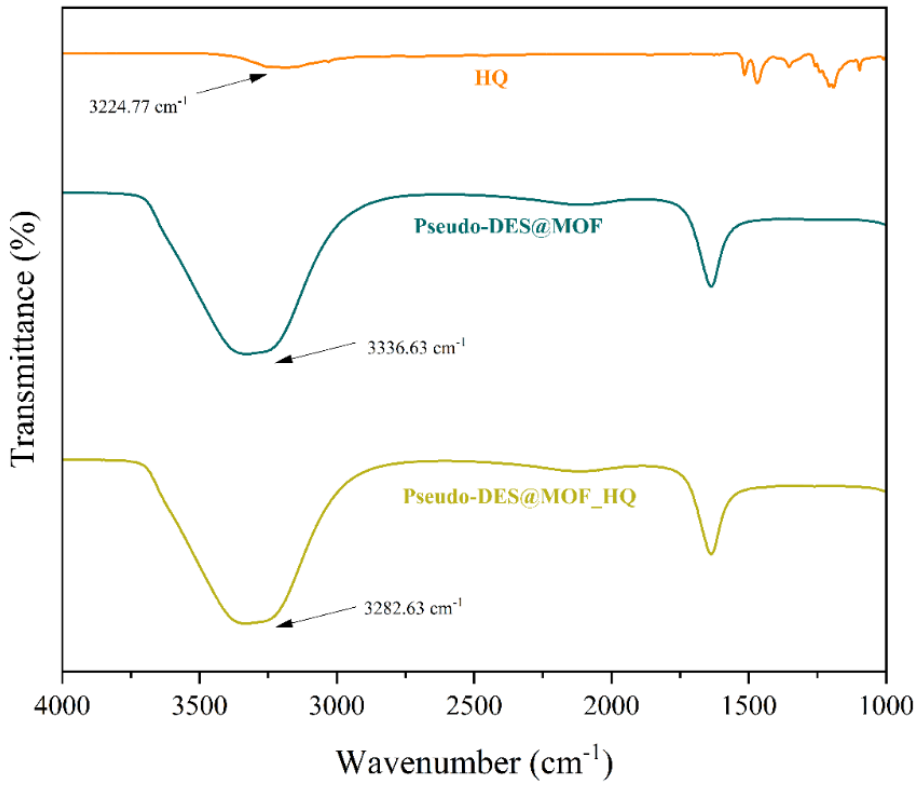

Fig. 42. FT-IR spectra of pure HQ, synthesized MOF@pseudo-DES, and MOF@pseudo-DES after HQ sorption

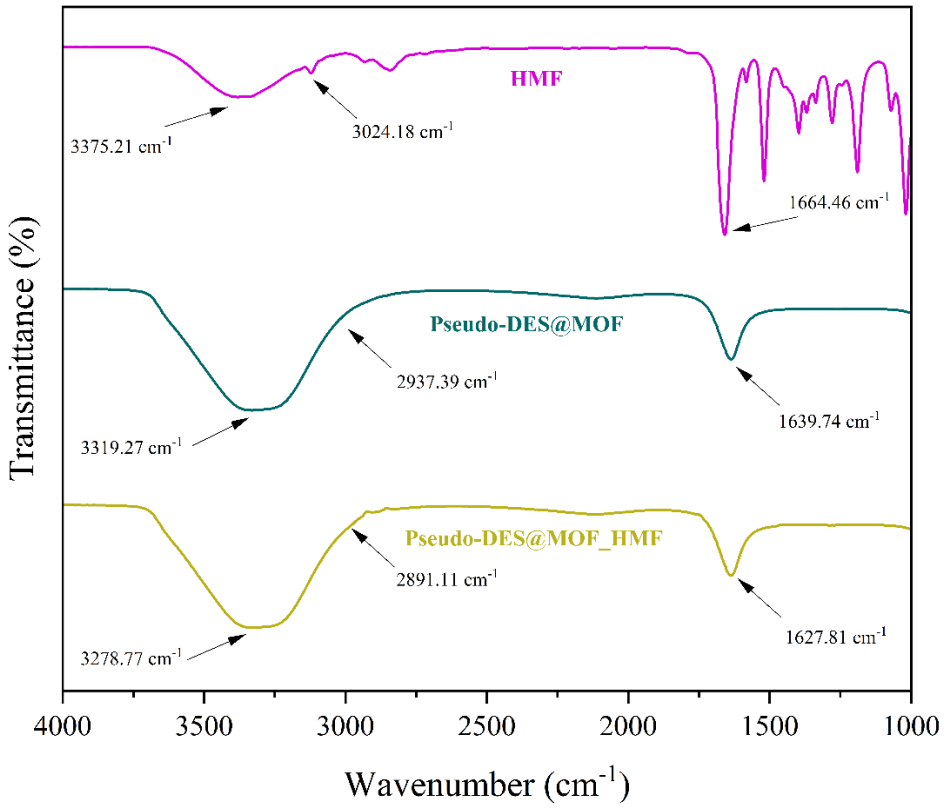

Fig. 43. FT-IR spectra of pure HMF, synthesized MOF@pseudo-DES, and MOF@pseudo-DES after HMF sorption [189].

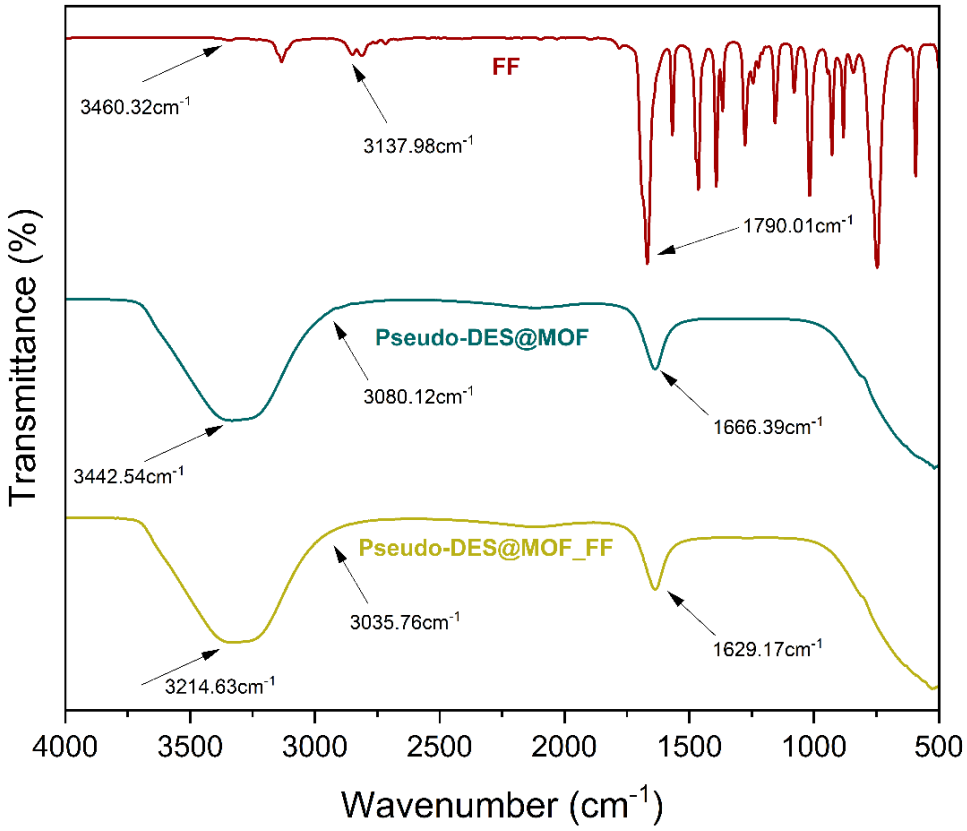

Fig. 44. FT-IR spectra of pure FF, synthesized MOF@pseudo-DES, and MOF@pseudo-DES after FF sorption [189].

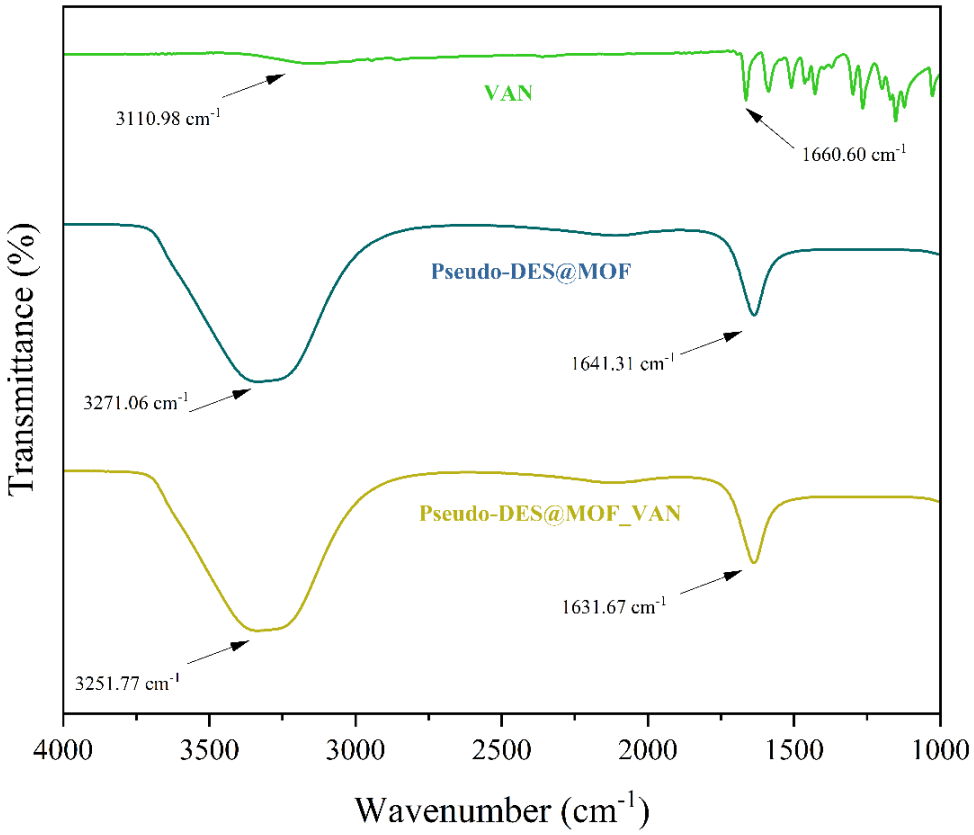

Fig. 45. FT-IR spectra of pure VAN, synthesized MOF@pseudo-DES, and MOF@pseudo-DES after VAN sorption [189].

13. CONCLUSIONS ON NH_2-UIO-66@PSEUDO-DES

The performance of NH_2-UiO-66@pseudo-DES as a novel sorbent for the removal of fermentation inhibitors from lignocellulosic hydrolysates was thoroughly evaluated. This material, synthesized by functionalizing the NH_2-UiO-66 metal-organic framework with a choline chloride-based pseudo-deep eutectic solvent, combines the high surface area and porosity of MOFs with the green and tunable properties of DESs, resulting in enhanced adsorption performance, eco-compatibility, and operational simplicity.

Using a Box–Behnken design, optimal conditions for inhibitor removal were established: pH 5.8, analyte concentration of 9 ppm, vortex time of 11 minutes, and an adsorbent dosage of 5 mg. Under these parameters, removal efficiencies of 62.08% for HQ, 56.09% for HMF, 45.29% for FF, and 83.46% for VAN were achieved in synthetic solutions, reflecting fast adsorption kinetics under ambient conditions ($20 \pm 1°C$). The material was then applied to real hydrolyzed and fermented biomass samples, where slight reductions in efficiency were observed due to matrix complexity and competing interactions. Nevertheless, respectable removal rates were maintained: HQ (51.73%), HMF (53.21%), FF (42.69%), and VAN (37.59%).

Characterization techniques including XRD, FTIR, BET, SEM, TGA, and EDX confirmed the successful functionalization of NH_2-UiO-66 with pseudo-DES. The structural analysis indicated retention of crystallinity and morphology, while FTIR and EDX confirmed the incorporation of choline chloride. Although a decrease in surface area was noted, the modification enhanced hydrophilicity and accessibility to sorption sites. The mechanism of adsorption was attributed to multiple interactions including hydrogen bonding, electrostatic attraction, π–π stacking, and van der Waals forces.

When benchmarked against conventional solvents and advanced extraction methods, NH_2-UiO-66@pseudo-DES demonstrated several advantages. Compared to traditional solvents like toluene or isobutyl acetate, which require longer extraction times and higher volumes, NH_2-UiO-66@pseudo-DES achieved efficient removal within 11 minutes at room temperature using lower solvent ratios. In comparison with HMDES and SUPRADES, NH_2-UiO-66@pseudo-DES offered broader selectivity and better operational simplicity, despite slightly lower removal percentages for some compounds. SUPRADES showed the highest RE for HQ (98.75%) but required longer contact time and alkaline pH, while HMDES was notable for its magnetic separability and rapid extraction.

Overall, NH_2-UiO-66@pseudo-DES presents a balanced and sustainable solution for inhibitor removal. It combines rapid action, eco-friendly composition, reusability, and high affinity for multiple inhibitory compounds. These features make it a promising candidate for industrial-scale applications in the detoxification of biomass hydrolysates, contributing to the development of more efficient and greener biorefinery systems.

14. RESULTS OF USING SUPRADES FOR REMOVING INHIBITOR COMPOUNDS

14.1. Optimization of SUPRADES extraction conditions

To optimize the extraction efficiency of inhibitory compounds using SUPRADES, a Plackett–Burman (PB) statistical design was employed to systematically evaluate the influence of critical parameters including pH, inhibitor concentration, SUPRADES volume, cyclodextrin content, stirring speed, sample volume, and contact time on the removal performance. The tested ranges and final optimized values for these variables are summarized in Table 6.

Table 6. Investigated ranges and recognized optimal conditions for the removal of inhibitory compounds using SUPRADES

Optimized parameter	Stirring speed (rpm)	Amount of cyclo (%)	SUPRADES volume (mL)	Sample Volume (mL)	pH	Inhibitors concentration (mgL^{-1})	Contact time (min)
Low value	600	5	5	5	6	1	10
High value	1200	10	20	20	9	30	60
Recognized optimal values	1200	5	20	5	9	30	60

Seven variables were initially selected based on literature review and preliminary trials: pH, inhibitor concentration, extraction time, cyclodextrin content in the SUPRADES phase, stirring speed, sample volume, and SUPRADES volume. A total of twelve experimental runs were designed according to the PB matrix, enabling the evaluation of main effects while assuming negligible two-factor interactions.

After completing the experiments under the PB design, the RE% of four major inhibitory compounds HQ, HMF, FF, and VAN were measured. The results were analyzed using standardized Pareto charts to determine the significance of each variable (Fig. 46a–d). The vertical reference line on each chart indicates the t-critical value for statistical significance at a 95% confidence level ($\alpha = 0.05$, $t = 2.776$).

The analysis revealed that, cyclodextrin concentration and sample volume were the most influential parameters for HQ removal. Sample volume had the highest impact on HMF extraction. Inhibitor concentration was the most significant for FF removal. Both inhibitor concentration and sample volume affected VAN removal efficiency.

These findings were further supported by the correlogram (Fig. 47), which illustrated the correlation between each factor and the removal efficiency of the tested inhibitors. Based on these insights, the run that demonstrated the highest average removal efficiency across all four target compounds was selected as the optimal condition, corresponding to the following parameters: pH 9,

inhibitor concentration 30 mgL^{-1}, SUPRADES volume 20 mL, cyclodextrin content 5%, stirring speed 1200 rpm, sample volume 5 mL, and contact time 60 minutes.

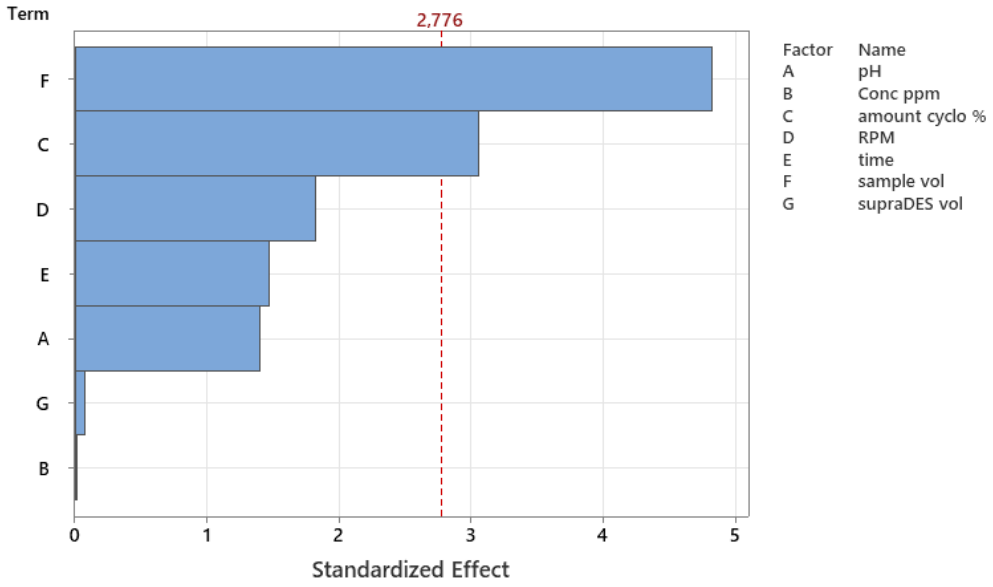

a)

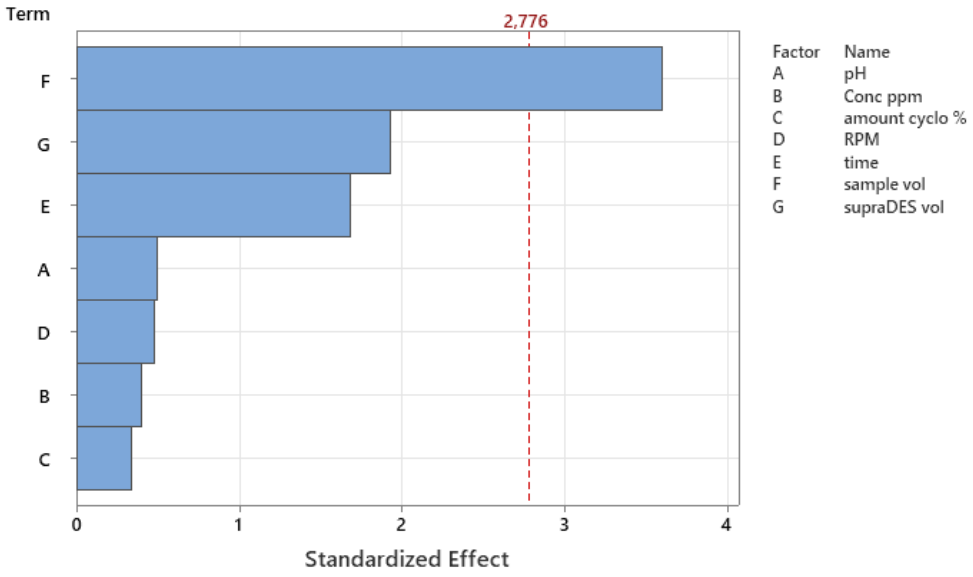

b)

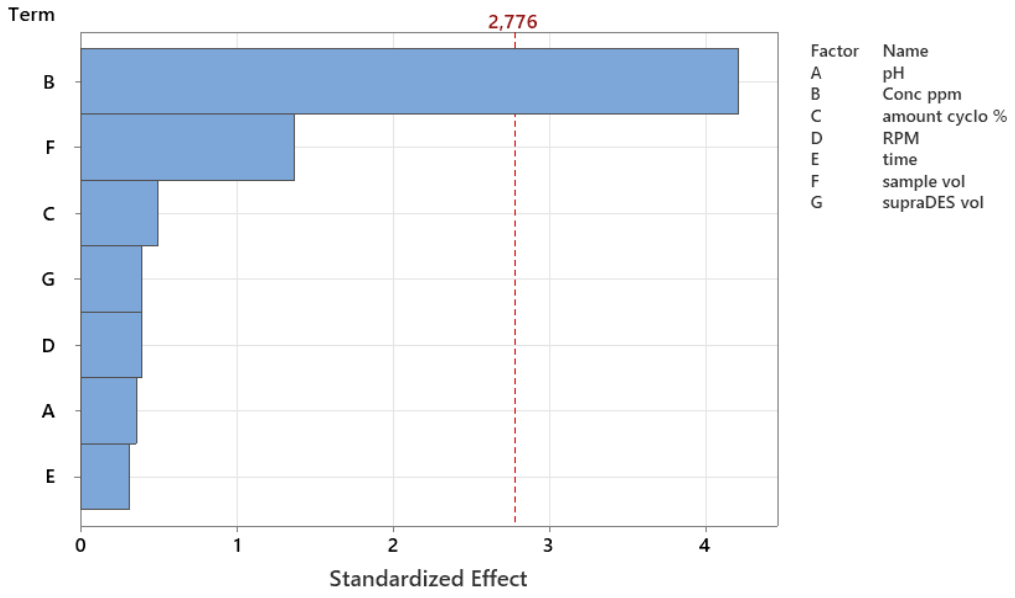

c)

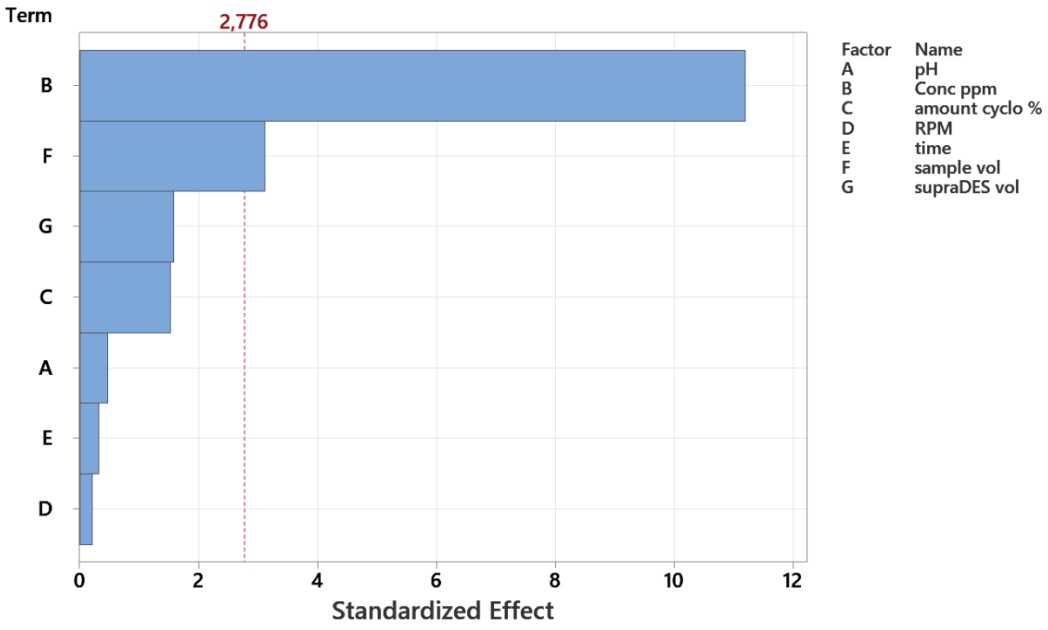

d)

Fig. 46. A Pareto Chart for the standardized effects, a) HQ, b) HMF, c) FF, d) VAN.

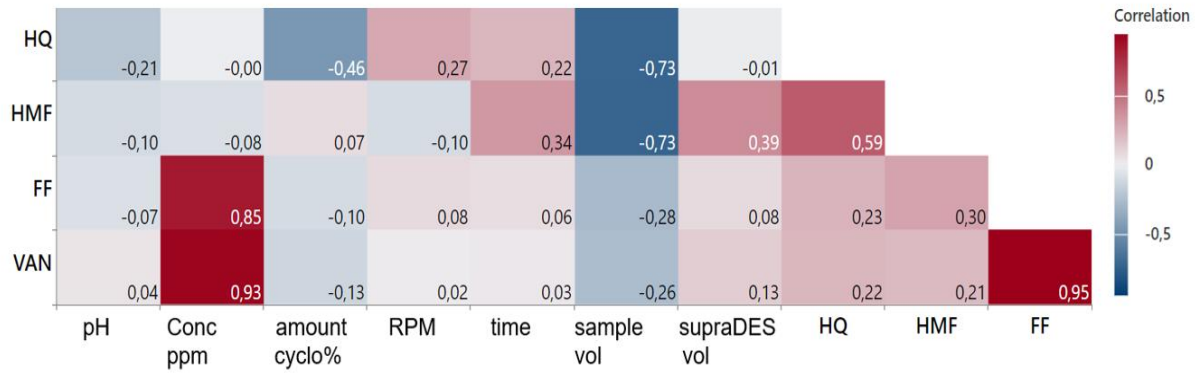

Fig. 47. Correlogram for the results and variables.

14.2. Characterization of SUPRADES

The physicochemical properties of SUPRADES, including viscosity, density, and surface tension, were evaluated under ambient conditions to gain insights into its behavior and performance. These properties play a fundamental role in determining the efficiency of mass transfer for inhibitory compounds within the solvent system. Density and viscosity are particularly crucial in chemical processes, as they directly influence fluid dynamics and mass transfer efficiency. Density provides essential data for fluid mechanics calculations and aids in the optimal design of chemical processes, ensuring accurate predictions of phase behavior. Viscosity, on the other hand, is indicative of a liquid's resistance to flow, which is governed by molecular interactions and structural arrangement [197, 198].

The measured density and viscosity of Ment:NA@MβCD were 898.53 kgm^{-3} and 222 mPa·s, respectively. The density was measured using a density densimeter (DMA 4500 M, Anton Paar, Graz, Austria), and the viscosity was determined using a BROOKFIELD LVDV-II+ viscometer (Labo-Plus, Warsaw, Poland). The high density suggests a closely packed molecular structure, a typical characteristic of DES containing organic acids and cyclic compounds. Moreover, the viscosity value, which is significantly higher than that of water and conventional organic solvents, highlights the presence of strong intermolecular forces and extensive hydrogen bonding between the constituents. The increased viscosity can also be attributed to MβCD, which contributes to steric hindrance and enhances the internal resistance to flow. These characteristics make Ment:NA@MβCD highly suitable for applications requiring enhanced solubilization, controlled diffusion, and selective extraction.

Additionally, the surface tension of Ment:NA@MβCD was found to be 28.9 $mN \cdot m^{-1}$, measured using a tensiometer (K11, KRÜSS, Germany). Compared to conventional DES formulations, this relatively low value indicates weaker intermolecular forces and reduced cohesive interactions within the system. A lower surface tension enhances the solvent's ability to spread across surfaces, improving film formation and interfacial interactions. This property is particularly advantageous in extraction and separation processes, where increased interfacial contact between phases can significantly enhance mass transfer efficiency.

Overall, the high density, elevated viscosity, and low surface tension of Ment:NA@MβCD demonstrate its unique physicochemical behavior, making it a promising solvent for specialized applications in extraction, separation, and targeted solubilization processes.

14.3. Effects of matrix composition in real sample

The performance of SUPRADES in extracting inhibitory compounds from real fermentation samples and model samples are presented in Fig. 48. Compared to model systems, a noticeable reduction in RE was observed for compounds such as HQ and VAN, with efficiencies dropping to 31.63% and 50%, respectively. This contrasts sharply with their extraction rates in simplified model media, where both exceeded 85%. Such discrepancies are largely attributed to the complex chemical environment present in real matrices.

HQ, a highly polar molecule with two hydroxyl groups, forms strong hydrogen bonds with surrounding water molecules. This feature restricts its migration into the hydrophobic domain of the extraction phase, particularly when pH and ionic strength conditions are suboptimal. Similarly, VAN possesses both hydroxyl and aldehyde functionalities, giving it partial polarity and amphiphilic character. This duality in solubility preference results in inconsistent partitioning between aqueous and organic phases, especially when competing molecules like organic acids or peptides are present.

The reduced extraction performance in real matrices also arises from the presence of co-solutes such as microbial metabolites, proteins, polysaccharides, and lignin-like macromolecules. These substances can bind to or shield the target inhibitors, limiting their accessibility to the extraction solvent. In addition, the relatively low concentrations of HQ and VAN in fermentation broth may weaken the mass transfer driving force, further hindering efficient removal [199].

In contrast, HMF demonstrated a higher removal efficiency in real samples (61.46%) than in the model system (55.2%), an outcome that was initially unexpected. This may be due to chemical transformations that HMF undergoes in fermentation environments, such as acid or base catalyzed degradation to levulinic acid and formic acid, polymerization into less water-soluble species, or reduction to 2,5-bis(hydroxymethyl)furan (BHMF). Furthermore, oxidative pathways may lead to the formation of 2,5-furandicarboxylic acid (FDCA), a compound with enhanced interaction potential with SUPRADES due to its increased polarity and functionality. These derivative forms of HMF, which may partition more readily into the extraction phase, collectively contribute to the observed improvement in extraction efficiency [200, 201].

FF, being less polar, showed the most consistent extraction profile across both sample types, with over 68% removal efficiency in the real sample closely matching the model value of 72.49%. Its hydrophobic character supports effective migration into the organic solvent phase, making it less susceptible to interference from matrix constituents.

So, the drop in RE for most compounds in real samples especially HQ and VAN can be attributed to matrix complexity, presence of interfering solutes, and lower target concentrations. Additionally, real matrices often contain components with functional groups (e.g., -OH, -COOH) that may interact with SUPRADES via hydrogen bonding or other intermolecular forces, reducing extraction specificity. These findings highlight the importance of considering real matrix effects in process optimization and suggest that strategies such as matrix pretreatment or solvent tuning may be required to enhance inhibitor removal under practical conditions.

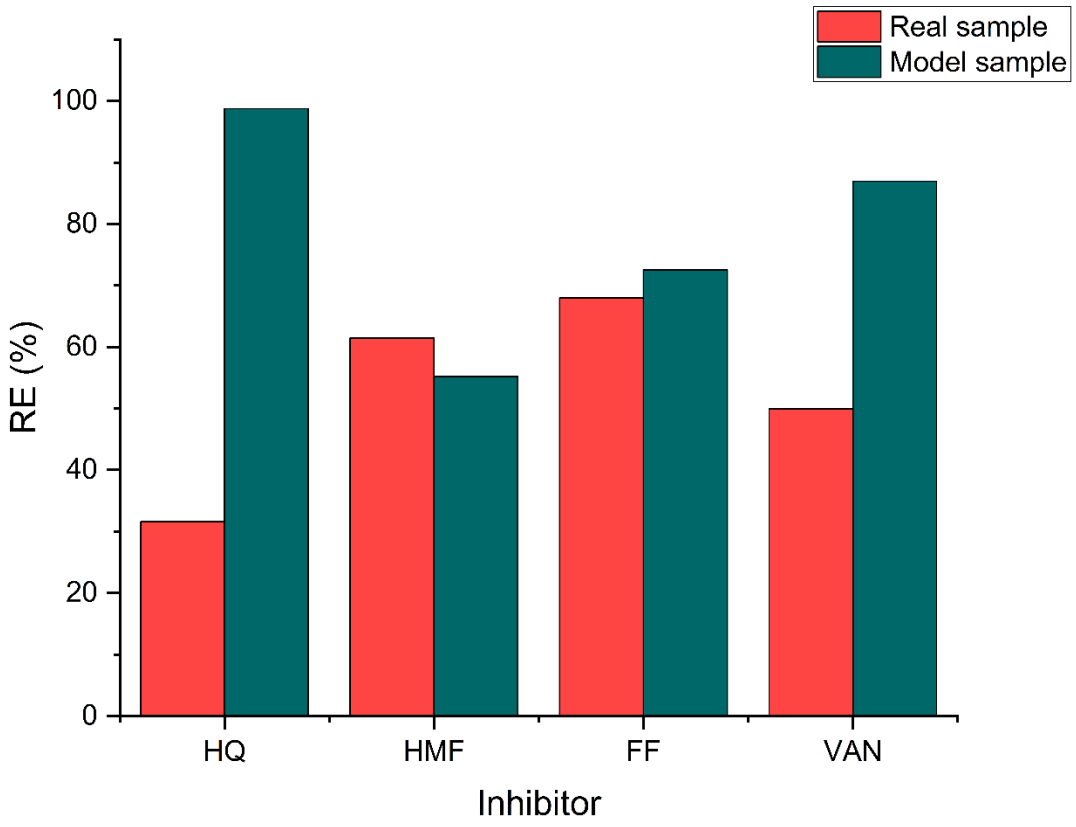

Fig. 48. Comparison of RE of inhibitory compounds in real and model fermentation samples using SUPRADES [202].

14.4. Comparison of SUPRADES with ordinary DES

When comparing the RE of SUPRADES (Menth:NA@MβCD) and conventional DES (Menth:NA) in extracting inhibitory compounds from model samples, a marked improvement is observed with SUPRADES, as illustrated in Fig. 49. This enhanced performance is mainly attributed to the integration of MβCD into the solvent, which introduces molecular recognition and complexation capabilities not found in traditional DES. The hydrophobic cavity within MβCD enables the

encapsulation of target compounds, improving their solubility and retention within the solvent, thereby resulting in significantly higher RE values for various inhibitors.

For instance, SUPRADES achieves a remarkable 98.75% RE for HQ, compared to only 67.44% with conventional DES. The substantial increase in efficiency is due to the specific interactions facilitated by MβCD's structure. The hydrophobic interactions and van der Waals forces within MβCD's cavity capture HQ molecules effectively, preventing re-release and stabilizing them within the solvent. Similarly, SUPRADES reaches an RE of 86.94% for VAN, which is much higher than the 61.35% obtained with DES. This further demonstrates how MβCD enhances the stability and specificity of the solvent.

A similar trend is seen with other inhibitory compounds. For FF, SUPRADES shows an RE of 72.49%, while DES only achieves 45.68%. The ability of MβCD to form dipole-dipole interactions, along with hydrophobic forces, increases the solvent's binding affinity for FF, resulting in more effective and sustained extraction. SUPRADES also outperforms DES in HMF removal, with an RE of 55.2%, compared to just 30.19% for DES, indicating that MβCD's interactions provide additional binding forces that DES lacks.

The enhanced effectiveness of SUPRADES can be attributed to the synergistic effects of improved solubility, stronger binding interactions, and the specific molecular recognition facilitated by MβCD. These characteristics enable SUPRADES to efficiently stabilize and retain inhibitory compounds, preventing their re-release into the solution. Consequently, SUPRADES emerges as a more reliable and efficient system for eliminating a wide array of inhibitory compounds, offering superior performance over conventional DES, particularly in applications where high selectivity and consistent extraction stability are essential.

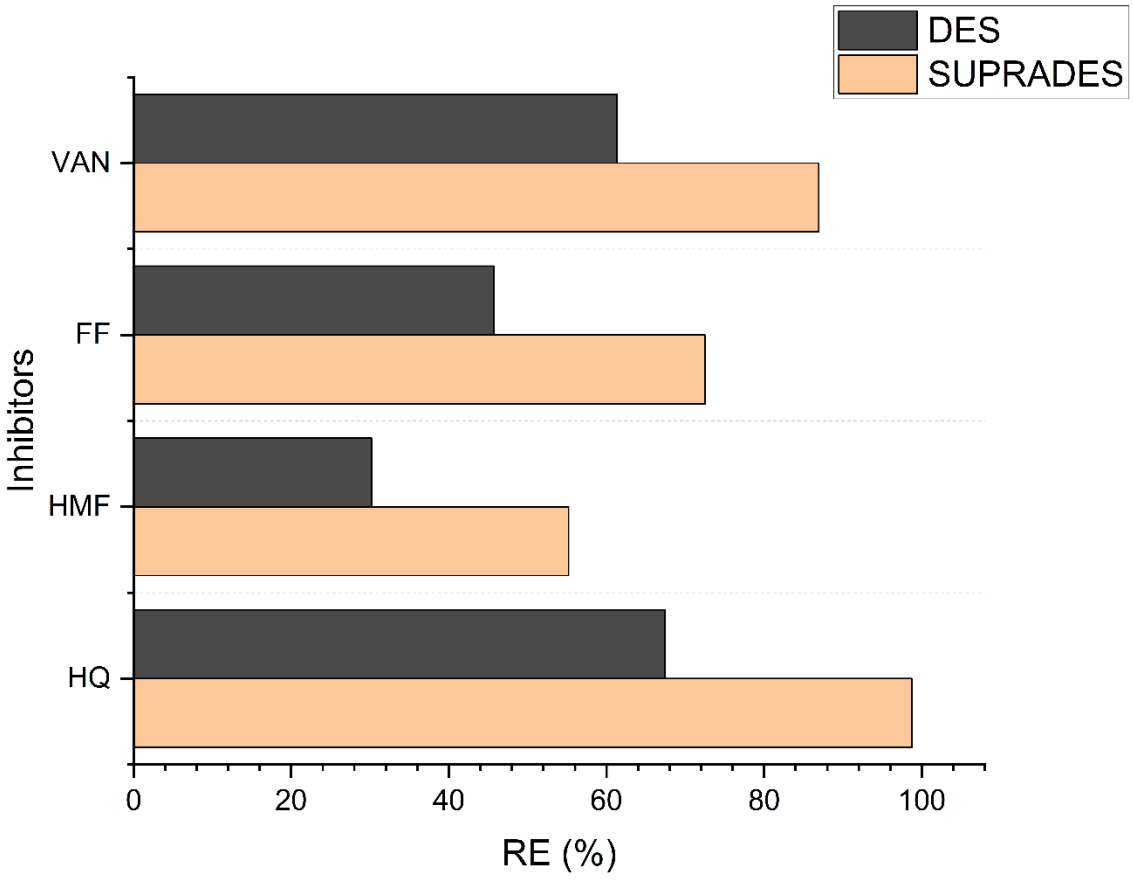

Fig. 49. Comparison of removal efficiency performance between SUPRADES and conventional DES under optimal conditions [202].

14.5. Reusability

Reusability is a critical factor in industrial processes, offering numerous benefits, such as enhancing sustainability, reducing the need for fresh materials, minimizing waste, and lowering costs. This, in turn, improves operational efficiency and promotes environmental friendliness. As shown in Fig. 50, the reusability of SUPRADES in the removal of inhibitor compounds reveals a progressive decline in RE% across six consecutive cycles. During the initial cycle, SUPRADES demonstrated excellent removal efficiencies, especially for HQ, where nearly 100% of the compound was removed. Vanillin also showed a strong performance, with approximately 85% removal efficiency. In contrast, HMF and FF displayed lower initial efficiencies, approximately 65% and 55%, respectively.

Over successive cycles, the efficiency of SUPRADES gradually decreased for all tested compounds. By the sixth cycle, HQ's removal efficiency had fallen to around 60%, while vanillin's decreased to approximately 50%. More significant reductions were observed for FF and HMF, with their efficiencies dropping to roughly 35% and 25%, respectively, by the final cycle. This reduction in

performance can likely be attributed to the saturation of active sites on the SUPRADES material or potential degradation of its extraction capability over time.

Despite these declines, SUPRADES maintained satisfactory removal efficiency, especially for HQ and vanillin, through the fourth cycle. The decreased performance in subsequent cycles highlights the need for either regeneration or replacement of the material after several uses to preserve optimal efficiency in practical applications.

Overall, while SUPRADES offers impressive initial removal capabilities for various inhibitor compounds, its effectiveness diminishes with extended use. This behavior indicates that SUPRADES is suitable for short-term applications, where high removal efficiency is required, but may not be ideal for long-term use without proper maintenance or replacement.

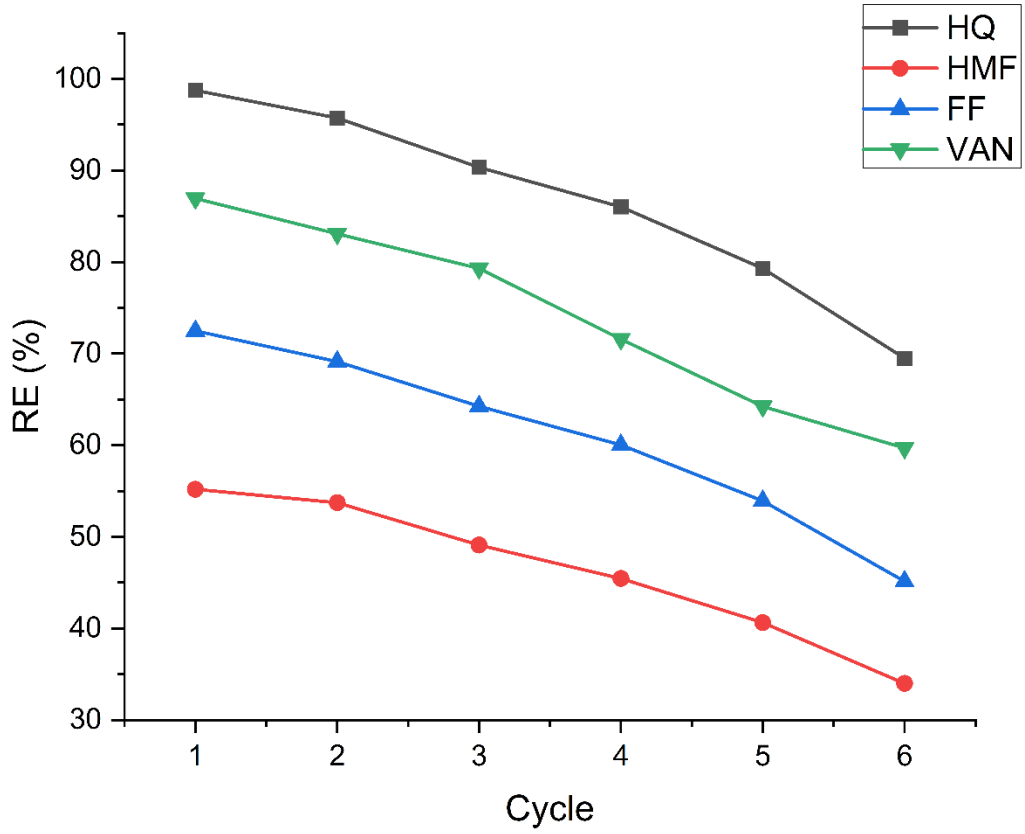

Fig. 50. Reusability of SUPRADES for removal efficiency of inhibitory compounds [202].

14.6. Mechanism of extraction

FTIR spectroscopy was employed to elucidate the interactions between SUPRADES and the inhibitory compounds, offering molecular-level insight into the extraction mechanism (Figs.51-54). Notable shifts in characteristic functional group bands after extraction indicate non-covalent interactions such as hydrogen bonding and dipole-dipole forces.

For HQ, shifts in the O-H and C=O stretching regions to lower wavenumbers, along with the appearance of bands at 916 cm^{-1} and 549 cm^{-1}, suggest strong hydrogen bonding between the solute and SUPRADES [203, 204]. Aromatic and hydroxyl group deformations observed in the 950-550 cm^{-1} range further support this interaction.

In the case of HMF, post-extraction spectra revealed O-H, C-H, and C=O stretching band shifts from 3384, 2873, and 1714 cm^{-1} to 3355, 2844, and 1704 cm^{-1}, respectively. These shifts indicate perturbation of the local environment due to solvent–solute interactions [158].

FF exhibited strong affinity for SUPRADES as evident from shifts in aldehyde C-H (2842.89 cm^{-1}), aromatic C=C (1600-1500 cm^{-1}), and furan ring-related C-O (1200-1000 cm^{-1}) and C-H out-of-plane bending bands (900-700 cm^{-1}). These observations confirm the role of hydrogen bonding and dipolar interactions in its extraction [205, 206].

Analysis of SUPRADES constituents showed characteristic bands: a broad O-H stretching region (3500-3000 cm^{-1}) attributed to MβCD and NA, C-H stretching between 2850-3000 cm^{-1} from menthol, a strong C=O peak at 1714 cm^{-1} from NA, and C-O-C stretches in 1000-1150 cm^{-1} and 900-950 cm^{-1} regions from glycosidic linkages in MβCD [207-209].

During FF extraction, the M:NA (1:2) mixture likely formed hydrogen bonds with FF, while MβCD contributed through inclusion complexation. Shifts in O-H (3384 to 3352 cm^{-1}), C=O, and C-O-C bands, alongside new bands at 592 cm^{-1} (shifting to 547 cm^{-1}), indicate substantial structural interactions [210, 211].

Vanillin's spectral features at 3170 and 1662 cm^{-1} (O-H and C=O stretching) also shifted upon extraction, confirming solvent–solute interaction and solubilization in SUPRADES [212].

Thus, FTIR analysis demonstrates that the extraction mechanism relies on a combination of hydrogen bonding, electrostatic attraction, and dipole-based interactions, enabling SUPRADES to efficiently stabilize and extract inhibitory compounds [213].

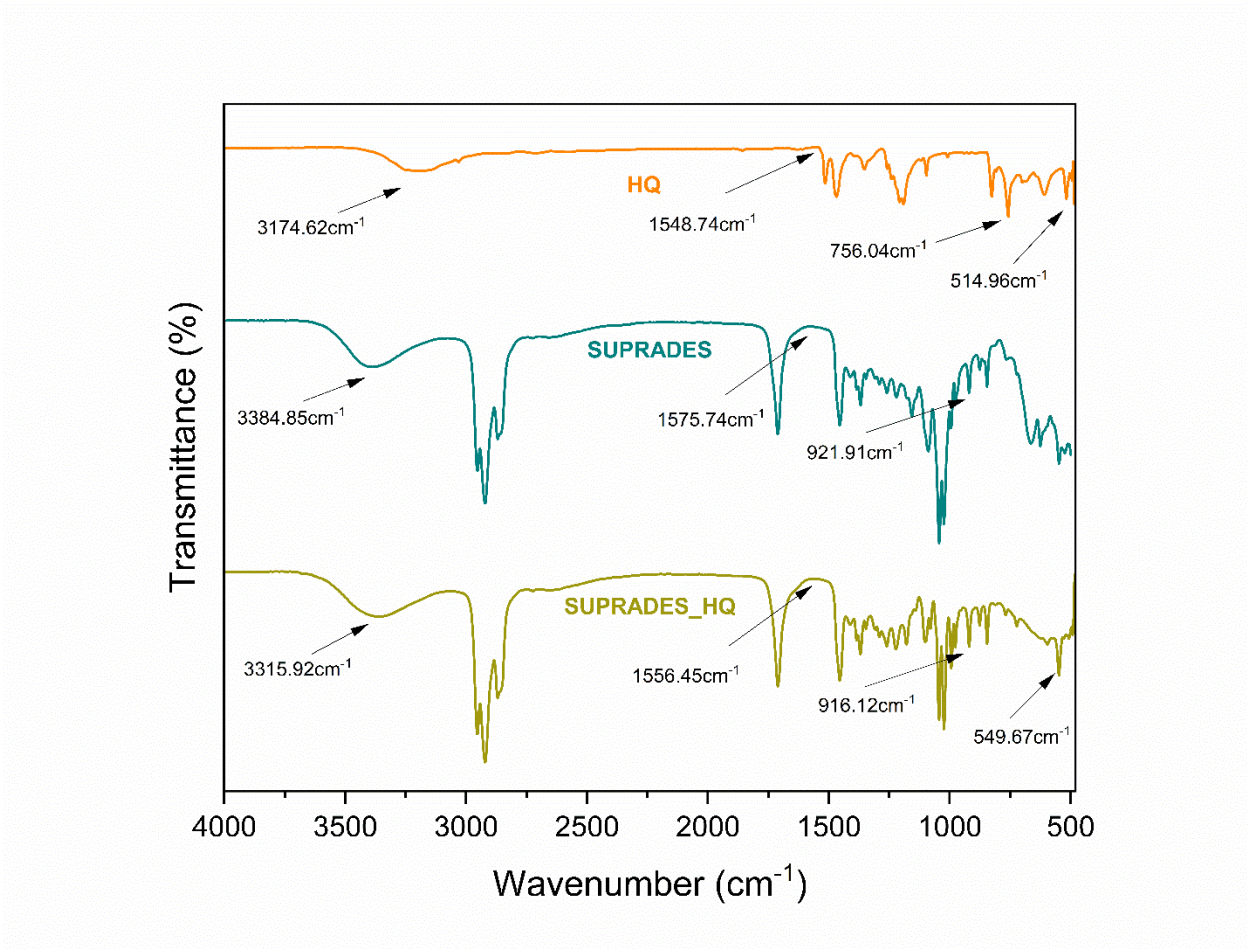

Fig. 51. FT-IR spectra of pure HQ, synthesized SUPRADES, and SUPRADES after HQ sorption [202] .

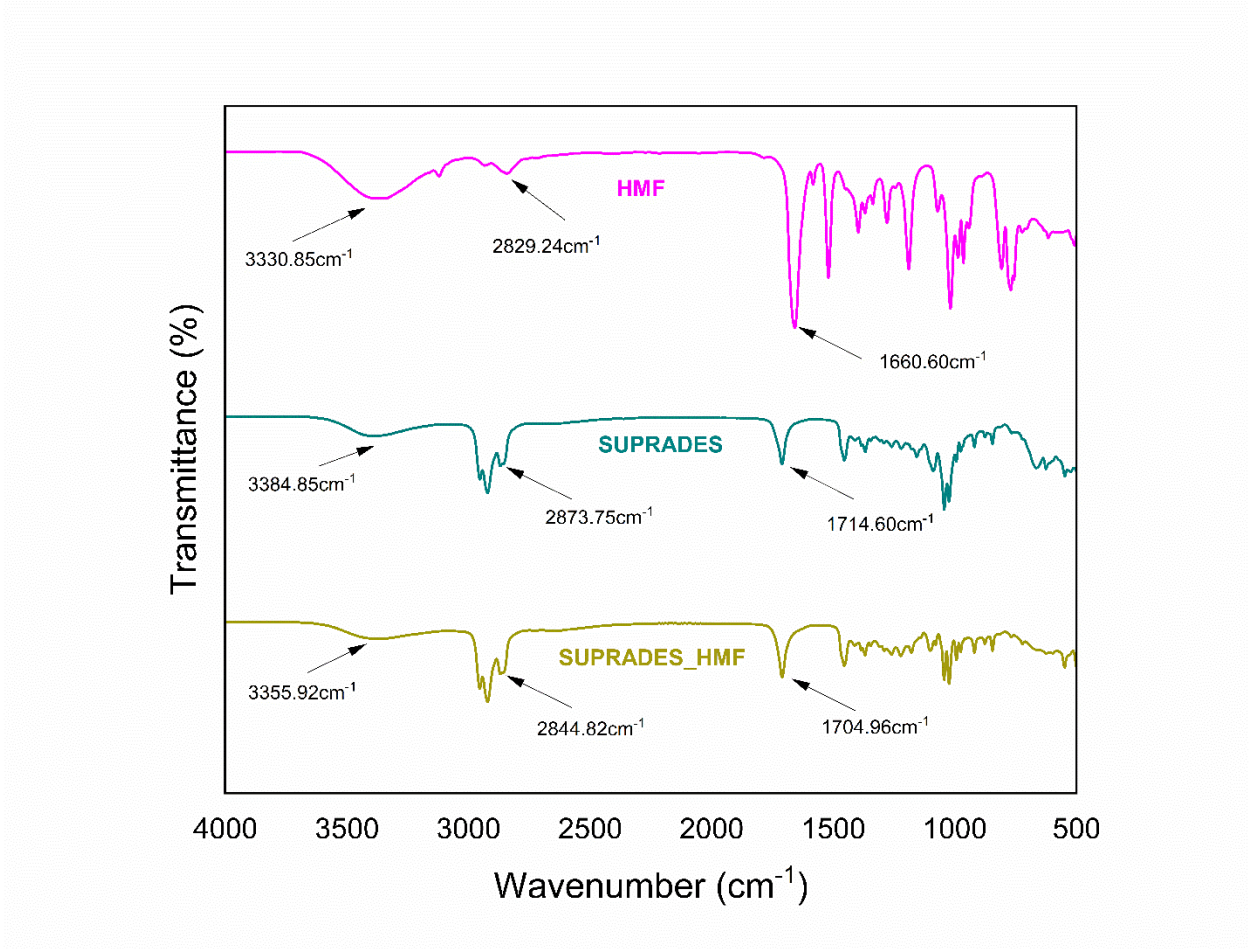

Fig. 52. FT-IR spectra of pure HMF, synthesized SUPRADES, and SUPRADES after HMF sorption [202].

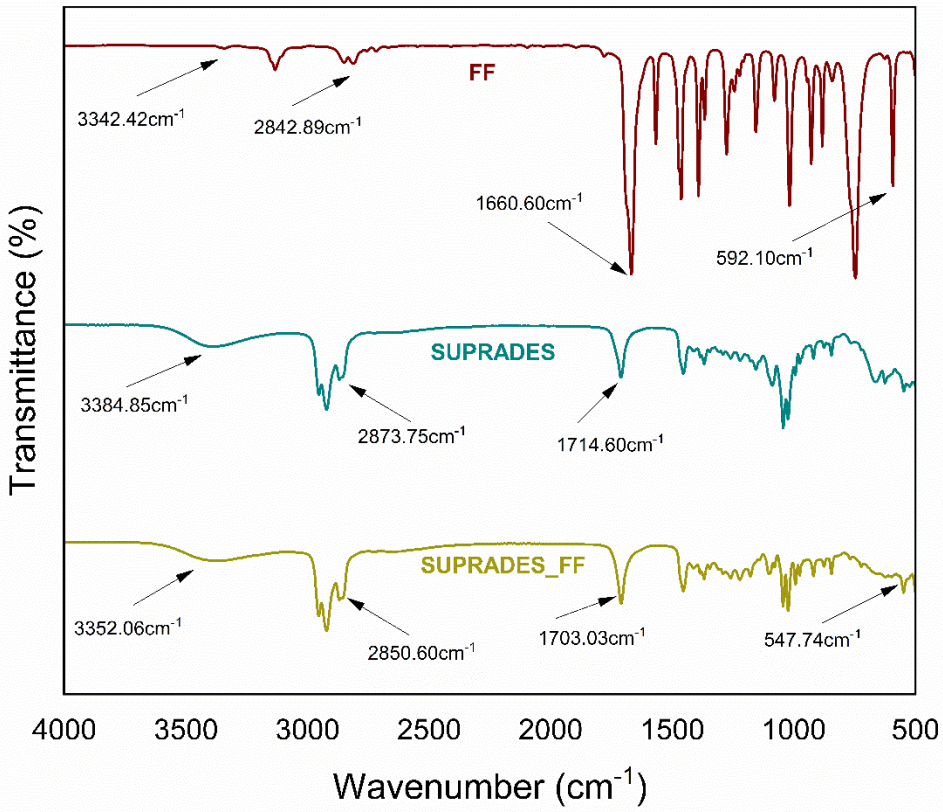

Fig. 53. FT-IR spectra of pure FF, synthesized SUPRADES, and SUPRADES after FF sorption [202].

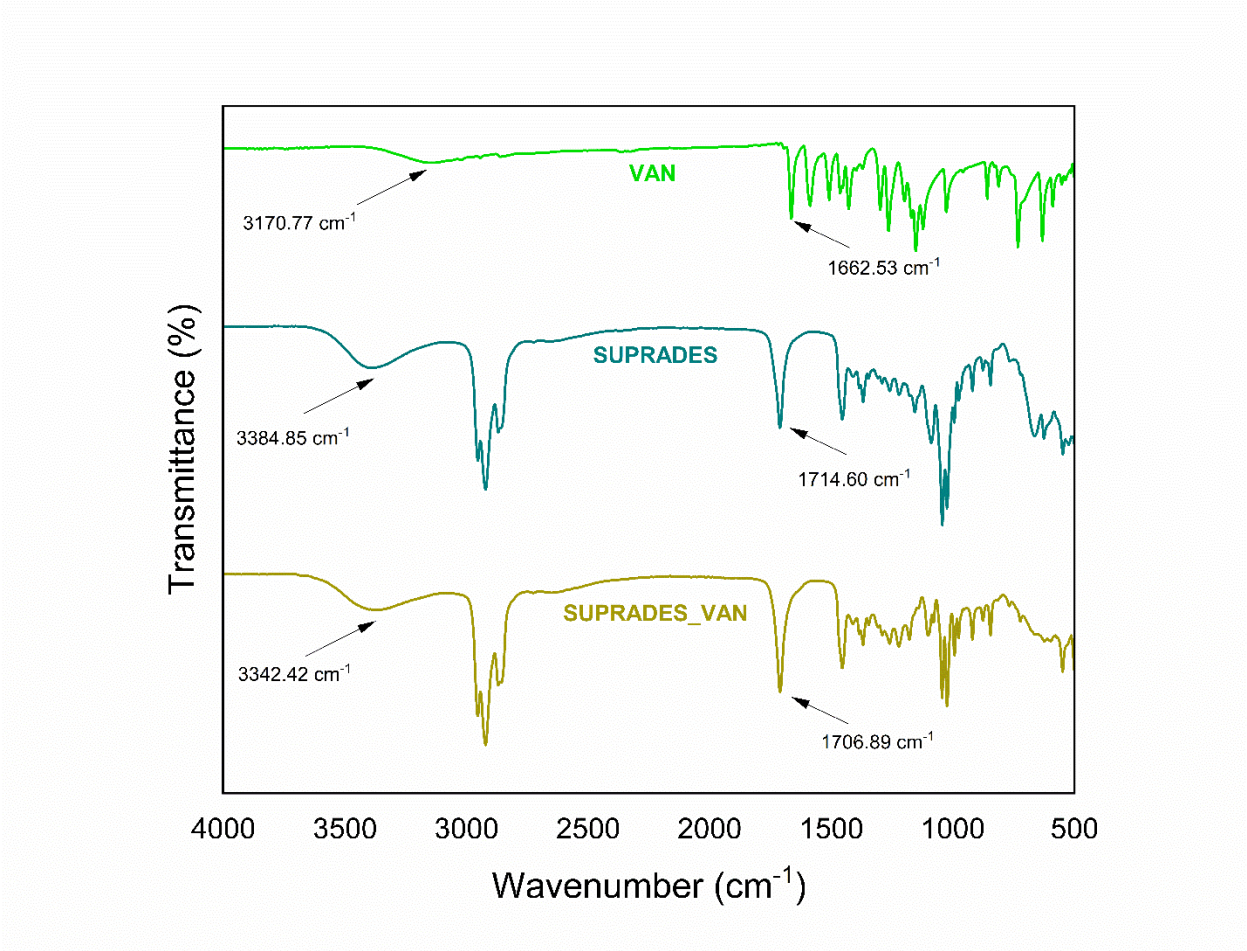

Fig. 54. FT-IR spectra of pure VAN, synthesized SUPRADES, and SUPRADES after VAN sorption [202].

14.7. Biohydrogen production performance

Gas composition during dark fermentation was assessed using calibration curves and flow rate measurements. *Enterobacter aerogenes* was employed as the fermentative microorganism, undergoing the typical four-phase growth pattern. Maximum hydrogen production occurred during the stationary phase, while the onset of the death phase, linked to nutrient depletion and methane-producing microbes, reduced net hydrogen output.

Fig.55 summarizes hydrogen production across four fermentation cycles in two bioreactors with different feedstocks. In the glucose control cycle, bioreactor 2 supplemented with casein produced significantly more hydrogen (0.0495 cm^3h^{-1}) than bioreactor 1 (0.0028 cm^3h^{-1}), highlighting the impact of nitrogen enrichment.

In Cycle 1, bio fraction waste was hydrolyzed with either 5% acetic acid (bioreactor 1) or SUPRADES (bioreactor 2). Bioreactor 2 achieved markedly higher hydrogen productivity (0.2188 cm^3h^{-}

^{1} vs. 0.0675 cm^3h^{-1}), indicating improved hydrolysate fermentability due to the SUPRADES pretreatment.

Cycle 2 confirmed this trend. Although bioreactor 1 showed improvement (0.1848 cm^3h^{-1}), bioreactor 2 still performed better (0.2134 cm^3h^{-1}). The slight efficiency drops in bioreactor 2 may relate to reduced nutrient availability or microbial fatigue, yet performance remained above control levels.

In Cycle 3, bioreactor 1 ceased hydrogen production entirely, likely due to inhibitory compounds remaining from acetic acid hydrolysis. In contrast, bioreactor 2 maintained stable production (0.1571 cm^3h^{-1}), underlining the detoxifying and stabilizing role of SUPRADES during hydrolysate preparation.

In conclusion, these findings underscore that the hydrolysis method significantly affects biohydrogen productivity. SUPRADES consistently improved microbial performance and hydrogen yield by reducing inhibitors and preserving fermentable substrates, positioning it as a promising strategy for large-scale hydrogen fermentation processes.

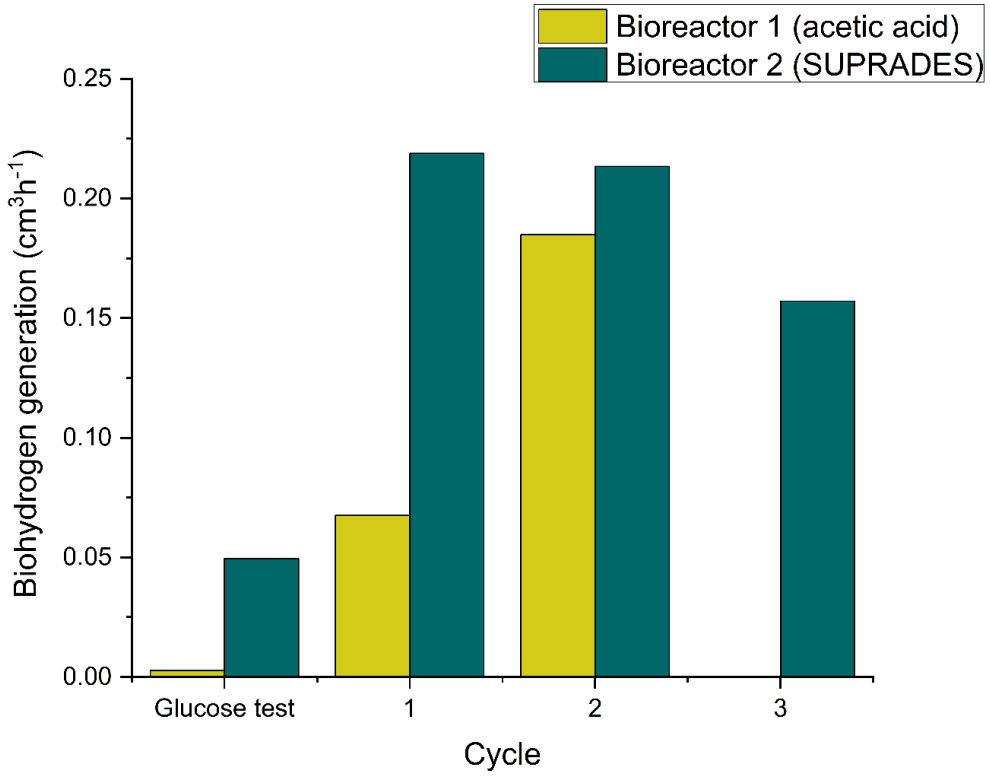

Fig. 55. Biohydrogen production rate in different cycles for Bioreactor 1 and Bioreactor 2 [202].

15. CONCLUSION ON SUPRADES

This study demonstrates that SUPRADES is a highly effective green solvent system for the removal of key inhibitory compounds generated during the hydrolysis of lignocellulosic biomass. Through systematic optimization of operational parameters, SUPRADES achieved high removal efficiencies in model samples, reaching 98.75% for HQ, 55.20% for HMF, 72.49% for FF, and 86.94% for VAN. These results indicate the establishment of optimal removal conditions tailored to target specific inhibitors effectively.

Under real-world conditions, although removal efficiency decreased due to the complexity of the hydrolysate matrix, significant extraction was still observed: 31.63% for HQ, 61.46% for HMF, 68.04% for FF, and 50% for VAN. These values confirm the practical applicability of SUPRADES, despite matrix interferences, in removing inhibitors from actual biomass hydrolysates.

When benchmarked against conventional approaches such as acetic acid pretreatment and unmodified DES systems, SUPRADES showed clear advantages. For instance, hydrogen yields from hydrolysates treated with SUPRADES were up to three times higher than those treated with acetic acid, highlighting its superior detoxification capability. Furthermore, incorporating Methyl-β-cyclodextrin (MβCD) into the SUPRADES formulation significantly enhanced its extraction performance, due to MβCD's molecular recognition and strong inclusion complexation, which facilitated more selective and efficient binding of inhibitory compounds. This gave SUPRADES a notable edge over other DES-based systems.

From a mechanistic perspective, the high removal efficiency of SUPRADES can be attributed to strong hydrogen bonding and dipole-dipole interactions with target molecules, coupled with the favorable physicochemical properties conferred by MβCD. Additionally, SUPRADES demonstrated good short-term reusability, maintaining high removal rates over four consecutive cycles before showing a decline, indicating its suitability for batch-wise applications and the potential need for regeneration strategies in extended use.

In summary, SUPRADES emerges as a promising pretreatment method for biohydrogen production processes, offering high inhibitor removal efficiency, environmental compatibility, operational simplicity, and the potential to outperform conventional methods. Its application can significantly improve microbial fermentation outcomes while minimizing ecological impact, making it a valuable tool for advancing sustainable biofuel technologies.

16. COMPARATIVE EVALUATION OF HMDES, MOF@PSEUDO-DES, AND SUPRADES FOR INHIBITOR REMOVAL

Efficient removal of inhibitory compounds such as HQ, HMF, FF, and VAN is crucial in the pretreatment and fermentation steps of lignocellulosic biomass conversion. In this study, three novel extraction and sorption systems HMDES, MOF@pseudo-DES, and SUPRADES were developed and systematically compared not only with each other, but also with previously reported methods (Fig.56 and Table 7). The evaluation was based on critical performance indicators including RE, contact time, operating conditions (temperature and pH), solvent-to-hydrolysate volume ratio, and environmental impact.

HMDES demonstrated rapid and highly selective removal of all four inhibitors, achieving REs above 80% within just 15 minutes. The highest REs was observed for HQ (92.97%) and VAN (95.12%), making it one of the most effective methods reported to date. Its operation at room temperature (20°C), pH 8, and magnetic separability eliminates the need for centrifugation or phase separation, making it ideal for scalable and fast extraction processes. In comparison, traditional solvents such as isobutyl acetate or toluene require 120-240 minutes to reach comparable efficiency for FF, while failing to remove HQ and VAN.

MOF@pseudo-DES enabled balanced removal of HQ (62.08%), HMF (56.09%), FF (62.08%), and VAN (83.46%) within a contact time of 11 minutes. The presence of amino-functional groups within the MOF facilitates hydrogen bonding with polar inhibitors, while pseudo-DES improves sorbent compatibility with aqueous systems. Its environmental credentials are enhanced by using biodegradable choline chloride and its ability to operate under mild conditions (20°C, pH 5.8). Although its performance was slightly lower than that of HMDES and SUPRADES, MOF@pseudo-DES outperforms ionic liquids like [C6mim][PF6] [214] and traditional solvents by offering higher selectivity for all four inhibitors in a much shorter time frame.

SUPRADES emerged as the most selective and environmentally sustainable system, achieving 98.75% RE for HQ and high removal for VAN (86.94%), FF (72.49%), and moderate efficiency for HMF (55.20%). This method uses completely biodegradable and green materials (menthol, nonanoic acid, methyl-β-cyclodextrin) and functions efficiently at pH 9 and 20°C within 60 minutes. Unlike ionic liquids or aromatic solvents like thymol or toluene, SUPRADES presents no environmental hazard and avoids the complexity of nanoparticle recovery seen in HMDES.

Traditional extraction solvents such as isobutyl acetate and toluene often display good RE for FF (up to 98.1%) and moderate for HMF (76.6%), but they are ineffective against HQ and VAN and require long extraction times (120-240 minutes). Ionic liquids such as [C6mim][PF6] [214] have good REs for HMF and FF but pose toxicity and cost concerns. Thymol-based systems work in highly acidic conditions (pH 3.6), limiting their application in real hydrolysates.

Recently reported systems like ChCl@MIL-101(Cr) [215] and GO-ZIF-67 composites [216] show promise for pesticide and drug extraction but lack selectivity for HQ or VAN. Other MOF and DES-based hybrids such as amorphous UiO-66 + DES [217] or MUiO-66-NH_2 + [BTBAC][Lac] [218] have shown efficiency for specific pharmaceuticals but not for typical lignocellulosic inhibitors.

In contrast to conventional extraction methods many of which are limited in selectivity, require long contact times, or involve hazardous solvents the three innovative systems developed in this study offer efficient, environmentally friendly, and fast solutions for removing a broader spectrum of inhibitory compounds. These methods operate under milder conditions, achieve higher removal efficiencies, and eliminate the need for intensive separation steps.

Each system offers distinct advantages that cater to different operational priorities. The SUPRADES system, based on biodegradable components such as menthol, nonanoic acid, and methyl-β-cyclodextrin, demonstrated the highest removal efficiency for HQ and VAN and is most suitable when selectivity and environmental safety are of primary concern. HMDES is a magnetically recoverable system that offers rapid extraction within 15 minutes and is particularly advantageous for industrial settings that require fast, scalable processes with minimal energy input. Meanwhile, MOF@pseudo-DES presents a structurally tunable and highly porous sorbent system, functionalized with ChCl-based pseudo-DES, providing fast kinetics and compatibility with a wide range of hydrolysate compositions while maintaining operation under near-neutral pH and ambient temperature.

Collectively, these three methods significantly outperform conventional solvent-based and ionic liquid-based approaches in key parameters such as removal efficiency, process time, environmental impact, and applicability across diverse hydrolysate matrices. They represent a new generation of sorbent technologies that combine selectivity, sustainability, and operational efficiency paving the way for scalable and eco-friendly purification processes in biomass valorization.

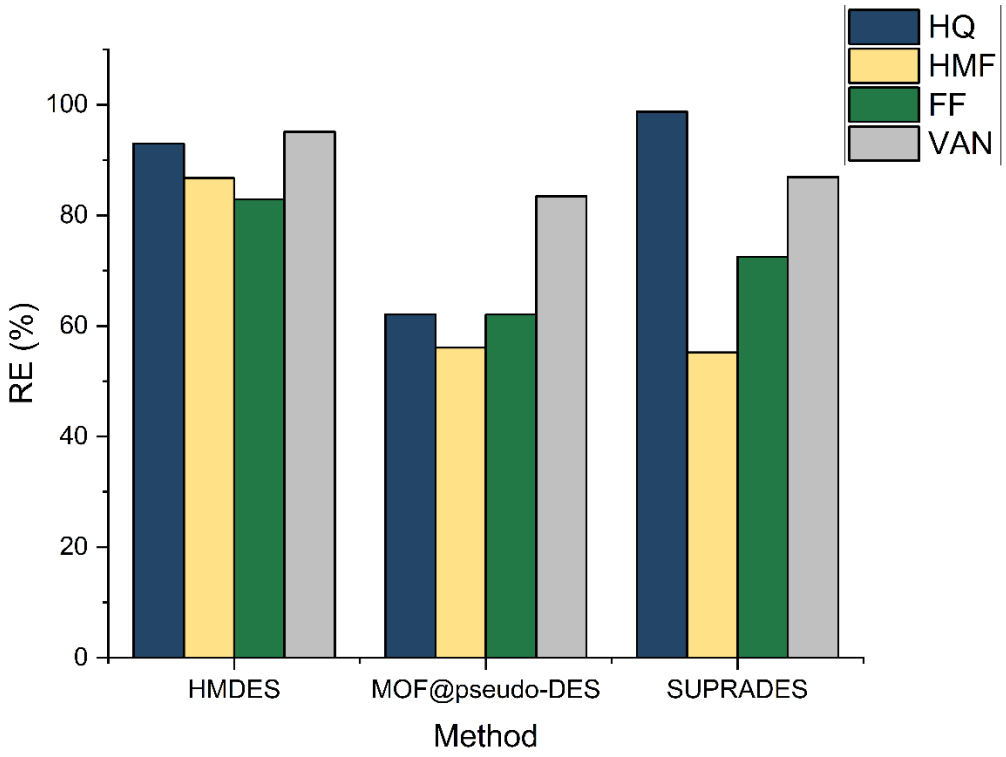

Fig. 56. Comparison of removal efficiencies for inhibitory compounds using HMDES, MOF@pseudo-DES and SUPRADES methods.

Table 7. Comparative overview of green and conventional methods for inhibitor removal from lignocellulosic hydrolysates

Method	RE (%)	Contact Time (min)	Temp (°C)	Green chemistry profile	Reusability	Selectivity (number of inhibitors)	Phase separation	ref
HMDES	Very high (up to 95%)	15	20	Biodegradable, Magnetic	Excellent (≥13 cycles)	Broad-spectrum (4 inhibitors)	Magnetic	this study
SUPRADES	Very high (up to 98%)	60	20	Fully green, biodegradable	High	Moderate (3-4 inhibitors)	Simple (phase split)	This study
MOF@pseudo-DES	High (up to 83%)	1	20	Partially green	Moderate (6 cycles)	Broad-spectrum (4 inhibitors)	Centrifuge	This study
Isobutyl Acetate	Moderate-High	240	25	Non-green, volatile	Poor	Limited (1-2 inhibitors)	Evaporation	[110]
Toluene	Low-Moderate	120	25	Hazardous	Poor	Limited	Evaporation	[111]
[C6mim][PF6]	Moderate-High	30	25	Nonbiodegradable	Limited	Moderate	Slow separation	[214]
Thymol:DecAc	Moderate (HMF only)	120	30	Natural but acidic	N/A	Single inhibitor (HMF)	Phase separation	[219]
Camphor:OA	High (up to 86.71%)	60	40	Semi-green	N/A	FF & HMF	Phase split	[142]
C:DOL (1:2)	Moderate-High	240	40	Green (natural solvents)	N/A	2 inhibitors (FF, HMF)	Phase split	[108]
Ment:Th:$FeCl_3$	High (up to 98.5%)	30	25	DES + metal salt	Limited	2 inhibitors (FF, HMF)	Requires separation	[141]
ChCl@MIL-101(Cr)	High (insecticide)	30	25	DES + MOF	Limited	Not for lignocellulosic inhibitors	N/A	[220]
GO-ZIF-67 composites	High (drugs)	50	N/A	MOF + GO + DES	Limited	Not lignocellulosic inhibitors	Centrifuge	[216]
Amorphous UiO-66 + DES	High (pesticides)	120	25	DES based	N/A	Non-specific inhibitors	Phase separation	[217]

17. SUMMARY, SCIENTIFIC NOVELTY, AND PURPOSE OF THE DOCTORAL DISSERTATION

The purpose of this doctoral dissertation is to develop and evaluate novel, efficient, and environmentally sustainable sorption-based methods for the removal of fermentation inhibitors generated during the hydrolysis and fermentation of lignocellulosic biomass. The accumulation of compounds such as HQ, HMF, FF, and VAN negatively affects microbial activity and biohydrogen production. Therefore, this research explores three distinct approaches: HMDES, SUPRADES, and a NH_2-UiO-66@pseudo-DES.

These methods were systematically studied in both model and real hydrolysates to assess their removal performance, reusability, and impact on fermentation outcomes. The goal was not only to eliminate inhibitors but also to improve hydrogen yield, operational stability, and process scalability. Ultimately, this work aims to provide practical and scalable solutions for industrial biorefinery systems, enabling more efficient and greener biofuel production.

These three sorption methods present a novel approach, as they have not been previously utilized in the literature for the removal of inhibitors from fermentation broth. It must be clearly stated that this is a new approach that has not yet been explored in the scientific literature, making it a significant contribution to the field.

The two sorption methods, UiO-66@pseudo-DES and SUPRADES, have never been applied to remove inhibitory compounds from the fermentation medium before or after fermentation. However, limited studies have been conducted on DES and Magnetic DES (MDES). Makoś et al. employed HDES to remove HMF and furfural from feedstocks intended for biofuel production (108). Dietz et al. examined the potential of HDES for extracting HMF and FF from biomass (111). In a comparative study, Makoś et al. evaluated 56 green HDES models for extracting inhibitors such as HMF, FF, and LA from fermentation media following biomass pretreatment (142). Similarly, Dietz et al. assessed the efficiency of eight different HDES types in extracting FF and HMF from biomass (219). Furthermore, Makoś et al. investigated the application of MDES for extracting FF and HMF from hydrolysis broth (141). However, these methods have primarily focused on the removal of inhibitors before fermentation rather than after the process.

In contrast, this study focuses on hydrophobic magnetic DES (HMDES) for the removal of four inhibitory compounds (HQ, HMF, FF, VAN) before and after fermentation, highlighting its distinct scientific novelty. Additionally, the application of HMDES for extracting inhibitory compounds from real anaerobic digestion samples represents one of the first reported advancements in this field. Therefore, these methods can be classified as novel approaches that have not yet been used for inhibitor removal at both stages of fermentation.

As a result, the newly proposed methods HMDES, SUPRADES, and MOF@pseudo-DES offer efficient, sustainable, and customizable solutions for the removal of inhibitory compounds from

fermentation broth. Their application leads to enhanced fermentation efficiency and improved product yields, making them a promising advancement in biomass processing and biofuel production.

The scientific relevance and effectiveness of these methods have been validated in peer-reviewed publications, including:

- Z. Honarmandrad, K. Kucharska, M. Kaykhaii, J. Gębicki, Removal of phenolic inhibitor compounds from hydrolysates and post-fermentation broths by using a hydrophobic magnetic deep eutectic solvent, *Journal of Environmental Chemical Engineering*, 12(3), 112621 (2024).
- Z. Honarmandrad, S.S.M. Khadem, K. Kucharska, M. Kaykhaii, J. Łuczak, J. Gebicki Enhanced sorption of inhibitory compounds from fermentation broth using a MOF@pseudo-DES composite, *Journal of Molecular Liquids*, 421, 126845 (2025).
- Z. Honarmandrad, K. Kucharska, E. Słupek, J. Cydejko, I. Strzelczyk, M. Kaykhaii J. Gębicki, SUPRADES: A novel approach for inhibitor compound removal from hydrolysates with concurrent enhancement of biohydrogen production, *International Journal of Hydrogen Energy*, 135, 361-371 (2025).

18. GENERAL CONCLUSIONS

This doctoral research aimed to develop and assess innovative, sustainable, and sorption-based strategies for the removal of fermentation inhibitors generated during the hydrolysis and fermentation of lignocellulosic biomass. The accumulation of compounds such as HQ, HMF, FF, and VAN impairs microbial activity and significantly reduces biohydrogen yield, making their effective removal a critical target in biorefinery operations.

To address this challenge, three novel sorbent systems were developed and evaluated:

Hydrophobic magnetic deep eutectic solvents (HMDES)

Supramolecular deep eutectic solvents (SUPRADES)

A functionalized metal-organic framework, NH_2-UiO-66@pseudo-DES

Each system was tested under both model and real conditions. The results confirmed their technical feasibility, environmental compatibility, and potential for industrial application.

HMDES exhibited excellent removal performance under optimized conditions (pH 8.0, 15 min, 1200 rpm, ambient temperature), achieving over 80% efficiency for all target inhibitors, even in real hydrolysates and fermentation broths. Its magnetic separability and stability over 13 reuse cycles further enhanced its practicality for continuous operations.

SUPRADES showed the highest removal efficiency for HQ (98.75%) and significantly improved biohydrogen production up to threefold compared to conventional acid pretreatment. Its superior performance in preserving essential nutrients and minimizing toxicity highlights its strong potential as a green detoxification agent. However, a gradual decline in performance after four cycles suggests the need for further research into regeneration protocols.

NH_2-UiO-66@pseudo-DES demonstrated fast adsorption kinetics (11 min), broad selectivity, and mild operational conditions (pH 5.8, 20°C). While its removal rates were slightly lower than the other methods in real matrices, its operational simplicity, structural tunability, and eco-friendliness offer advantages in applications requiring tailored sorbent design.

Extraction mechanism studies revealed that the main sorption mechanisms were governed by hydrogen bonding, π-π stacking, electrostatic forces, and van der Waals interactions. Compared to conventional solvents such as toluene and isobutyl acetate, the proposed sorbents exhibited superior removal efficiency, faster kinetics, lower energy demand, and reduced environmental impact.

While each method has distinct advantages, a comparative analysis indicates that HMDES is best suited for rapid, reusable, and scalable operations, SUPRADES for biohydrogen-oriented pretreatment, and NH_2-UiO-66@pseudo-DES for eco-compatible selective detoxification under mild conditions.

These findings represent a substantial scientific contribution, especially given the first-time application of these systems to real post-fermentation matrices. Moreover, they provide a foundation for integrating such technologies into industrial biorefineries.

Limitations such as matrix interference, partial inhibitor selectivity, and the need for regeneration strategies remain, but do not undermine the practical value of these systems.

In conclusion, this research delivers three robust, scalable, and green detoxification approaches that can significantly enhance the efficiency of biohydrogen production. With further optimization, they hold strong potential to revolutionize inhibitor management in sustainable biorefinery systems.

*Comprehensive literature review on the formation of inhibitors during biomass hydrolysis and their impact on fermentation efficiency:

A detailed literature review confirmed that HQ, HMF, FF, and VAN are major phenolic inhibitors formed during hydrolysis, and their accumulation significantly reduces microbial viability and hydrogen production efficiency.

*Synthesis of novel green solvents, including hydrophobic magnetic deep eutectic solvents (HMDES), SUPRADES, and MOF-based pseudo-DES:

All three sorbents HMDES, SUPRADES, and NH_2-UiO-66@pseudo-DES were successfully synthesized and applied for the first time in the removal of fermentation inhibitors from lignocellulosic biomass.

* Physicochemical characterization of the developed methods:

SUPRADES were characterized by density, viscosity, and surface tension measurements, while MOF@pseudo-DES was extensively analyzed using FTIR, XRD, SEM, BET, and TGA techniques.

*Optimization of extraction conditions for maximum inhibitor removal using statistical models like Plackett–Burman and Box–Behnken designs:

The extraction conditions were optimized using Plackett-Burman and Box-Behnken design models, identifying vortex time, pH, analyte concentration, and sorbent dosage as significant variables.

*Comparison of performance between the proposed green solvents and conventional methods in terms of efficiency, selectivity, and reusability:

The proposed green solvents outperformed conventional solvents such as toluene and ionic liquids by offering higher removal efficiency, shorter extraction times, better selectivity, and excellent reusability over multiple cycles.

*Application of the optimized systems to real fermentation broths to validate performance under practical conditions:

The sorption systems were successfully applied to real hydrolysates; however, data from post-fermentation broths were limited and excluded from final analysis due to lack of HQ detection. *Evaluation of biohydrogen production improvement after detoxification, confirming the positive impact of inhibitor removal on microbial hydrogen generation:

The removal of inhibitory compounds using HMDES and SUPRADES enhanced hydrogen yields during fermentation, confirming the effectiveness of detoxification in improving microbial performance.

19. FUTURE RESEARCH DIRECTIONS

Based on the promising results of this research, several directions can be followed in future studies:

- ✓ Improving Reusability and Regeneration Methods: While HMDES showed good performance over 13 cycles, SUPRADES lost efficiency after 4 uses. Future work should focus on developing easy and cost-effective regeneration methods, such as using activated carbon, vacuum drying, or green solvents, to extend the lifespan of these sorbents.
- ✓ Better Understanding of Extraction Mechanisms: Although FTIR analysis provided useful insights, more advanced tools such as NMR spectroscopy, in-situ Raman analysis, or molecular dynamics simulations can help better understand how the inhibitors interact with the sorbents at the molecular level.
- ✓ Testing in Real Industrial or Continuous Systems: To evaluate how practical these methods are for industrial use, they should be tested in pilot-scale or continuous flow systems where pH, temperature, and inhibitor levels may vary. This will help confirm their reliability under real working conditions.
- ✓ Designing New or Combined Sorbents: Future research can explore new materials, such as biodegradable magnetic DESs or MOFs combined with other functional materials (e.g., carbon-based nanomaterials or enzymes), to improve removal efficiency and selectivity.
- ✓ Application in Other Bioprocesses: Since similar inhibitory compounds are also found in other bioprocesses like bioethanol or biobutanol production, these extraction systems could be tested in those processes to widen their range of application.
- ✓ Life Cycle and Economic Assessments: Performing life cycle analysis (LCA) and techno-economic assessment (TEA) will help evaluate the environmental impact and economic feasibility of these methods and guide their development for large-scale and sustainable use.

These future studies can help improve the performance, stability, and practical application of the developed systems and support their integration into cleaner and more efficient biorefinery processes.

REFERENCES

1. Kaltschmitt M, Streicher W, Wiese A. Renewable energy: technology, economics and environment: Springer Science & Business Media; 2007.

2. Twidell J. Renewable energy resources: Routledge; 2021.

3. Shankar S, Shikha. Renewable and Nonrenewable Energy Resources: Bioenergy and Biofuels. In: Singh RL, editor. Principles and Applications of Environmental Biotechnology for a Sustainable Future. Singapore: Springer Singapore; 2017. p. 293-314.

4. Oladeji J. Environmental and Health Implications of Processing, Harvesting, Distribution and Using both Renewable and Non-renewable Energy Sources. Journal of Energy Technologies and Policy. 2015;5(7):40-5.

5. Peng L, Fu D, Chu H, Wang Z, Qi H. Biofuel production from microalgae: a review. Environmental Chemistry Letters. 2020;18:285-97.

6. Lelieveld J, Klingmüller K, Pozzer A, Burnett R, Haines A, Ramanathan V. Effects of fossil fuel and total anthropogenic emission removal on public health and climate. Proceedings of the National Academy of Sciences. 2019;116(15):7192-7.

7. Inumaru J, Hasegawa T, Shirai H, Nishida H, Noda N, Ohyama S. 1 - Fossil fuels combustion and environmental issues. In: Ozawa M, Asano H, editors. Advances in Power Boilers. 2: Elsevier; 2021. p. 1-56.

8. Patrick DL, Murray TP, Sullivan R, Kimmell K. Health & environmental effects of air pollution. Commonwealth of Massachusetts Departement of Environmental Protection MassDepp. 2015.

9. Usikalu M. Health impact of climate change due to combustion of fossil fuel. International Journal of Physical Sciences. 2009;4(13):880-4.

10. Caldeira K, Bala G, Cao L. The science of geoengineering. Annual Review of Earth and Planetary Sciences. 2013;41:231-56.

11. Raftery AE, Zimmer A, Frierson DM, Startz R, Liu P. Less than 2 C warming by 2100 unlikely. Nature climate change. 2017;7(9):637-41.

12. Doney SC, Fabry VJ, Feely RA, Kleypas JA. Ocean acidification: the other CO2 problem. Annual review of marine science. 2009;1:169-92.

13. Lubchenco J, McNutt MK, Dreyfus G, Murawski SA, Kennedy DM, Anastas PT, et al. Science in support of the Deepwater Horizon response. Proceedings of the National Academy of Sciences. 2012;109(50):20212-21.

14. Alrikabi N. Renewable energy types. Journal of Clean Energy Technologies. 2014;2(1):61-4.

15. Ellabban O, Abu-Rub H, Blaabjerg F. Renewable energy resources: Current status, future prospects and their enabling technology. Renewable and sustainable energy reviews. 2014;39:748-64.

16. Stančin H, Mikulčić H, Wang X, Duić N. A review on alternative fuels in future energy system. Renewable and Sustainable Energy Reviews. 2020;128:109927.

17. Srirangan K, Akawi L, Moo-Young M, Chou CP. Towards sustainable production of clean energy carriers from biomass resources. Applied energy. 2012;100:172-86.

18. Sriram N, Shahidehpour M, editors. Renewable biomass energy. IEEE Power Engineering Society General Meeting, 2005; 2005: IEEE.

19. Reddy B, Srinivas T, editors. Biomass based energy systems to meet the growing energy demand with reduced global warming: role of energy and exergy analyses. 2013 International Conference on Energy Efficient Technologies for Sustainability; 2013: IEEE.

20. Byrne J, Kurdgelashvili L, Mathai M, Kumar A, Yu J, Zhang X, et al. World solar energy review: technology, markets and policies. Center for Energy and Environmental Policies Report. 2010.

21. Kaygusuz K. Wind power for a clean and sustainable energy future. Energy Sources, Part B. 2009;4(1):122-33.

22. Wang Q, Yang T, editors. Sustainable hydropower development: international perspective and challenges for China. 2011 International Conference on Multimedia Technology; 2011: IEEE.

23. Yan Q, Wang A, Wang G, Yu W, Chen Q, editors. Resource evaluation of global geothermal energy and the development obstacles. 2010 International conference on advances in energy engineering; 2010: IEEE.

24. Ishaq H, Dincer I. Comparative assessment of renewable energy-based hydrogen production methods. Renewable and Sustainable Energy Reviews. 2021;135:110192.

25. Arcos JMM, Santos DM. The hydrogen color spectrum: techno-economic analysis of the available technologies for hydrogen production. Gases. 2023;3(1):25-46.

26. Dash SK, Chakraborty S, Elangovan D. A brief review of hydrogen production methods and their challenges. Energies. 2023;16(3):1141.

27. Agyekum EB, Nutakor C, Agwa AM, Kamel S. A critical review of renewable hydrogen production methods: factors affecting their scale-up and its role in future energy generation. Membranes. 2022;12(2):173.

28. Aly HH, El-Hawary ME, editors. State of the art for tidal currents electric energy resources. 2011 24th Canadian Conference on Electrical and Computer Engineering (CCECE); 2011: IEEE.

29. Mansoori GA, Agyarko LB, Estevez LA, Fallahi B, Gladyshev G, Santos RGd, et al. Fuels of the future for renewable energy sources (ammonia, biofuels, hydrogen). arXiv preprint arXiv:210200439. 2021.

30. Hassan Q, Viktor P, Al-Musawi TJ, Ali BM, Algburi S, Alzoubi HM, et al. The renewable energy role in the global energy Transformations. Renewable Energy Focus. 2024;48:100545.

31. Pablo-Romero M, Román R, Sánchez-Braza A, Yñiguez R. Renewable energy, emissions, and health. Renewable Energy: Utilisation and System Integration. 2016;173.

32. Bridgwater T. Biomass for energy. Journal of the Science of Food and Agriculture. 2006;86(12):1755-68.

33. Rodionova MV, Poudyal RS, Tiwari I, Voloshin RA, Zharmukhamedov SK, Nam HG, et al. Biofuel production: challenges and opportunities. International Journal of Hydrogen Energy. 2017;42(12):8450-61.

34. Rafiee A, Khalilpour KR, Prest J, Skryabin I. Biogas as an energy vector. Biomass and Bioenergy. 2021;144:105935.

35. Mignogna D, Ceci P, Cafaro C, Corazzi G, Avino P. Production of Biogas and Biomethane as Renewable Energy Sources: A Review. Applied Sciences. 2023;13(18):10219.

36. Kabeyi MJB, Olanrewaju OA. Biogas production and applications in the sustainable energy transition. JEner. 2022;2022(1):8750221.

37. Raghulchandrana R, Tamizhini A, Snehya A, Pandey RP. Pretreatment Studies of Biohydrogen Production from Agro-Industrial Waste. 2020.

38. Singh T, Alhazmi A, Mohammad A, Srivastava N, Haque S, Sharma S, et al. Integrated biohydrogen production via lignocellulosic waste: Opportunity, challenges & future prospects. Bioresource Technology. 2021;338:125511.

39. Chandrasekhar K, Lee Y-J, Lee D-W. Biohydrogen production: strategies to improve process efficiency through microbial routes. Int J Mol Sci. 2015;16(4):8266-93.

40. Albuquerque MM, Sartor GdB, Martinez-Burgos WJ, Scapini T, Edwiges T, Soccol CR, et al. Biohydrogen Produced via Dark Fermentation: A Review. Methane. 2024;3(3):500-32.

41. El-Sayad RM, Khalil AS. Wastewater treatment and hydrogen production via Microbial electrolysis cells (MECs) and fermentation methods: A comparative review. Journal of Contemporary Technology and Applied Engineering. 2023;2(1):29-41.

42. Xie D, Kong L, Hu J, Li H, Wang Y. A comparative review of biohydrogen and biomethane production from biowaste through photo-fermentation. Green Chemistry. 2025.

43. Demirbaş A. Biomass resource facilities and biomass conversion processing for fuels and chemicals. Energy conversion and Management. 2001;42(11):1357-78.

44. Yoon TP, Ischay MA, Du J. Visible light photocatalysis as a greener approach to photochemical synthesis. Nature chemistry. 2010;2(7):527-32.

45. Demirbas A. Production of combustible gas from triglycerides via pyrolysis. Energy Sources, Part A. 2009;31(10):870-5.

46. Reddy SN, Nanda S, Dalai AK, Kozinski JA. Supercritical water gasification of biomass for hydrogen production. International Journal of Hydrogen Energy. 2014;39(13):6912-26.

47. Soudagar MEM, Upadhyay VV, Bhooshanam NN, Singh RP, Rabadiya D, Venkatesh R, et al. Organic municipal solid waste derived hydrogen production through supercritical water gasification process configured with K2CO3/SiO2: performance study. Biomass and Bioenergy. 2024;190:107379.

48. Khetkorn W, Rastogi RP, Incharoensakdi A, Lindblad P, Madamwar D, Pandey A, et al. Microalgal hydrogen production–A review. Bioresource technology. 2017;243:1194-206.

49. Anjana K, Kaushik A. Enhanced hydrogen production by immobilized cyanobacterium Lyngbya perelegans under varying anaerobic conditions. Biomass and Bioenergy. 2014;63:54-7.

50. Mona S, Kumar SS, Kumar V, Parveen K, Saini N, Deepak B, et al. Green technology for sustainable biohydrogen production (waste to energy): a review. Science of the Total Environment. 2020;728:138481.

51. Bhatia SK, Jagtap SS, Bedekar AA, Bhatia RK, Rajendran K, Pugazhendhi A, et al. Renewable biohydrogen production from lignocellulosic biomass using fermentation and integration of systems with other energy generation technologies. Science of the Total Environment. 2021;765:144429.

52. Soltanian S, Aghbashlo M, Almasi F, Hosseinzadeh-Bandbafha H, Nizami A-S, Ok YS, et al. A critical review of the effects of pretreatment methods on the exergetic aspects of lignocellulosic biofuels. Energy Conversion and Management. 2020;212:112792.

53. Das D, Khanna N, Dasgupta CN. Biohydrogen production: fundamentals and technology advances: CRC Press; 2014.

54. Honarmandrad Z, Kucharska K, Gębicki J. Processing of Biomass Prior to Hydrogen Fermentation and Post-Fermentative Broth Management. Molecules. 2022;27(21):7658.

55. Mahmoodi P, Karimi K, Taherzadeh MJ. Efficient conversion of municipal solid waste to biofuel by simultaneous dilute-acid hydrolysis of starch and pretreatment of lignocelluloses. Energy conversion and management. 2018;166:569-78.

56. Ren N, Wang A, Cao G, Xu J, Gao L. Bioconversion of lignocellulosic biomass to hydrogen: potential and challenges. Biotechnology Advances. 2009;27(6):1051-60.

57. Ren N-Q, Cao G-L, Guo W-Q, Wang A-J, Zhu Y-H, Liu B-f, et al. Biological hydrogen production from corn stover by moderately thermophile Thermoanaerobacterium thermosaccharolyticum W16. International Journal of Hydrogen Energy. 2010;35(7):2708-12.

58. De Vrije T, De Haas G, Tan G, Keijsers E, Claassen P. Pretreatment of Miscanthus for hydrogen production by Thermotoga elfii. International journal of hydrogen energy. 2002;27(11-12):1381-90.

59. Ntaikou I, Gavala HN, Kornaros M, Lyberatos G. Hydrogen production from sugars and sweet sorghum biomass using Ruminococcus albus. International Journal of Hydrogen Energy. 2008;33(4):1153-63.

60. Sharma R, Joshi R, Kumar D. Present status and future prospect of genetic and metabolic engineering for biofuels production from lignocellulosic biomass. Genetic and Metabolic Engineering for Improved Biofuel Production from Lignocellulosic Biomass: Elsevier; 2020. p. 171-92.

61. Baig K. Interaction of enzymes with lignocellulosic materials: causes, mechanism and influencing factors. Bioresources and bioprocessing. 2020;7(1):1-19.

62. Vu HP, Nguyen LN, Vu MT, Johir MAH, McLaughlan R, Nghiem LD. A comprehensive review on the framework to valorise lignocellulosic biomass as biorefinery feedstocks. Science of the Total Environment. 2020;743:140630.

63. Scelsi E, Angelini A, Pastore C. Deep eutectic solvents for the valorisation of lignocellulosic biomasses towards Fine Chemicals. Biomass. 2021;1(1):29-59.

64. Zoghlami A, Paës G. Lignocellulosic biomass: understanding recalcitrance and predicting hydrolysis. Frontiers in chemistry. 2019;7:874.

65. Ashokkumar V, Venkatkarthick R, Jayashree S, Chuetor S, Dharmaraj S, Kumar G, et al. Recent advances in lignocellulosic biomass for biofuels and value-added bioproducts - A critical review. Bioresource Technology. 2022;344:126195.

66. Chuetor S, Ruiz T, Barakat A, Laosiripojana N, Champreda V, Sriariyanun M. Evaluation of rice straw biopowder from alkaline-mechanical pretreatment by hydro-textural approach. Bioresource Technology. 2021;323:124619.

67. Bhatia SK, Jagtap SS, Bedekar AA, Bhatia RK, Patel AK, Pant D, et al. Recent developments in pretreatment technologies on lignocellulosic biomass: effect of key parameters, technological improvements, and challenges. Bioresource technology. 2020;300:122724.

68. Amin FR, Khalid H, Zhang H, Rahman SU, Zhang R, Liu G, et al. Pretreatment methods of lignocellulosic biomass for anaerobic digestion. Amb Express. 2017;7:1-12.

69. Baruah J, Nath BK, Sharma R, Kumar S, Deka RC, Baruah DC, et al. Recent trends in the pretreatment of lignocellulosic biomass for value-added products. Frontiers in Energy Research. 2018;6:141.

70. Loow Y-L, Wu TY, Md. Jahim J, Mohammad AW, Teoh WH. Typical conversion of lignocellulosic biomass into reducing sugars using dilute acid hydrolysis and alkaline pretreatment. Cellulose. 2016;23:1491-520.

71. Nazli RI, Gulnaz O, Kafkas E, Tansi V. Comparison of different chemical pretreatments for their effects on fermentable sugar production from miscanthus biomass. Biomass Conversion and Biorefinery. 2021:1-9.

72. Bhatia R, Lad JB, Bosch M, Bryant DN, Leak D, Hallett JP, et al. Production of oligosaccharides and biofuels from Miscanthus using combinatorial steam explosion and ionic liquid pretreatment. Bioresource Technology. 2021;323:124625.

73. Jędrzejczyk M, Soszka E, Czapnik M, Ruppert AM, Grams J. Physical and chemical pretreatment of lignocellulosic biomass. Second and third generation of feedstocks: Elsevier; 2019. p. 143-96.

74. Yao K, Wu Q, An R, Meng W, Ding M, Li B, et al. Hydrothermal pretreatment for deconstruction of plant cell wall: Part II. Effect on cellulose structure and bioconversion. AIChE Journal. 2018;64(6):1954-64.

75. Escobar ELN, Da Silva TA, Pirich CL, Corazza ML, Pereira Ramos L. Supercritical fluids: a promising technique for biomass pretreatment and fractionation. Frontiers in Bioengineering and Biotechnology. 2020;8:252.

76. Jönsson LJ, Martín C. Pretreatment of lignocellulose: formation of inhibitory by-products and strategies for minimizing their effects. Bioresource technology. 2016;199:103-12.

77. Batog J, Wawro A. Chemical and biological deconstruction in the conversion process of sorghum biomass for bioethanol. Journal of Natural Fibers. 2022;19(13):5827-38.

78. Łukajtis R, Hołowacz I, Kucharska K, Glinka M, Rybarczyk P, Przyjazny A, et al. Hydrogen production from biomass using dark fermentation. Renewable and Sustainable Energy Reviews. 2018;91:665-94.

79. da Rosa A. Chapter 16 - Ocean Engines. In: da Rosa A, editor. Fundamentals of Renewable Energy Processes (Third Edition). Boston: Academic Press; 2013. p. 765-92.

80. Argun H, Kargi F. Bio-hydrogen production by different operational modes of dark and photo-fermentation: an overview. International Journal of Hydrogen Energy. 2011;36(13):7443-59.

81. Adessi A, De Philippis R. Hydrogen production: photofermentation. Microbial technologies in advanced biofuels production. 2012:53-75.

82. Rai PK, Singh S. Integrated dark-and photo-fermentation: Recent advances and provisions for improvement. International journal of hydrogen energy. 2016;41(44):19957-71.

83. Eroglu E, Melis A. Photobiological hydrogen production: recent advances and state of the art. Bioresource technology. 2011;102(18):8403-13.

84. Phuttaro C, Sawatdeenarunat C, Surendra K, Boonsawang P, Chaiprapat S, Khanal SK. Anaerobic digestion of hydrothermally-pretreated lignocellulosic biomass: Influence of pretreatment temperatures, inhibitors and soluble organics on methane yield. Bioresource technology. 2019;284:128-38.

85. Ghosh S, Falyouna O, Malloum A, Othmani A, Bornman C, Bedair H, et al. A general review on the use of advance oxidation and adsorption processes for the removal of furfural from industrial effluents. Microporous and Mesoporous Materials. 2022;331:111638.

86. Kaykhaii M, Honarmandrad Z, Gębicki J. Effect of Microplastics Pollution on Hydrogen Production from Biomass: A Comprehensive Review. Industrial & Engineering Chemistry Research. 2023;62(9):3835-43.

87. OECD. Test No. 303: Simulation Test - Aerobic Sewage Treatment -- A: Activated Sludge Units; B: Biofilms2001.

88. Balasundaram G, Banu R, Varjani S, Kazmi AA, Tyagi VK. Recalcitrant compounds formation, their toxicity, and mitigation: Key issues in biomass pretreatment and anaerobic digestion. Chemosphere. 2022;291:132930.

89. Anish R, Rao M. Bioethanol from lignocellulosic biomass part III hydrolysis and fermentation. Handbook of plant-based biofuels. 2009:159-73.

90. Canilha L, Chandel AK, Suzane dos Santos Milessi T, Antunes FAF, Luiz da Costa Freitas W, das Graças Almeida Felipe M, et al. Bioconversion of sugarcane biomass into ethanol: an overview about composition, pretreatment methods, detoxification of hydrolysates, enzymatic saccharification, and ethanol fermentation. BioMed Research International. 2012;2012.

91. Grzenia DL, Schell DJ, Ranil Wickramasinghe S. Membrane extraction for detoxification of biomass hydrolysates. Bioresource Technology. 2012;111:248-54.

92. Chandel AK, da Silva SS, Singh OV. Detoxification of lignocellulosic hydrolysates for improved bioethanol production. Biofuel production-recent developments and prospects. 2011;10:225.

93. Canilha L, Carvalho W, Giulietti M, Felipe MDGA, Almeida E Silva JB. Clarification of a wheat straw-derived medium with ion-exchange resins for xylitol crystallization. Journal of Chemical Technology & Biotechnology: International Research in Process, Environmental & Clean Technology. 2008;83(5):715-21.

94. Gírio FM, Fonseca C, Carvalheiro F, Duarte LC, Marques S, Bogel-Łukasik R. Hemicelluloses for fuel ethanol: a review. Bioresource technology. 2010;101(13):4775-800.

95. Antunes F, Milessi T, Oliveira I, Chandel A, Silva S, editors. Characterization of sugarcane bagasse hemicellulosic hydrolysate after detoxification with overliming and activated charcoal. Proceedings of the 20th European Biomass Conference and Exhibition; 2012.

96. Carvalho W, Canilha L, Silva SS. Semi-continuous xylose-to-xylitol bioconversion by Ca-alginate entrapped yeast cells in a stirred tank reactor. Bioprocess and Biosystems Engineering. 2008;31:493-8.

97. Converti A, Domínguez JM, Perego P, Da Silva S, Zilli M. Wood hydrolysis and hydrolyzate detoxification for subsequent xylitol production. Chemical Engineering & Technology: Industrial Chemistry-Plant Equipment-Process Engineering-Biotechnology. 2000;23(11):1013-20.

98. Cantarella M, Cantarella L, Gallifuoco A, Spera A, Alfani F. Comparison of different detoxification methods for steam-exploded poplar wood as a substrate for the bioproduction of ethanol in SHF and SSF. Process biochemistry. 2004;39(11):1533-42.

99. Hou-Rui Z, Xiang-Xiang Q, Silva SS, Sarrouh BF, Ai-Hua C, Yu-Heng Z, et al. Novel isolates for biological detoxification of lignocellulosic hydrolysate. Applied biochemistry and biotechnology. 2009;152:199-212.

100. Chandel AK, Chandrasekhar G, Radhika K, Ravinder R, Ravindra P. Bioconversion of pentose sugars into ethanol: a review and future directions. Biotechnol mol biol rev. 2011;6(1):008-20.

101. Moreno AD, Ibarra D, Fernández JL, Ballesteros M. Different laccase detoxification strategies for ethanol production from lignocellulosic biomass by the thermotolerant yeast Kluyveromyces marxianus CECT 10875. Bioresource Technology. 2012;106:101-9.

102. Parawira W, Tekere M. Biotechnological strategies to overcome inhibitors in lignocellulose hydrolysates for ethanol production. Critical reviews in biotechnology. 2011;31(1):20-31.

103. Prabhune A, Dey R. Green and sustainable solvents of the future: Deep eutectic solvents. Journal of Molecular Liquids. 2023;379:121676.

104. Pan L, He M, Wu B, Wang Y, Hu G, Ma K. Simultaneous concentration and detoxification of lignocellulosic hydrolysates by novel membrane filtration system for bioethanol production. Journal of Cleaner Production. 2019;227:1185-94.

105. Doddapaneni TRKC, Jain R, Praveenkumar R, Rintala J, Romar H, Konttinen J. Adsorption of furfural from torrefaction condensate using torrefied biomass. Chemical Engineering Journal. 2018;334:558-68.

106. Carvalho GB, Mussatto SI, Cândido EJ, Almeida e Silva JB. Comparison of different procedures for the detoxification of eucalyptus hemicellulosic hydrolysate for use in fermentative processes. Journal of Chemical Technology & Biotechnology. 2006;81(2):152-7.

107. Ludwig D, Amann M, Hirth T, Rupp S, Zibek S. Development and optimization of single and combined detoxification processes to improve the fermentability of lignocellulose hydrolyzates. Bioresource Technology. 2013;133:455-61.

108. Makoś P, Słupek E, Gębicki J. Extractive detoxification of feedstocks for the production of biofuels using new hydrophobic deep eutectic solvents–Experimental and theoretical studies. Journal of Molecular Liquids. 2020;308:113101.

109. Hanson C. Recent advances in liquid-liquid extraction. 2013.

110. Roque LR, Morgado GP, Nascimento VM, Ienczak JL, Rabelo SC. Liquid-liquid extraction: A promising alternative for inhibitors removing of pentoses fermentation. Fuel. 2019;242:775-87.

111. Dietz CH, Gallucci F, van Sint Annaland M, Held C, Kroon MC. 110th anniversary: distribution coefficients of furfural and 5-hydroxymethylfurfural in hydrophobic deep eutectic solvent+ water systems: experiments and perturbed-chain statistical associating fluid theory predictions. Industrial & Engineering Chemistry Research. 2019;58(10):4240-7.

112. Cui P, Liu H, Xin K, Yan H, Xia Q, Huang Y, et al. Liquid-liquid equilibria for the ternary system of water+ furfural+ solvents at 303.15 and 323.15 K under atmospheric pressure. The Journal of Chemical Thermodynamics. 2018;127:134-44.

113. Makoś P, Boczkaj G. Deep eutectic solvents based highly efficient extractive desulfurization of fuels–Eco-friendly approach. Journal of Molecular Liquids. 2019;296:111916.

114. Smink D, Kersten SR, Schuur B. Recovery of lignin from deep eutectic solvents by liquid-liquid extraction. Separation and purification technology. 2020;235:116127.

115. Makoś P, Słupek E, Gębicki J. Hydrophobic deep eutectic solvents in microextraction techniques–A review. Microchemical journal. 2020;152:104384.

116. Makoś P, Przyjazny A, Boczkaj G. Hydrophobic deep eutectic solvents as “green” extraction media for polycyclic aromatic hydrocarbons in aqueous samples. Journal of Chromatography A. 2018;1570:28-37.

117. Makoś P, Fernandes A, Przyjazny A, Boczkaj G. Sample preparation procedure using extraction and derivatization of carboxylic acids from aqueous samples by means of deep eutectic solvents for gas chromatographic-mass spectrometric analysis. Journal of Chromatography A. 2018;1555:10-9.

118. Florindo C, Branco L, Marrucho I. Development of hydrophobic deep eutectic solvents for extraction of pesticides from aqueous environments. Fluid Phase Equilibria. 2017;448:135-42.

119. Zubeir LF, Van Osch DJ, Rocha MA, Banat F, Kroon MC. Carbon dioxide solubilities in decanoic acid-based hydrophobic deep eutectic solvents. Journal of Chemical & Engineering Data. 2018;63(4):913-9.

120. Słupek E, Makoś P, Gębicki J. Deodorization of model biogas by means of novel non-ionic deep eutectic solvent. Archives of Environmental Protection. 2020;46(1).

121. Słupek E, Makoś P. Absorptive desulfurization of model biogas stream using choline chloride-based deep eutectic solvents. Sustainability. 2020;12(4):1619.

122. Boldrini CL, Manfredi N, Perna FM, Capriati V, Abbotto A. Designing eco-sustainable dye-sensitized solar cells by the use of a menthol-based hydrophobic eutectic solvent as an effective electrolyte medium. Chemistry–A European Journal. 2018;24(67):17656-9.

123. Tolmachev D, Lukasheva N, Ramazanov R, Nazarychev V, Borzdun N, Volgin I, et al. Computer simulations of deep eutectic solvents: Challenges, solutions, and perspectives. Int J Mol Sci. 2022;23(2):645.

124. Ferreira C, Sarraguça M. A Comprehensive Review on Deep Eutectic Solvents and Its Use to Extract Bioactive Compounds of Pharmaceutical Interest. Pharmaceuticals. 2024;17(1):124.

125. Zainal-Abidin MH, Hayyan M, Wong WF. Hydrophobic deep eutectic solvents: Current progress and future directions. Journal of Industrial and Engineering Chemistry. 2021;97:142-62.

126. Brouwer T, Dielis BC, Bock JM, Schuur B. Hydrophobic deep eutectic solvents for the recovery of bio-based chemicals: Solid–liquid equilibria and liquid–liquid extraction. Processes. 2021;9(5):796.

127. Cheng H, Huang Y, Lv H, Li L, Meng Q, Yuan M, et al. Insights into the liquid extraction mechanism of actual high-strength phenolic wastewater by hydrophobic deep eutectic solvents. Journal of Molecular Liquids. 2022;368:120609.

128. Makoś-Chełstowska P, Kaykhaii M, Płotka-Wasylka J, de la Guardia M. Magnetic deep eutectic solvents–Fundamentals and applications. Journal of Molecular Liquids. 2022;365:120158.

129. Aguirre MÁ, Canals A. Magnetic deep eutectic solvents in microextraction techniques. TrAC Trends in Analytical Chemistry. 2022;146:116500.

130. Farooq MQ, Tryon-Tasson N, Biswas A, Anderson JL. Preparation of ternary hydrophobic magnetic deep eutectic solvents and an investigation into their physicochemical properties. Journal of Molecular Liquids. 2022;365:120000.

131. Khezeli T, Daneshfar A. Synthesis and application of magnetic deep eutectic solvents: Novel solvents for ultrasound assisted liquid-liquid microextraction of thiophene. Ultrasonics Sonochemistry. 2017;38:590-7.

132. Liu Q, Huang X, Liang P. Preconcentration of copper and lead using deep eutectic solvent modified magnetic nanoparticles and determination by inductively coupled plasma optical emission spectrometry. At Spectrosc. 2020;41(1):36-42.

133. Pochivalov A, Cherkashina K, Sudarkin A, Osmolowsky M, Osmolovskaya O, Krekhova F, et al. Liquid-liquid microextraction with hydrophobic deep eutectic solvent followed by magnetic phase separation for preconcentration of antibiotics. Talanta. 2023;252:123868.

134. Qu Q, Tang W, Tang B, Zhu T. Highly selective purification of ferulic acid from wheat bran using deep eutectic solvents modified magnetic nanoparticles. Separation Science And Technology. 2017;52(6):1022-30.

135. Hai X, Shi F, Zhu Y, Ma L, Wang L, Yin J, et al. Development of magnetic dispersive micro-solid phase extraction of four phenolic compounds from food samples based on magnetic chitosan nanoparticles and a deep eutectic supramolecular solvent. Food Chemistry. 2023;410:135338.

136. Chen Z, Ragauskas A, Wan C. Lignin extraction and upgrading using deep eutectic solvents. Industrial crops and products. 2020;147:112241.

137. Kumar AK, Parikh BS, Cotta MA. Application of natural deep eutectic solvents in biomass pretreatment, enzymatic saccharification and cellulosic ethanol production. Materials Today: Proceedings. 2018;5(11):23057-63.

138. Wang Z-K, Li H, Lin X-C, Tang L, Chen J-J, Mo J-W, et al. Novel recyclable deep eutectic solvent boost biomass pretreatment for enzymatic hydrolysis. Bioresource technology. 2020;307:123237.

139. Lu Y, He Q, Fan G, Cheng Q, Song G. Extraction and modification of hemicellulose from lignocellulosic biomass: A review. Green Processing and Synthesis. 2021;10(1):779-804.

140. Honarmandrad Z, Kucharska K, Kaykhaii M, Gębicki J. Removal of phenolic inhibitor compounds from hydrolysates and post-fermentation broths by using a hydrophobic magnetic deep eutectic solvent. Journal of Environmental Chemical Engineering. 2024;12(3):112621.

141. Makoś-Chełstowska P, Kucharska K, Słupek E, Gębicki J, de la Guardia M. Magnetic deep eutectic solvents as efficient media for extraction of furfural and 5-hydroxymethylfurfural from aqueous samples. Journal of Molecular Liquids. 2023;390:122945.

142. Makoś-Chełstowska P, Słupek E, Kucharska K, Kramarz A, Gębicki J. Efficient Extraction of Fermentation Inhibitors by Means of Green Hydrophobic Deep Eutectic Solvents. Molecules. 2021;27(1):157.

143. Alam MA, Muhammad G, Khan MN, Mofijur M, Lv Y, Xiong W, et al. Choline chloride-based deep eutectic solvents as green extractants for the isolation of phenolic compounds from biomass. Journal of cleaner production. 2021;309:127445.

144. de Almeida Pontes PV, Shiwaku IA, Maximo GJ, Batista EAC. Choline chloride-based deep eutectic solvents as potential solvent for extraction of phenolic compounds from olive leaves: Extraction optimization and solvent characterization. Food Chemistry. 2021;352:129346.

145. Vorobyova V, Skiba M, Vasyliev G. Extraction of phenolic compounds from tomato pomace using choline chloride–based deep eutectic solvents. Journal of Food Measurement and Characterization. 2022;16(2):1087-104.

146. Dance I. What is supramolecular? New Journal of Chemistry. 2003;27(1):1-2.

147. Lehn J-M. Supramolecular chemistry: Vch, Weinheim New York; 1995.

148. Ariga K, Kunitake T. Supramolecular chemistry-fundamentals and applications: advanced textbook: Springer Science & Business Media; 2006.

149. Janicka P, Kaykhaii M, Płotka-Wasylka J, Gębicki J. Supramolecular deep eutectic solvents and their applications. Green Chemistry. 2022;24(13):5035-45.

150. Zhang J, Yao L, Li S, Li S, Wu Y, Li Z-G, et al. Green materials with promising applications: Cyclodextrins-based deep eutectic supramolecular polymers. Green Chemistry. 2023.

151. El Achkar T, Moufawad T, Ruellan S, Landy D, Greige-Gerges H, Fourmentin S. Cyclodextrins: from solute to solvent. Chemical communications. 2020;56(23):3385-8.

152. Morin-Crini N, Fourmentin S, Fenyvesi É, Lichtfouse E, Torri G, Fourmentin M, et al. 130 years of cyclodextrin discovery for health, food, agriculture, and the industry: A review. Environmental Chemistry Letters. 2021;19(3):2581-617.

153. Crini G. A history of cyclodextrins. Chemical reviews. 2014;114(21):10940-75.

154. Moufawad T, Moura L, Ferreira M, Bricout H, Tilloy Sb, Monflier E, et al. First evidence of cyclodextrin inclusion complexes in a deep eutectic solvent. ACS Sustainable Chemistry & Engineering. 2019;7(6):6345-51.

155. Sereshti H, Karami F, Nouri N. A green dispersive liquid-liquid microextraction based on deep eutectic solvents doped with β-cyclodextrin: Application for determination of tetracyclines in water samples. Microchemical Journal. 2021;163:105914.

156. Di Pietro ME, Ferro M, Mele A. Drug encapsulation and chiral recognition in deep eutectic solvents/β-cyclodextrin mixtures. Journal of Molecular Liquids. 2020;311:113279.

157. Tilloy S, Genin E, Hapiot F, Landy D, Fourmentin S, Genêt JP, et al. Water-Soluble Triphenylphosphane-3, 3′, 3″-tricarboxylate (m-TPPTC) Ligand and Methylated Cyclodextrins: A New Combination for Biphasic Rhodium-Catalyzed Hydroformylation of Higher Olefins. Advanced synthesis & catalysis. 2006;348(12-13):1547-52.

158. Farooq MQ, Zeger VR, Anderson JL. Comparing the extraction performance of cyclodextrin-containing supramolecular deep eutectic solvents versus conventional deep eutectic solvents by headspace single drop microextraction. Journal of Chromatography A. 2021;1658:462588.

159. Panda S, Fourmentin S. Cyclodextrin-based supramolecular low melting mixtures: efficient absorbents for volatile organic compounds abatement. Environmental Science and Pollution Research. 2022:1-7.

160. Tian B, Liu Y, Liu J. Smart stimuli-responsive drug delivery systems based on cyclodextrin: A review. Carbohydrate polymers. 2021;251:116871.

161. Wan H, Wang J, Sheng X, Yan J, Zhang W, Xu Y. Removal of polystyrene microplastics from aqueous solution using the metal–organic framework material of ZIF-67. Toxics. 2022;10(2):70.

162. Furukawa H, Cordova KE, O'Keeffe M, Yaghi OM. The chemistry and applications of metal-organic frameworks. Science. 2013;341(6149):1230444.

163. Kaykhaii M, Hashemi SH. Miniaturized solid phase extraction. Emerging Freshwater Pollutants: Elsevier; 2022. p. 49-61.

164. Kaykhaii M, Hashemi SH, Andarz F, Piri A, Sargazi G. Chromium-based metal organic framework for pipette tip micro-solid phase extraction: an effective approach for determination of methyl and propyl parabens in wastewater and shampoo samples. BMC chemistry. 2021;15(1):60.

165. Sajid M. Nanomaterials: types, properties, recent advances, and toxicity concerns. Current Opinion in Environmental Science & Health. 2022;25:100319.

166. Kuang X, Ma Y, Su H, Zhang J, Dong Y-B, Tang B. High-performance liquid chromatographic enantioseparation of racemic drugs based on homochiral metal–organic framework. Analytical Chemistry. 2014;86(2):1277-81.

167. Wang T, Zhao P, Lu N, Chen H, Zhang C, Hou X. Facile fabrication of Fe3O4/MIL-101 (Cr) for effective removal of acid red 1 and orange G from aqueous solution. Chemical Engineering Journal. 2016;295:403-13.

168. James SL. Metal-organic frameworks. Chemical Society Reviews. 2003;32(5):276-88.

169. Yaghi O, Li H. Hydrothermal synthesis of a metal-organic framework containing large rectangular channels. Journal of the American Chemical Society. 1995;117(41):10401-2.

170. Tian H, Peng J, Lv T, Sun C, He H. Preparation and performance study of MgFe2O4/metal–organic framework composite for rapid removal of organic dyes from water. Journal of Solid State Chemistry. 2018;257:40-8.

171. Yengin C, Gumus ZP, Ilktac R, Elci A, Soylak M. Vortex-assisted solid phase extraction on MIL-101(Cr) of parabens in waters and cosmetics by HPLC–DAD. Journal of the Iranian Chemical Society. 2023;20(6):1383-93.

172. Ozalp O, Gumus ZP, Soylak M. Metal-organic framework functionalized with deep eutectic solvent for solid-phase extraction of Rhodamine 6G in water and cosmetic products. J Sep Sci. 2023:e2300190.

173. Wei X, Wang Y, Chen J, Xu P, Xu W, Ni R, et al. Poly (deep eutectic solvent)-functionalized magnetic metal-organic framework composites coupled with solid-phase extraction for the selective separation of cationic dyes. Analytica Chimica Acta. 2019;1056:47-61.

174. Salamat Q, Soylak M. Novel magnetic deep eutectic solvent/Zn-MOF composite for extraction of Carmoisine from water and food samples. Journal of Food Composition and Analysis. 2024:105997.

175. Alipanahpour Dil E, Ghaedi M, Asfaram A, Tayebi L, Mehrabi F. A ferrofluidic hydrophobic deep eutectic solvent for the extraction of doxycycline from urine, blood plasma and milk samples prior to its determination by high-performance liquid chromatography-ultraviolet. Journal of Chromatography A. 2020;1613:460695.

176. Li H, Chu H, Ma X, Wang G, Liu F, Guo M, et al. Efficient heterogeneous acid synthesis and stability enhancement of UiO-66 impregnated with ammonium sulfate for biodiesel production. Chemical Engineering Journal. 2021;408:127277.

177. Akbarian M, Sanchooli E, Oveisi AR, Daliran S. Choline chloride-coated UiO-66-Urea MOF: A novel multifunctional heterogeneous catalyst for efficient one-pot three-component synthesis of 2-amino-4H-chromenes. Journal of Molecular Liquids. 2021;325:115228.

178. Florindo C, Lima F, Branco LC, Marrucho IM. Hydrophobic deep eutectic solvents: a circular approach to purify water contaminated with ciprofloxacin. ACS Sustainable Chemistry & Engineering. 2019;7(17):14739-46.

179. Almashjary KH, Khalid M, Dharaskar S, Jagadish P, Walvekar R, Gupta TCSM. Optimisation of extractive desulfurization using Choline Chloride-based deep eutectic solvents. Fuel. 2018;234:1388-400.

180. Farooq MQ, Ocaña-Rios I, Anderson JL. Analysis of persistent contaminants and personal care products by dispersive liquid-liquid microextraction using hydrophobic magnetic deep eutectic solvents. Journal of Chromatography A. 2022;1681:463429.

181. Rykowska I, Ziemblińska J, Nowak I. Modern approaches in dispersive liquid-liquid microextraction (DLLME) based on ionic liquids: A review. Journal of molecular liquids. 2018;259:319-39.

182. Sas OG, Castro M, Domínguez Á, González B. Removing phenolic pollutants using deep eutectic solvents. Separation and Purification Technology. 2019;227:115703.

183. Lu W, Liu S. Choline chloride–based deep eutectic solvents (Ch-DESs) as promising green solvents for phenolic compounds extraction from bioresources: State-of-the-art, prospects, and challenges. Biomass Conversion and Biorefinery. 2020:1-14.

184. Yonten V, Ince M, Tanyol M, Yildirim N. Adsorption of bisphenol A from aqueous solutions by Pleurotus eryngii immobilized on Amberlite XAD-4 using as a new adsorbent. Desalination and Water Treatment. 2016;57(47):22362-9.

185. Piao H, Jiang Y, Qin Z, Ma P, Sun Y, Wang X, et al. Application of an in-situ formulated magnetic deep eutectic solvent for the determination of triazine herbicides in rice. Talanta. 2021;222:121527.

186. Peng F, Liu M, Wang X, Ding X. Synthesis of low-viscosity hydrophobic magnetic deep eutectic solvent: Selective extraction of DNA. Analytica Chimica Acta. 2021;1181:338899.

187. Kocúrová L, Balogh IS, Andruch V. A glance at achievements in the coupling of headspace and direct immersion single-drop microextraction with chromatographic techniques. Journal of separation science. 2013;36(23):3758-68.

188. Daliran S, Ghazagh-Miri M, Oveisi AR, Khajeh M, Navalón S, Âlvaro M, et al. A Pyridyltriazol Functionalized Zirconium Metal–Organic Framework for Selective and Highly Efficient Adsorption of Palladium. ACS Applied Materials & Interfaces. 2020;12(22):25221-32.

189. Honarmandrad Z, Khadem SSM, Kucharska K, Kaykhaii M, Łuczak J, Gebicki J. Enhanced sorption of inhibitory compounds from fermentation broth using a MOF@pseudo-DES composite. Journal of Molecular Liquids. 2025;421:126845.

190. Sarker M, Song JY, Jhung SH. Carboxylic-acid-functionalized UiO-66-NH2: A promising adsorbent for both aqueous- and non-aqueous-phase adsorptions. Chemical Engineering Journal. 2018;331:124-31.

191. Du C, Zhao B, Chen X-B, Birbilis N, Yang H. Effect of water presence on choline chloride-2urea ionic liquid and coating platings from the hydrated ionic liquid. Scientific reports. 2016;6(1):29225.

192. Chakarova K, Strauss I, Mihaylov M, Drenchev N, Hadjiivanov K. Evolution of acid and basic sites in UiO-66 and UiO-66-NH2 metal-organic frameworks: FTIR study by probe molecules. Microporous and Mesoporous Materials. 2019;281:110-22.

193. Strauss I, Chakarova K, Mundstock A, Mihaylov M, Hadjiivanov K, Guschanski N, et al. UiO-66 and UiO-66-NH2 based sensors: Dielectric and FTIR investigations on the effect of CO2 adsorption. Microporous and Mesoporous Materials. 2020;302:110227.

194. Navazeni M, Zolfigol MA, Torabi M, Khazaei A. Application of magnetic deep eutectic solvents as an efficient catalyst in the synthesis of new 1, 2, 3-triazole-nicotinonitrile hybrids via a cooperative vinylogous anomeric-based oxidation. RSC advances. 2024;14(47):34668-78.

195. Timofeev KL, Kulinich SA, Kharlamova TS. NH2-modified UiO-66: structural characteristics and functional properties. Molecules. 2023;28(9):3916.

196. Li Z, Sun W, Chen C, Guo Q, Li X, Gu M, et al. Deep eutectic solvents appended to UiO-66 type metal organic frameworks: Preserved open metal sites and extra adsorption sites for CO2 capture. Applied Surface Science. 2019;480:770-8.

197. Janicka P, Przyjazny A, Boczkaj G. Novel “acid tuned” deep eutectic solvents based on protonated L-proline. Journal of Molecular Liquids. 2021;333:115965.

198. Koca HD, Doganay S, Turgut A, Tavman IH, Saidur R, Mahbubul IM. Effect of particle size on the viscosity of nanofluids: A review. Renewable and Sustainable Energy Reviews. 2018;82:1664-74.

199. Harvey D. Modern analytical chemistry: McGraw Hill; 2000.

200. Tippkötter N, Deterding A, Ulber R. Determination of Acetic Acid in Fermentation Broth by Gas-Diffusion Technique. Eng Life Sci. 2008;8(1):62-7.

201. Hu L, Lin L, Wu Z, Zhou S, Liu S. Recent advances in catalytic transformation of biomass-derived 5-hydroxymethylfurfural into the innovative fuels and chemicals. Renewable and Sustainable Energy Reviews. 2017;74:230-57.

202. Honarmandrad Z, Kucharska K, Słupek E, Cydejko J, Strzelczyk I, Kaykhaii M, et al. SUPRADES: A novel approach for inhibitor compound removal from hydrolysates with concurrent enhancement of biohydrogen production. International Journal of Hydrogen Energy. 2025;135:361-71.

203. Kung K-H, McBride M. Electron transfer processes between hydroquinone and iron oxides. Clays Clay Miner. 1988;36(4):303-9.

204. Kubinyi MJ, Keresztury G, editors. Infrared and Raman spectra of hydroquinone crystalline modifications. Progress in Fourier Transform Spectroscopy: Proceedings of the 10th International Conference, August 27–September 1, 1995, Budapest, Hungary; 1997: Springer.

205. Chawananon S, Asselin P, Claus JA, Goubet M, Roucou A, Georges R, et al. Rovibrational Spectroscopy of Trans and Cis Conformers of 2-Furfural from High-Resolution Fourier Transform and QCL Infrared Measurements. Molecules. 2023;28(10):4165.

206. Ong H, Sashikala M. Identification of furfural synthesized from pentosan in rice husk. J Trop Agric Food Sci. 2007;35:305-12.

207. Chromá R, Vilková M, Shepa I, Makoś-Chełstowska P, Andruch V. Investigation of tetrabutylammonium bromide-glycerol-based deep eutectic solvents and their mixtures with water by spectroscopic techniques. Journal of Molecular Liquids. 2021;330:115617.

208. Adeoye DO, Gano ZS, Ahmed OU, Shuwa SM, Atta AY, Iwarere SA, et al. Synthesis and Characterisation of Menthol-Based Hydrophobic Deep Eutectic Solvents. Chemistry Proceedings. 2023;14(1):98.

209. Hadadian M, Allahyari R, Mahdavi B, Rezaei-Seresht E. Design, characterization, and in vitro evaluation of magnetic carboxymethylated β-cyclodextrin as a pH-sensitive carrier system for amantadine delivery: a novel approach for targeted drug delivery. RSC advances. 2025;15(1):446-59.

210. Allen G, Bernstein H. Internal rotation: VIII. The infrared and Raman spectra of furfural. Canadian Journal of Chemistry. 1955;33(6):1055-61.

211. Mudi I, Hart A, Ingram A, Wood J. A Kinetic Model of Furfural Hydrogenation to 2-Methylfuran on Nanoparticles of Nickel Supported on Sulfuric Acid-Modified Biochar Catalyst. Catalysts. 2024;14(1):54.

212. Peng H, Xiong H, Li J, Xie M, Liu Y, Bai C, et al. Vanillin cross-linked chitosan microspheres for controlled release of resveratrol. Food chemistry. 2010;121(1):23-8.

213. Shi Y, Zhang Z, Jiang W, Wang R, Wang Z. Infrared spectral-shift induced by hydrogen bonding cooperativity in cyclic and prismatic water clusters. Journal of Molecular Liquids. 2019;286:110940.

214. Pei Y, Wu K, Wang J, Fan J. Recovery of furfural from aqueous solution by ionic liquid based liquid–liquid extraction. Separation Science and Technology. 2008;43(8):2090-102.

215. Ozalp O, Gumus ZP, Soylak M. MIL-101(Cr) metal–organic frameworks based on deep eutectic solvent (ChCl: Urea) for solid phase extraction of imidacloprid in tea infusions and water samples. Journal of Molecular Liquids. 2023;378:121589.

216. Liu Y, Cao S, Liu Z, Wu D, Luo M, Chen Z. Adsorption of amphetamine on deep eutectic solvents functionalized graphene oxide/metal-organic framework nanocomposite: Elucidation of hydrogen bonding and DFT studies. Chemosphere. 2023;323:138276.

217. Yin Y, Fan C, Shan Y, Cheng L. Fabrication of amorphous metal-organic framework in deep eutectic solvent for boosted organophosphorus pesticide adsorption. Journal of Environmental Chemical Engineering. 2023;11(3):109963.

218. Wei X, Wang Y, Chen J, Xu F, Liu Z, He X, et al. Adsorption of pharmaceuticals and personal care products by deep eutectic solvents-regulated magnetic metal-organic framework adsorbents: Performance and mechanism. Chemical Engineering Journal. 2020;392:124808.

219. Dietz CH, Erve A, Kroon MC, van Sint Annaland M, Gallucci F, Held C. Thermodynamic properties of hydrophobic deep eutectic solvents and solubility of water and HMF in them: Measurements and PC-SAFT modeling. Fluid Phase Equilibria. 2019;489:75-82.

220. Ozalp O, Gumus ZP, Soylak M. MIL-101 (Cr) metal–organic frameworks based on deep eutectic solvent (ChCl: Urea) for solid phase extraction of imidacloprid in tea infusions and water samples. Journal of Molecular Liquids. 2023;378:121589.

LIST OF FIGURES

LIST OF TABLES

Achievements

Publication

Title: SUPRADES: A novel approach for inhibitor compound removal from hydrolysates with concurrent enhancement of biohydrogen production.

Authors: Zhila Honarmandrad, Karolina Kucharska, Edyta Słupek, Jakub Cydejko, Ilona Strzelczyk, Massoud Kaykhaii, Jacek Gebicki.

Journal: International Journal of Hydrogen Energy.

Year: 2025

Doi: 10.1016/j.ijhydene.2025.04.351

Title: Enhanced sorption of inhibitory compounds from fermentation broth using a MOF@ pseudo-DES composite.

Authors: Zhila Honarmandrad, Seyed Soroush Mousavi Khadem, Karolina Kucharska, Massoud Kaykhaii, Justyna Łuczak, Jacek Gebicki.

Journal: Journal of Molecular Liquids

Doi: 10.1016/j.molliq.2025.126845

Title: Removal of phenolic inhibitor compounds from hydrolysates and post-fermentation broths by using a hydrophobic magnetic deep eutectic solvent

Authors: Zhila Honarmandrad, Karolina Kucharska, Massoud Kaykhaii, Jacek Gębicki

Journal: Journal of Environmental Chemical Engineering

Year: 2024

Doi: 10.1016/j.jece.2024.112621

Title: Removal of phenolic inhibitor compounds from hydrolysates and post-fermentation broths by using a hydrophobic magnetic deep eutectic solvent.

Authors: Zhila Honarmandrad, Karolina Kucharska, Massoud Kaykhaii, Jacek Gębicki.

Journal: Journal of Environmental Chemical Engineering.

Year: 2024

Doi: 10.1016/j.jece.2024.112621

Title: Microplastics removal from aqueous environment by metal organic frameworks

Authors: Zhila Honarmandrad, Massoud Kaykhaii, Jacek Gębicki

Journal: BMC chemistry

Year: 2023

Doi: 10.1186/s13065-023-01032-y

Title: Effect of Microplastics Pollution on Hydrogen Production from Biomass: A Comprehensive Review.

Authors: Massoud Kaykhaii, Zhila Honarmandrad, Jacek Gębicki.

Journal: Industrial & Engineering Chemistry Research.

Year: 2023

Doi: 10.1021/acs.iecr.2c04499

Title: Processing of biomass prior to hydrogen fermentation and post fermentative broth management.

Authors: Zhila Honarmandrad, Karolina Kucharska, Jacek Gebicki.

Journal: Molecules

Year: 2022

Doi: 10.3390/molecules27217658

Conference

Title: Application of hydrophobic magnetic deep eutectic solvent for rapid and effective removal of inhibitor compounds from post-fermentation broth media.

Authors: Zhila Honarmandrad, karolina Kucharska, Massoud Kaykhaii, Jacek Gebicki

Name of conference: 7th International Congress on Water, Waste and Energy Management (WWEM-24)

Year: 2024

Publisher: Lisbon, Portugal

Title: Detoxification methods for the production of more biohydrogen from biomass hydrolysis: a review.

Authors: Zhila Honarmandrad, Massoud Kaykhaii, karolina Kucharska, Jacek Gebicki

Name of conference: 64 Zjazd Polskiego Towarzystwa Chemicznego

Year: 2022

Publisher: Lublin, Poland

Indexing database	H-Index	Citation
Scopus	9	462
Web of Science	6	339